

SU(2) LATTICE GAUGE THEORY IN
COULUMB GAUGE AT ZERO AND FINITE
TEMPERATURE

Songvudhi Chimchinda

A Thesis Submitted in Partial Fulfillment of the Requirements for the

Degree of Doctor of Philosophy in Physics

Suranaree University of Technology

Academic Year 2009

ทฤษฎีเกจผลึก $SU(2)$ ในเกจลออมป์ที่อนุหภูมิศูนย์ และอนุหภูมิจำกัด

นายทรงวุฒิ นิมจินดา

วิทยานิพนธ์นี้เป็นส่วนหนึ่งของการศึกษาตามหลักสูตรปริญญาวิทยาศาสตรดุษฎีบัณฑิต

สาขาวิชาฟิสิกส์

มหาวิทยาลัยเทคโนโลยีสุรนารี

ปีการศึกษา 2552

**$SU(2)$ LATTICE GAUGE THEORY IN COULUMB GAUGE
AT ZERO AND FINITE TEMPERATURE**

Suranaree University of Technology has approved this thesis submitted in partial fulfillment of the requirements for the Degree of Doctor of Philosophy.

Thesis Examining Committee

(Asst. Prof. Dr. Chinorat Kobdaj)

Chairperson

(Prof. Dr. Yupeng Yan)

Member (Thesis Advisor)

(Dr. Nupan Kheaomaingam)

Member

(Dr. Sampart Cheedket)

Member

(Dr. Khanchai Khosonthongkee)

Member

(Prof. Dr. Sukit Limpijumnong)

Vice Rector for Academic Affairs

(Assoc. Prof. Dr. Prapun Manyum)

Dean of Institute of Science

ทรงวุฒิ จิมจินดา : ทฤษฎีเกจผลึก $SU(2)$ ในเกจคูลอมป์ที่อุณหภูมิศูนย์และอุณหภูมิจำกัด
($SU(2)$ LATTICE GAUGE THEORY IN COULOMB GAUGE AT ZERO AND FINITE
TEMPERATURE) อาจารย์ที่ปรึกษา : ศาสตราจารย์ ดร.ยูเป็ง แขน, 101 หน้า.

เราศึกษาลักษณะของการกักกันในพลศาสตร์สี่ควอนตัมแบบวิธีการไม่รบกวนซึ่งคือ การจำลองผลึกทฤษฎีแอง-มิลล์ $SU(2)$ ในเกจคูลอมป์ซึ่งยอมให้เราดึงข้อมูลของวัตถุสามอย่าง คือ ตัวแผ่กระจายกลูออน ตัวรูปสี่ และศักย์คูลอมป์ซึ่งสัมพันธ์กับการกักกันของควาร์กและกลูออน เราพิจารณาการทำให้ไม่ต่อเนื่องของทฤษฎีแอง-เมิลล์ในเกจคูลอมป์ และภาพการกักกันของมัน ซึ่งถูกชื้อออกมาโดยกริโบว เรากล่าวถึงวิธีการผลึกเพื่อการปฏิบัติการสร้างการจำลอง สิ่งที่น่าสนใจได้ถูกวัดจากตัวเหมือนเกจที่ดีที่สุด การตรงใจของเราได้ถูกปรับปรุงโดยการสร้างทางเลือกของวงโคจรเกจโดยใช้ความเป็นปฏิภาคของผลึก

เรารายงานผลของตัวแผ่กระจายกลูออนและตัวรูปสี่ ที่อุณหภูมิศูนย์และอุณหภูมิจำกัด ทุกๆ สิ่งที่น่าสนใจได้ วัดที่ผลึกเวลาเท่ากัน ผลลัพธ์ของกลูออนแสดงให้เห็นการลดลงที่บริเวณอินฟราเรด ทั้งมิติ $D = 2 + 1$ และ $D = 3 + 1$ ซึ่งไม่ขัดกับผลเชิงวิเคราะห์ก่อนหน้านี้ ผลลัพธ์ของตัวรูปสี่ได้แสดงถึงความสูงไม่มีที่สิ้นสุดที่บริเวณอินฟราเรด ซึ่งไม่ขัดกันกับผลวิเคราะห์ของกลุ่มวิจัยอื่นเช่นกัน เรายังได้จำลองตัวแผ่กระจายกลูออน และตัวรูปสี่ที่อุณหภูมิจำกัด ซึ่งรวมในช่วงเฟสของการกักกันและไม่กักกันไว้ แต่ศักย์คูลอมป์ เราได้รับผลลัพธ์ที่ไม่ปกติที่อุณหภูมิศูนย์ เราจึงไม่กล้าที่จะทำการจำลองต่อไปที่อุณหภูมิจำกัด

สาขาวิชาฟิสิกส์
ปีการศึกษา 2552

ลายมือชื่อนักศึกษา _____
ลายมือชื่ออาจารย์ที่ปรึกษา _____
ลายมือชื่ออาจารย์ที่ปรึกษาร่วม _____

SONGVUDHI CHIMCHINDA : $SU(2)$ LATTICE GAUGE THEORY IN
COULOMB GAUGE AT ZERO AND FINITE TEMPERATURE.

THESIS ADVISOR : PROF. YUPENG YAN, Ph.D. 101 PP.

LATTICE / GAUGE / COULOMB / QCD / YANG-MILLS THEORY

We study the feature of confinement in quantum chromodynamics in the non-perturbative method of lattice simulations of the $SU(2)$ Yang-Mills theory in Coulomb gauge which allows one to extract three objects: gluon propagator, ghost form factor, and Coulomb potential which are related to the confinement of quarks and gluon. We consider the quantization of Yang-Mills in Coulomb gauge and its confinement scenario as pointed out by Gribov. The lattice methods are reviewed for implementing the simulations. Observables are measured from the best gauge copies for avoiding the Gribov gauge copies. Our gauge fixing is improved by making more choices of gauge orbit by using the antiperiodic of lattice.

We report the results of gluon propagator and ghost form factor at zero and finite temperature. All the observables are measured at equal-time slice of lattice. Our result of gluon propagator shows the glowing down at IR regime for both dimensions $D = 2 + 1$ and $D = 3 + 1$, which is consistent with previous analytic results. The result of ghost form factors has shown the divergence at IR regime, which is again consistent with analytic works of the other research group. We have also simulated both gluon propagator and ghost form factor at finite temperature which includes the range of confinement and de-confinement phase. But for the Coulomb potential we have obtained a peculiar result at zero temperature, which makes us hesitate to do further simulation at finite temperature.

School of Physics

Academic Year 2009

Student's Signature _____

Advisor's Signature _____

Co-Advisor's Signature _____

ACKNOWLEDGEMENTS

I am grateful to Prof. Dr. H. Reinhardt, Prof. Dr. M. Quandt and Dr. G. Burgio at Institut für Theoretische Physik, Universität Tübingen, Germany for training me the lattice computation, and to Prof. Dr. Y. Yan and Asst. Prof. Dr. C. Kobdaj at Suranaree University of Technology, Thailand, for encouraging me to study in Germany. The simulations have been done with facilities at Tübingen, the PTWAP cluster of computers, and the SUT-HPCC (Suranaree University of Technology - High Performance Computing Cluster), especially, Asst Prof. Dr. Eckart Schulz who have developed the grid computing at SUT.

This work has been supported by the German Academic Exchange Service (DAAD) scholarship during October, 2005 to September, 2006, the Commission on Higher Education's scholarship of Thailand during October, 2006 to September, 2007, the scholarship from Fakultät für Mathematik und Physik, Universität Tübingen and the Nuclear and Particle Physics Group at SUT with managing by Asst. Prof. Dr. Chinorat Kobdaj, SUT during October, 2007 - March, 2008.

I would like to thank my parents, my friends, and my colleagues especially Dr. Chakrit Nualchimplee and Dr. Ayut Limphirat for their encouragement over the period of my writing thesis.

Songvudhi Chimchinda

CONTENTS

	Page
ABSTRACT IN THAI	I
ABSTRACT IN ENGLISH	II
ACKNOWLEDGEMENTS	III
CONTENTS	IV
LIST OF TABLES	VIII
LIST OF FIGURES	IX
CHAPTER	
I INTRODUCTION	1
II YANG-MILLS THEORY IN COULOMB GAUGE	6
2.1 Path integral	6
2.1.1 Feynman path integral	6
2.1.2 Euclidean path integral	8
2.1.3 Partition function	8
2.2 Introductory Yang-Mills theory	9
2.3 Quantization of Yang-Mills theory	12
2.4 Gribov copies	14
2.5 Gribov's confinement of color charge	16
III LATTICE METHOD ON COULOMB GAUGE	18
3.1 Lattice forming into gauge field theory	18
3.2 Monte Carlo method	20
3.2.1 Heatbath algorithm	22
3.3 Observable as averaging from partition function	27
3.4 Coulomb gauge fixing	28

CONTENTS (Continued)

	Page
3.4.1 Iterated overrelaxation	29
3.5 Gribov's copy effect on Coulomb gauge	30
3.5.1 Finding best gauge copy	31
3.5.2 Flip Trick	31
3.6 Renormalization	32
3.7 Observables	32
3.7.1 Gluon propagator	33
3.7.2 Ghost form factor	33
3.7.3 Coulomb form factor	34
3.8 Set up at finite temperature	34
IV LATTICE RESULTS	36
4.1 Gibov gauge copies effect	36
4.2 Gluon propagator	36
4.2.1 Result: at zero temperature	36
4.2.2 Result: at finite temperature	38
4.3 Ghost form factor	39
4.3.1 Result: curve fitting at IR and UV region	39
4.3.2 Result: curve fitting for all range	43
4.4 Coulomb potential	45
V SUMMARY	49
APPENDICES	
APPENDIX A LIST OF NOTATION	57
APPENDIX B GLOSSARY	59
APPENDIX C LIE GROUP BACKGROUND	62

CONTENTS (Continued)

	Page
C.1 $SU(N)$ algebra	62
C.2 Lagrangian	63
APPENDIX D FLOWCHART OF PROGRAM	64
D.1 For gluon propagator measurement	64
D.2 For ghost form factor measurement	65
D.3 For Coulomb potential measurement	66
APPENDIX E LATTICE CONVENTIONS	67
E.1 convention and notation	67
E.2 Covariant derivative - Gauge potential	67
E.3 Lattice notation	68
E.4 Lattice gauge potential	70
E.5 Lattice gauge-covariant derivative	70
E.6 Lattice gauge fixing	71
E.7 Gluon propagator	72
E.8 Faddeev-Popov operator	72
E.9 Coulomb potential	77
APPENDIX F LATTICE ALGORITHM	80
F.1 Heatbath algorithm : pseudocode	80
F.2 Relaxation	81
F.2.1 Overrelaxation	82
F.2.2 Flip trick	83
F.3 Conjugate gradient method	83
F.4 Preconditioned conjugate gradient method	85
APPENDIX G PUBLICATION PAPER	87

CONTENTS (Continued)

	Page
CURRICULUM VITAE	101

LIST OF TABLES

Table		Page
4.1	Parameters from curve fitting of the ghost form factor for UV region at zero temperature.	43
4.2	Parameters from curve fitting of the ghost form factor for IR region at zero temperature.	43
4.3	Parameters from curve fitting of the ghost form factor for all range at zero temperature.	43
4.4	Parameters from curve fitting of ghost form factor for all range at finite temperature.	45

LIST OF FIGURES

Figure		Page
2.1	The gauge field space by considering its gauge functional values is divided in region C_n according to the number of n negative eigenvalue of the Faddeev-Popov operator.	15
3.1	Each lattice site x has its links associating neighbour direction. . .	19
3.2	The link variables $U_\mu(n)$ connecting n and $n + \hat{\mu}$ and $U_{-\mu}(n)$ connecting n and $n - \hat{\mu}$	19
3.3	The four link variables perform the plaquette $U_{\mu\nu}(n)$. The circle specifies the order that the link are multiplied in the product. . . .	21
3.4	For each link $U_\mu(x)$, there are other nearest-neighbour link variables which have contribution to sampling.	24
4.1	Gribov copies influence to gluon propagator at minimum momentum, p_{\min} , for lattice 24^4 at $\beta = 2.2$	37
4.2	The suppression of Ghost propagator at lowest momentum.	38
4.3	Gluon propagator in 2+1 dimensions at zero temperature	39
4.4	Gluon propagator in 3+1 dimensions at zero temperature.	40
4.5	The gluon propagator at finite temperature.	41
4.6	The gluon propagator at finite temperature after renormalizing data at high energy.	41
4.7	Ghost form factor at zero temperature, measured from best gauge copy of lattice 24^4	42
4.8	Ghost form factor at zero temperature, measured from best gauge copy of lattice 24^4	44

LIST OF FIGURES (Continued)

Figure		Page
4.9	Ghost form factor at finite temperature, measured from the best gauge copy lattice $24^4, 32^4, 36^4$	46
4.10	The dimensionless $p^2V(p)$ measured from lattice 36^4	47
4.11	$p^4V_{\text{Coul}}(p)$ in unit of the string tension σ , the result of our project, lattice 16^4	47
4.12	$p^4V_{\text{Coul}}(p)$ in unit of the string tension σ , extracted from (Langfeld and Moyaert, 2004).	48

CHAPTER I

INTRODUCTION

Quantum field theory (QFT) is the theory combining quantum mechanics and special relativity. Its role is to explain any phenomena in particle physics. In QFT we describe the state of a system by the so-called *field* associated with any interaction. The field plays its role as an operator acting on the vacuum state for creating some quantum state in a point of space-time. Quantum chromodynamics (QCD) is a branch of QFT, which describes the strong interaction of particle, e.g. the confinement of quark and gluon in nucleon.

The foundation of field theory has begun since Maxwell combined the electricity and magnetism into one picture. The classical electrodynamics gives the idea of *gauge invariance* which means any new magnetic vector potential can be redefined without any change to electromagnetic laws. The idea was also adopted to quantum electrodynamics (QED), one branch of QFT, by considering the gauge invariance of the $U(1)$ unitary transformation. In a similar way, Yang and Mills adopted the idea of gauge invariance to the non-Abelian gauge transformation $SU(N)$ and constructed the famous Yang-Mills field, which is the corner stone of the electroweak interaction and Quantum Chromodynamics (QCD).

Quantum Chromodynamics is believed the right theory describing the interactions of the quarks and gluons which make up hadrons. Its main point is that each quark flavor has three additional quark numbers, the so-called color and that the strong interaction is invariant under the color $SU(3)$ transformation. Associated with the eight generators of $SU(3)$ group, eight vector fields must be introduced to make the QCD Lagrangian invariant under the $SU(3)$ local gauge transformation.

The eight vector fields are now called gluons. The $SU(3)$ gauge invariant QCD Lagrangian takes the form

$$\mathcal{L}_{\text{QCD}} = \bar{\psi}_r^i (i\gamma^\mu D_\mu^{ij} - m_i^r \delta_{ij}^{rs}) \psi_s^j - \frac{1}{4} G_{\mu\nu}^\alpha G_\alpha^{\mu\nu} \quad (1.1)$$

with

$$D_\mu^{ij} = \delta_{ij} \partial_\mu - ig T_{ij}^\alpha \gamma^\mu G_\mu^\alpha \quad (1.2)$$

$$G_{\mu\nu}^a = \partial_\mu G_\nu^a - \partial_\nu G_\mu^a - gf^{abc} G_\mu^b G_\nu^c \quad (1.3)$$

where $\psi_i(x)$ ($i = 1, 2, 3$) are quark fields in the fundamental representation of $SU(3)$ group, $G_\mu^\alpha(x)$ ($\alpha = 1, 2, \dots, 8$) are gluon fields in the adjoint representation of $SU(3)$ group, and T^α the generators of $SU(3)$ group, connecting the fundamental, antifundamental and adjoint representations. The QCD Lagrangian is invariant under the $SU(3)$ local gauge transformation:

$$\psi(x) \Rightarrow U(x)\psi(x) \quad (1.4)$$

$$G_\mu^\alpha(x) T^\alpha \Rightarrow U(x) G_\mu^\alpha(x) T^\alpha U^{-1}(x) + \frac{1}{g} U(x) \partial_\mu U^{-1}(x) \quad (1.5)$$

where

$$U(x) = e^{-i\theta^\alpha(x) T^\alpha} \quad (1.6)$$

Note that the interaction described by Eq. (1.1) is flavor blind.

The effective coupling constants of gauge theories may be derived from perturbative calculation,

$$g^2(Q^2) = \frac{g^2(Q_0^2)}{1 + \frac{11C_2(G) - 4T(R)N_f}{48\pi^2} g^2(Q_0^2) \ln \frac{Q^2}{Q_0^2}} \quad (1.7)$$

with

$$\sum_{\alpha, \beta} f^{\alpha\beta\gamma} f^{\alpha\beta\delta} = C_2(G) \delta_{\gamma\delta}, \quad \text{Tr}(T^\alpha \cdot T^\beta) = T(R) \delta_{\alpha\beta} \quad (1.8)$$

where the $T(R)$ term stems from the interaction between the quark and gauge field (gluon) while the $C_2(G)$ term is a result of the self-interaction among gluons. For QCD $G_2(G) = 3$ and $T(R) = \frac{1}{2}$, one gets

$$g^2(Q^2) = \frac{g^2(Q_0^2)}{1 + \frac{33-2N_f}{48\pi^2} g^2(Q_0^2) \ln \frac{Q^2}{Q_0^2}} \quad (1.9)$$

From the above equation one derive $g^2(Q^2) = 0$ when $Q^2 \rightarrow \infty$ and $N_f \leq 16$. This is the so-called asymptotic freedom of the strong interaction, that is, for very high energy reactions quarks and gluons interact very weakly. the *asymptotic* freedom was first predicted in the early 1970s and confirmed later by a number of experiments and awarded the 2004 Nobel Prize in Physics. After confirmation of the *asymptotic* freedom, QCD has been believed as the correct theory for the strong interaction.

The asymptotic freedom of the strong interaction is only one face of QCD. There is another peculiar property, the confinement, that is, quarks and gluons are confined to form hadrons. Although analytically unproven, confinement is widely believed to be true because no free quark has been observed up to now. Considering the great success of QCD for hard processes, it has been dreamed for long that QCD should lead to structures and properties of hadrons; hadron interactions, especially the nuclear force; and the understanding of quark masses.

Since no free quark has been observed so far in nature as separate entities, the confinement of quarks or color confinement has been investigated since beginning by finding its cause from the first principle, the QCD Lagrangian. The investigation of the color confinement is still one of the millennium problems at present. It is found, however, that analytic or perturbative solutions in QCD at low energies are hard or impossible due to the highly nonlinear nature of the strong force. Among the non-perturbative methods for numerical simulations of QCD, the lattice gauge theory is a successful tool, because it simulates QCD on the lattice of discretized space-time, and any coupling constants can be varied for covering all range of non-perturbative effects. The lattice approach was used to explore the confinement mechanisms by

generating the field configuration, and implementing some gauge fixing into the lattice. Then the lattice were measured some certain observables responsible for confining properties of QCD in the considered gauge. In particular, there are two previous confinement mechanisms which can be simulated by lattice framework. The first confinement mechanism has basic idea that a pair quark-antiquark can produce the chromoelectric field being tuned up by dual Meissner effect into Abrikosov flux tubes in the same way as the magnetic field is confined in the superconductor of type II (Di Giacomo, 1988), by borrowing the idea of monopole as the end point of a magnetic flux tube which proposed by Dirac. This confinement mechanism is to consider the condensation of chromomagnetic monopoles in the vacuum in which the monopole behaves likes a dual superconductor which means that the roles of electric and magnetic quantities is interchanged by comparing to ordinary superconductors (Di Giacomo et al., 2000a; Di Giacomo et al., 2000b). However, on the lattice gauge theory, there is the reason for confinement in topological objects, such as instantons, monopole and vortices. The latter object was first suggested by t'Hooft ('t Hooft, 1981). Another mechanism was introduced by considering that confinement arises from the percolation of center vortices in the vacuum. Since it is explained that there exists a phase transition from the confinement phase to a deconfinement phase or the quark-gluon plasma which corresponds to a percolation-depercolation phase transition of center vortices (Greensite, 2003).

In the standard QCD, the symmetry group is $SU(3)$ which deals with the transformation among three colors. In our work we will use $SU(2)$ in stead of $SU(3)$ as the symmetry group, dealing with two color symmetry. It has been found that the properties of the $SU(2)$ and $SU(3)$ QCD are equivalent at low-energy (Cucchieri and Mendes, 2007). And one clear advantage of considering $SU(2)$ is that the numerical burden will be largely reduced. And furthermore we study on the pure gluon part, which called Yang-Mills part of QCD action.

The study of Green functions (Gluon propagator or correlation function) in Coulomb gauge provides the potential of two static coloured charges, which is a confinement scenario in Coulomb gauge proposed by Gibov (Gribov, 1978). Gribov pointed out that there exist many configurations of $SU(N)$ satisfying the Coulomb gauge condition, which is called “gauge copies” or *Gribov* copies. Nowadays only few information (Cucchieri and Zwanziger, 2001a; Langfeld and Moyaert, 2004; Voigt et al., 2008; Quandt et al., 2007) is known. This thesis is to study the $SU(2)$ Yang-Mills theory at zero and finite temperature by lattice gauge simulation.

The thesis is arranged as follows: Chapter II is devoted to the Yang-Mills theory on Coulomb gauge, describing its quantization which is related to the confinement problem. Chapter III is about lattice method, consisting of gauge fixing and measurement of any observable. Chapter IV gives the results of our simulation, and finally in the last chapter we summary our results and outlook for the future research we hope to do.

CHAPTER II

YANG-MILLS THEORY IN COULOMB GAUGE

This chapter is devoted to review Yang-Mills theory in the Coulomb gauge and its relation to the problem of color confinement. We will begin by briefly mention about path integral and Yang-Mills theory. Then we will explain how to quantize Yang-Mills theory in Coulomb gauge which relates to the problem of quark confinement.

2.1 Path integral

In analytical calculation of quantum field theory, the functional integral formalism is the powerful tool to be used. To make the numerical simulation which is corresponding to the functional integral formalism, we can construct from the Feynman path integral. We review Feynman path integral as the beginning to any creation of computational task.

2.1.1 Feynman path integral

In quantum mechanics, we calculate the probability amplitude for a particle moving from point y to point x during the time interval t is

$$\langle x|e^{-iHt}|y\rangle \tag{2.1}$$

where $|y\rangle$ denotes an eigenstate of the position operator, H is the Hamiltonian, and we let $\hbar = 1$. In general case, if the particle moves in a potential $V(\mathbf{x})$,

$$H = H_0 + V(\mathbf{x}), \tag{2.2}$$

where $H_0 \equiv \mathbf{p}^2/2m$. In order to calculating the probability amplitude $\langle x|e^{-iHt}|y\rangle$, we can divide the time interval t into small time interval

$$\epsilon = \frac{t}{N}, \quad (2.3)$$

and insert $N - 1$ complete sets of position eigenstates:

$$\langle x|e^{-iHt}|y\rangle = \lim_{N \rightarrow \infty} \int dx_1 \cdots dx_{N-1} \langle x|W_\epsilon|x_1\rangle \cdots \langle x_{N-1}|W_\epsilon|y\rangle \quad (2.4)$$

where

$$W_\epsilon = \exp\left(-iV\frac{\epsilon}{2}\right) \exp\left(-iH_0\epsilon\right) \exp\left(-iV\frac{\epsilon}{2}\right). \quad (2.5)$$

Then Eq. (2.4) becomes

$$\begin{aligned} \langle x|e^{-iHt}|y\rangle &= \lim_{N \rightarrow \infty} \left(\frac{m}{2\pi i\epsilon}\right)^{N/2} \int dx_1 \cdots dx_{N-1} \\ &\quad \exp\left\{i\frac{m}{2\epsilon}[(x-x_1)^2 + \dots + (x_{N-1}-y)^2] \right. \\ &\quad \left. - i\epsilon\left[\frac{1}{2}V(x) + V(x_1) + \dots + V(x_{N-1}) + \frac{1}{2}V(y)\right]\right\}. \end{aligned} \quad (2.6)$$

The term in exponent is called as iS_ϵ . The classical action S of a particle moving from y to x along to the trajectory $x(t)$ is

$$S = \int_0^t dt \left[\frac{m}{2}\dot{x}^2 - V(x)\right] = S_\epsilon + \mathcal{O}(\epsilon^2) \quad (2.7)$$

Then we can write the probability amplitude as

$$\langle x|e^{-iHt}|y\rangle = \int Dx e^{iS}, \quad (2.8)$$

where Dx is abbreviated from

$$Dx = \lim_{N \rightarrow \infty} \left(\frac{m}{2\pi i\epsilon}\right)^{N/2} dx_1 \cdots dx_{N-1}. \quad (2.9)$$

Eq. (2.8) is the quantum mechanical amplitude averaging over all classical paths which being weighted by the exponential of i multiplying by the classical action. By using the infinite dimensional integral, the quantum operator have been eliminated. This is called the *path integral* or *functional integral* method.

2.1.2 Euclidean path integral

We can change the real time t to be the imaginary time by

$$t = -i\tau, \quad \text{where } \tau > 0. \quad (2.10)$$

Then the probability amplitude Eq. (2.8) becomes

$$\langle x|e^{-H\tau}|y\rangle = \int Dx e^{-S_E}, \quad (2.11)$$

where S_E denote the *Euclidean* action which is defined by

$$S_E = \int_0^\tau d\tau \left[\frac{m}{2} \dot{x}^2 + V(x) \right]. \quad (2.12)$$

The usual action S is related to the Euclidean action S_E by

$$S = iS_E. \quad (2.13)$$

The change of working on the real time t to the imaginary time τ is equivalent to change from Minkowsky space into Euclidean space. We call this process, the *wick rotation*. The benefit of using Euclidean action is to allow to deal with quantum field both in theoretical calculation and computational work of any simulations.

2.1.3 Partition function

After knowing the Feynman path integral, we adopt the advantage of the connection between quantum statistical mechanics and quantum field theory. This can be accomplished by observing that there is analogy between the quantum field in Euclidean formalism and quantum statistical mechanics in the canonical ensemble, but in D dimensional space-time.

The fundamental quantity which expresses the probability distribution of each state of configuration in quantum statistical mechanics is the partition function:

$$\begin{aligned} Z[\beta] &= \text{Tr}[\exp\{-\beta H\}] \\ &= \text{Tr}[\exp\{\langle n| \{-\beta H\} |n\rangle\}], \end{aligned} \quad (2.14)$$

where H is a Hermitian operator representing the Hamiltonian of the whole ensemble. And we can set $\beta = 1/(k_B T)$, where T is temperature and k_B is Boltzmann's constant. The states, $|n\rangle$, is the set of complete and orthonormal basis and the summation is taken from all possible states. The expectation value of an operator \hat{O} is calculated from

$$\langle \hat{O} \rangle = \frac{1}{Z} \text{Tr}[\hat{O} \exp\{\langle n | \{-\beta H\} | n \rangle\}]. \quad (2.15)$$

In our framework, we deal with the gauge transformation, $U_\mu(x)$, which transforms the quark fields by $\Psi(x) \rightarrow U_\mu \Psi(x)$.

Therefore, our partition functions and expectation value must be evaluated from averaging over transformation $U_\mu(x)$:

$$Z = \int dU \exp\{-\beta S_{SU(N)}\} \quad (2.16)$$

and

$$\langle \hat{O} \rangle = \frac{1}{Z} \int dU O[U] \exp\{-\beta S_{SU(N)}\}. \quad (2.17)$$

2.2 Introductory Yang-Mills theory

There are two kinds of symmetry which are *global symmetries*, where the law of physics does not change, whether the field we consider is rotated in internal space or not, and *local symmetries*, where for each point in space-time is able to be rotated independently, even in intrinsic (or internal) space. When our field has local symmetries properties, we refer it has *gauge symmetries*.

It has been established that the strong interactions appear in nucleon is invariant under isospin transformation which is a local symmetry. In 1954 (Yang and Mills, 1954) Yang-Mills proposed that the concept of global phase invariance should be consistent with the principle of local field theory. They regarded the strong interactions, the proton and neutron could be composed to a 2-component field $\begin{pmatrix} p \\ n \end{pmatrix}$, which is the isospinor. It means the proton and neutron are considered

as the same particle and differ by projection of isospin. For the quarks which are constituents of the hadron. We can represent the quark field by the 3-vector in color space

$$\Psi = \begin{pmatrix} \Psi_{\text{red}} \\ \Psi_{\text{blue}} \\ \Psi_{\text{green}} \end{pmatrix}, \quad (2.18)$$

where each component is a 4-component spinor.

In nuclear physics, we consider that the isospin is a conserved quantum number as the spin is. This implies that the nucleon system should be invariant under global isospin transformation, and the law of physics should be independent of rotation with intrinsic (internal) space. For the strong interaction, we believe that it have color symmetry. That is, the internal rotation is performed within 3-dimensional color space of the quark field

$$\Psi(x) \rightarrow \Omega\Psi(x), \quad \text{with } \Omega \in SU(3) \quad (2.19)$$

with no change appears in the law of physics which we call gauge invariant. The conserving of $\Psi^\dagger\Psi = \Psi^\dagger\Omega^\dagger\Omega\Psi$ requires Ω must be a three-dimensional unitary matrix which is an element of $SU(3)$ group.

The color symmetry is one kind of internal symmetry, which is also the local symmetry (independent of each point of space-time). Therefore, the quarks which appear at different space-time should not correlated and we can perform the color rotations at each space-time points:

$$\Psi(x) \rightarrow \Omega\Psi(x). \quad (2.20)$$

We can introduce the *gauge field* for ensuring the gauge invariant under gauge transformation. In addition, it allows us to include the kinetic energy of quark or matter interaction.

We can write the Lagrange density of the quarks (one kind of fermions) as

$$\mathcal{L}_0 = \bar{\Psi}(x)(i\cancel{\partial} + g_0\cancel{A} - m)\Psi(x), \quad \text{where } \cancel{A} = \gamma^\mu A_\mu \quad (2.21)$$

and with introducing the gauge potential A_μ , the Lagrange density transforms as the following transformation

$$A_\mu \rightarrow A_\mu^\Omega = \Omega A_\mu \Omega^\dagger + \frac{i}{g_0} \Omega \partial_\mu \Omega^\dagger. \quad (2.22)$$

The symmetry group usually relate to the gauge symmetry. We can map each point x of space-time, R^4 into a gauge group G :

$$x \in R^4 \rightarrow \Omega(x) \in G. \quad (2.23)$$

The gauge group can be $SU(N)$ which has an element by

$$\Omega = e^{i\Lambda^a t^a}, \quad (2.24)$$

where t^a denotes the hermitian generators, (see Appendix E) and $\Lambda^a(x)$ is the numbers depending on space-time. Therefore, Ω is the gauge transformation which allowing the gauge potential can have the adjoint representation:

$$A_\mu(x) = A_\mu^a(x) t^a. \quad (2.25)$$

We can also define the covariant derivative by

$$D_\mu = \partial_\mu - ig_0 A_\mu^a t^a, \quad (2.26)$$

and define the field strength tensor by

$$\begin{aligned} -ig_0 F_{\mu\nu} &= [D_\mu, D_\nu] \\ &= -ig_0 (\partial_\mu A_\nu - \partial_\nu A_\mu - ig_0 [A_\mu, A_\nu]). \end{aligned} \quad (2.27)$$

Since the gauge potential is represented as matrix, therefore it is obvious that

$$[A_\mu, A_\nu] \neq 0. \quad (2.28)$$

In general, the field strength is quadratic in the term of gauge potential

$$F_{\mu\nu}^\alpha = \partial_\mu A_\nu^\alpha - \partial_\nu A_\mu^\alpha - g_0 \epsilon^{\alpha\beta\gamma} A_\mu^\beta A_\nu^\gamma. \quad (2.29)$$

This is the field strength in non-Abelian gauge theory which leads to different physical consequence as QED has in Abelian gauge theory, that is the confinement of quarks.

The classical $SU(2)$ Yang-Mills theory is defined by the Lagrangian density

$$\mathcal{L} = -\frac{1}{4}F_{\mu\nu}^\alpha F_\alpha^{\mu\nu}, \quad (2.30)$$

where α is the internal-symmetry index running from 1 to 3, and $F_{\mu\nu}^\alpha$ is defined in terms of its gauge potentials.

2.3 Quantization of Yang-Mills theory

We start from the Lagrangian density of a non-Abelian gauge theory of gauge group $SU(N)$:

$$\mathcal{L} = -\frac{1}{4}F_{\mu\nu}^a F_a^{\mu\nu} - ig_0 A_\mu^a J_a^\mu, \quad (2.31)$$

where A_μ^a are the gauge field, $F_{\mu\nu}^a$ is the strength tensor, J_a^μ is the external source, and g_0 is the bare coupling constant.

The canonical conjugated momentum are given by

$$\Pi_a^0 = 0, \quad (2.32)$$

$$\Pi_a^i = F_a^{i0}. \quad (2.33)$$

This is the primary constraints of Lagrangian Eq. (2.31), and the next constraint we consider is the Coulomb gauge condition, $\vec{\nabla} \cdot \vec{A} = 0$, which is

$$\partial_i A_a^i = 0. \quad (2.34)$$

By using the Faddeev-Popov method of using part integral for making the partition function Z finite, the Euclidean partition functions of non-Abelian gauge field (Yang-Mills fields) in Coulomb gauge is

$$Z[J] = \int DA \exp \left\{ \int \mathcal{L} d^4x \right\} \delta(\partial_i A_a^i) \text{Det}[-\nabla \cdot \mathbf{D}] \quad (2.35)$$

where $\text{Det}[-\nabla \cdot \mathbf{D}]$ is the Faddeev-Popov determinant (\mathbf{D} is the covariant derivative), and Eq. (2.35) is used for performing the simulation of our work. There is the relation between the functional integral formulation and the Hamiltonian formulation of Coulomb gauge Yang-Mills theory developed by (Cucchieri and Zwanziger, 2001b), by which the partition is expressed as

$$Z[J] = \int DA_{\perp} D\Pi_{\perp} \exp \left\{ \int d^4x (i\Pi_{\perp,i}^a \dot{A}^{i,a} - \mathcal{H}_{\perp}) \right\}, \quad (2.36)$$

where the Hamiltonian density \mathcal{H}_{\perp} is derived from the Coulomb gauge Hamiltonian $H = \int d^3x \mathcal{H}_{\perp}$, which is result of elimination of longitudinal degrees of freedom. Here H is

$$H = \int d^3x \left[\frac{1}{2} (\Pi_{\perp}^2 + B^2) + g_0 \mathbf{A} \cdot \mathbf{J} \right] - \frac{1}{2C_2} \int d^3x d^3y \rho(t, \mathbf{x}) V_{\text{Coul}}(\mathbf{x}, \mathbf{y}) \rho(t, \mathbf{y}), \quad (2.37)$$

where C_2 is the Casimir of the gauge group $SU(N)$, in our case for $SU(2)$, $C_2 = 3/4$. The ρ is the new quantity we have introduced it as the color charge density at $x = (t, \mathbf{x})$

$$\rho(x) = f^{abc} A_i^b(x) \Pi_{\perp,i}^c(x) + J_0(x). \quad (2.38)$$

The quantity V_{Coul} is the Coulomb potential which is measured from averaging over the gauge field by

$$V_{\text{Coul}}(\mathbf{x}, \mathbf{y}) = -C_2 g_0^2 M^{-1} (-\nabla) M^{-1} \Big|_{(\mathbf{x}, \mathbf{y})}, \quad (2.39)$$

where

$$M = -\nabla \cdot \mathbf{D} \quad (2.40)$$

is the Faddeev-Popov operator.

It was shown that the Coulomb potential is not equal to the Wilson potential V_{W} (Zwanziger, 2003; Zwanziger, 1998) which is used to be an order parameter for confinement. For the large spatial distance r , the Coulomb potential is an upper

bound of the rise of the Wilson potential:

$$V_W(r) \leq -\frac{4}{3}V_{\text{Coul}}(r). \quad (2.41)$$

That is, the confinement comes with Coulomb confinement, and the Coulomb string tension is the upper limit of the Wilson string tension:

$$\sigma_W \leq -\frac{4}{3}\sigma_{\text{Coul}}. \quad (2.42)$$

2.4 Gribov copies

Consider the Coulomb gauge condition, Eq. (2.34). For a given gauge potential \mathbf{A} which satisfied the condition of transversality, $\nabla \cdot \mathbf{A} = 0$, we observe that there should be many gauge field \mathbf{A} which transformed along gauge orbit as

$$\mathbf{A}^g = g\mathbf{A}g^{-1} - \frac{i}{g_0}(\nabla g)g^{-1} \quad (2.43)$$

which satisfying the Coulomb gauge,

$$\nabla \cdot \mathbf{A}^g = 0. \quad (2.44)$$

This condition may be seem as only helping us to reduce the redundant degree of freedom of gauge field theory, but Gribov (Gribov, 1978) pointed out that the equation does allow to have the non-trivial solution of g in the case non-Abelian theories, and consequently, the quantization of Yang-Mills theory is destroyed by the presence of the gauge copies, which we called them as *Gribov copies*.

Considering the gauge transformation of the gauge potential in Eq. (2.43) by $g = \exp(ig_0\omega_a T^a)$. By keeping only the first term of ω , we obtain (see. Appendix E.2) $\mathbf{A}^g = \mathbf{A} + D\omega$ and replace \mathbf{A}^g in Eq. (2.44), we have the Faddeev-Popov operator as

$$\begin{aligned} \nabla \cdot \mathbf{D}\omega^a &= 0 \\ \nabla \cdot (\nabla - g_0 f^{abc} A^b)\omega^a &= 0 \\ -\Delta\omega^a - g_0 f^{abc} \mathbf{A}^b \cdot \nabla\omega^c &= \epsilon[\mathbf{A}]\omega^a \end{aligned} \quad (2.45)$$

where $\epsilon[\mathbf{A}]$ is zero eigenvalue. When potential \mathbf{A} is small, Eq. (2.45) can be solved for positive ϵ and obtain the trivial solution $\omega = 0$. This domain of gauge field is free of gauge copies. For some significance magnitude of \mathbf{A} which let the lowest eigenvalue of the Faddeev-Popov vanishes, this domain of gauge field will give the non-trivial solution of Eq. (2.45). When the magnitude of \mathbf{A} increases, we will have the negative ϵ solution. For another value of magnitude \mathbf{A} , we will meet another $\epsilon = 0$ solution appears as the second bound state, and so on. The space of gauge field by considering from the gauge functional can be divided into regions C_n with respect to the number n of the negative eigenvalue of the Faddeev-Popov operator as shown in Fig. 2.1.

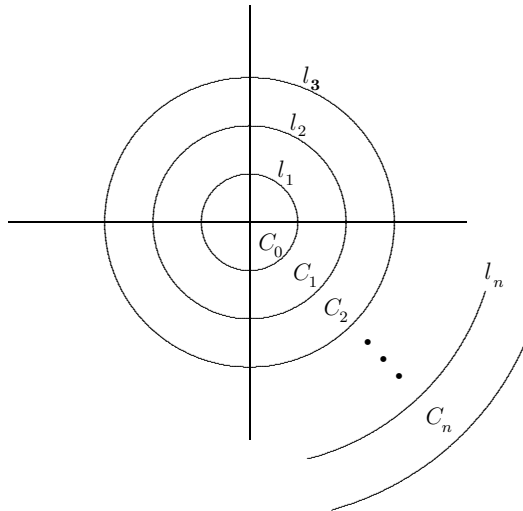


Figure 2.1 The gauge field space by considering its gauge functional values is divided in region C_n according to the number of n negative eigenvalue of the Faddeev-Popov operator.

Gribov pointed out that in a second gauge configurations which is the neighbourhood of the boundary of C_0 . Then we can write the field as

$$A_\mu = C_\mu + a_\mu, \quad (2.46)$$

where C_μ lies on l_1 , and a_μ is small compared to C_μ . Therefore, there must exist ϕ_0

decreasing at infinity and satisfying the equation

$$\partial_\mu[\nabla(C), \phi_0] = 0, \quad (2.47)$$

or

$$\mathbf{a}^g = \mathbf{a} + \mathbf{D}[\mathbf{C}]\phi_0. \quad (2.48)$$

The ϕ_0 is a zero-mode of the Faddeev-Popov operator, and providing that if one of \mathbf{A} or \mathbf{A}^g lies in C_0 then another one lies in C_1 . Therefore, it is possible to found

$$\epsilon[\mathbf{A}] = -\epsilon[\mathbf{A}^g] \quad (2.49)$$

which implies that there exists a bound state for one of the fields but not for another one. Any gauge transformation will bright the field from C_1 into C_0 , and the other transformations from C_0 into C_2, C_3, \dots can be possible. Therefore, any field which is not in C_0 can be transformed from the field in C_0 . Gribov considered that if we want to get rid of this gauge ambiguities, we must restrict the functional integrations in the region C_0 which we call now, the *Gribov region*, and the lowest eigenvalue of the Faddeev-Popov operator vanishes is called, the *first Gribov horizon*.

2.5 Gribov's confinement of color charge

For Coulomb gauge, Gribov proposed to restrict only the physical configurations space for the region $\Omega_t = \{A | (\partial_i A_i)^a(t, \vec{x}) = 0 \wedge M^{ab}(x, y)|_t \geq 0\}$ which now we call *Gribov region*. By the lattice method, we can simulate the thermalized lattice configuration $\{U_{\mu(x)}\}$ belonging to the region Ω_t by minimizing the functional $F_t^g[g(t, x)]$ into a local minimum.

The additional gauge condition proposed by Gribov is not important for the perturbative regime, but it is important in IR (infrared) region, (Gribov, 1978). Gribov has shown that when the functional integral is restricted to the region Ω_t , at each time slice, the ghost propagator $G(t, \vec{p})$ is enhanced in IR region. And

the transverse gluon propagator $D(t, \vec{p})$ go to zero in the IR region. The latter implies the violation of reflection positivity* which indicates the confinement of gluon (Alkofer and Smekal, 2001).

*Reflection positivity is the principle for ensuring that the Euclidean correlation functions can be back to Minkowski space.

CHAPTER III

LATTICE METHOD ON COULOMB GAUGE

In this chapter, we describe our numerical procedure of simulation by starting from forming the lattice into gauge field theory, then we will show how to simulate it by Monte Carlo method. Later we explain how to implement Coulomb gauge fixing on lattice. And by facing with the Gribov copy effect, we use flip trick and choosing the best gauge copy for measurement. This procedures allow us to study the three objects featuring the confinement of quark-antiquark in Coulomb gauge scenario.

3.1 Lattice forming into gauge field theory

We can discretize the space-time into lattice as D -dimensional lattice with lattice spacing a . The lattice site is assigned to have the integer parameter N_0, N_1, N_2, N_3 and the lattice volume is the dimensionless number $V = N_0 \times N_1 \times \dots \times N_3$.

In gauge field theory, the gauge potential A_μ in continuum is the connection in the space-times by gauge group. Suppose $\psi(x)$ is a field at a space-time x , another different field in its space-time $x + dx$ can be expressed as

$$\psi(x + dx) = U(x)\psi(x) \tag{3.1}$$

where $U(x)$ defined by

$$U(x) = e^{iA_\mu(x)dx^\mu}. \tag{3.2}$$

The matrix $U(x)$ is an element of the gauge group G which specifies the internal rotation with internal degree of freedom. The $U(x)$ has its role as transport between

the nearest-neighbour space-time point x and $x + dx$. The matrix $A_\mu(x)$ belongs to the Lie algebra associated to G . We can see that the potentials A_μ hidden in its transporter $U(x)$. For each lattice site x , there are D links corresponding to each space-time direction $x = (x_0, \vec{x})$. Its D nearest-neighbour links are expressed as unit vector $x + a\mathbf{e}_1$, (See Fig. 3.1).

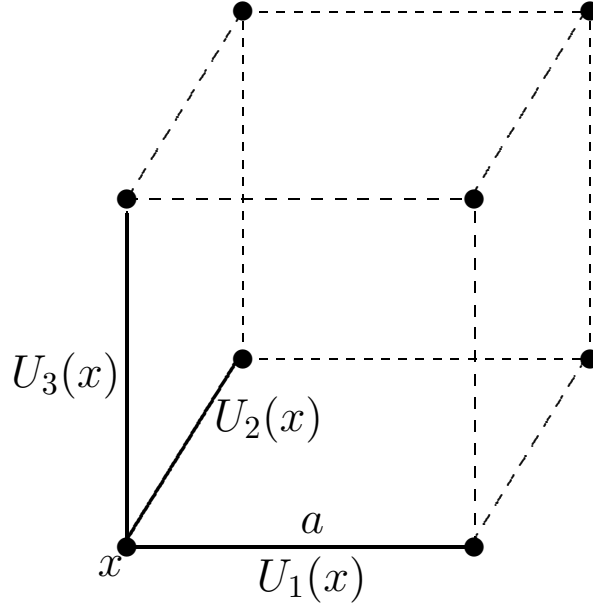


Figure 3.1 Each lattice site x has its links associating neighbour direction.

We may label each site x_μ as $x_\mu = n\hat{\mu}$, then the links connecting $x + a\mathbf{e}_\mu$ back to x is given by the inverse element unitary operator $U_\mu^{-1}(x) = U_{-\mu}(x)$ (See Fig. 3.2).

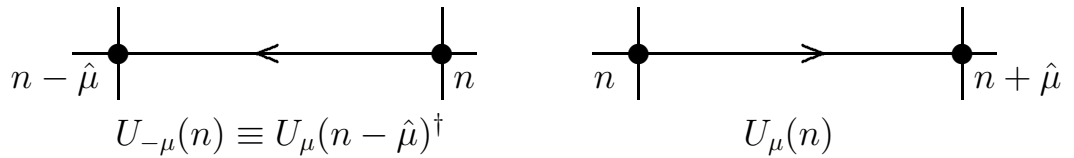


Figure 3.2 The link variables $U_\mu(n)$ connecting n and $n + \hat{\mu}$ and $U_{-\mu}(n)$ connecting n and $n - \hat{\mu}$.

For any $U_\nu(x + \hat{\nu})$,

$$U_{-\nu}(x + \hat{\nu}) \equiv U_\nu^\dagger(x). \quad (3.3)$$

Therefore, the links are variables which describing the fundamental dynamical degrees of freedom and each state of system is indicated by all possible ensemble $\{U_\mu(x)\}$. The gauge transformation at each site x is defined by

$$U_\mu^g = g(x + \hat{\mu})U_\mu(x)g^\dagger(x), \quad (3.4)$$

where $g(x), g^\dagger(x + \hat{\mu}) \in G$. In our work, we use $G = SU(2)$, a link $U_\mu(x)$ can be represented in quaternion form as

$$U(x) = a_0(x) + \mathbf{a} \cdot \boldsymbol{\sigma} \quad \text{or} \quad U = \cos\theta + i\boldsymbol{\sigma} \cdot \mathbf{n} \sin\theta, \quad (3.5)$$

where a_μ is a read four-vector of unit length

$$a_0^2(x) + \sum_{i=1}^3 a_i^2(x) = 1. \quad (3.6)$$

In the continuum limit of gauge theory, the field strength $F_{\mu\nu}$ appears in the gauge action of infinitesimal closed loop on any space-time x . That is

$$U_{P_{\mu\nu}}(x) = \exp(iF_{\mu\nu}dx^\mu dx^\nu). \quad (3.7)$$

The term $F_{\mu\nu}dx^\mu dx^\nu$ is corresponding to *Wilson loop*, $-\oint A_\mu dx^\mu$, which is the gauge invariance quantity. On lattice, these paths are taken along any squares, which are called *plaquettes* and let $U_{P_{\mu\nu}}(n)$ is the product of the links forming the plaquette (See Fig. 3.3):

$$U_{P_{\mu\nu}}(n) \equiv U_\nu^\dagger(n) \cdot U_\mu^\dagger(n + \nu) \cdot U_\nu^\dagger(n + \mu) \cdot U_\mu(n). \quad (3.8)$$

The plaquette $U_{P_{\mu\nu}}(n)$ can be transformed according to $U_{P_{\mu\nu}}^\Omega(n) = \Omega(n)U_{P_{\mu\nu}}(n)\Omega^{-1}(n)$ under gauge transformation. Anyone who interests in study lattice gauge theories can consult Rothe's book (Rothe, 2005), Montvay and Münster're book (Montvay and Münster, 1994) and Creutz' book (Creutz, 1983).

3.2 Monte Carlo method

For this section, we explain about the basic Monte Carlo method being used in lattice gauge field theory. We start from forming lattice of four dimensional space-

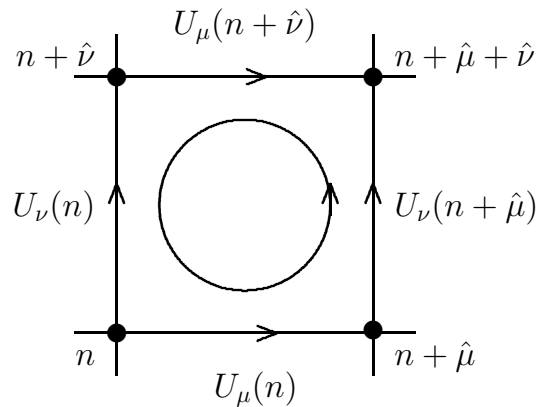


Figure 3.3 The four link variables perform the plaquette $U_{\mu\nu}(n)$. The circle specifies the order that the link are multiplied in the product.

times $\{x = (ax_0, ax_1, ax_2, ax_3)\}$ where x_μ is integer and a is *lattice spacing*. Any lattice we implement on computation must be satisfied with boundary conditions $x_\mu + L_\mu = x_\mu$ where L_μ is the number of lattice site. At each link between two sites connects by a link variable $U_\mu(x)$. The variable \mathbf{U} is defined as the set of all link variables U_μ residing on the links of the lattice. When we want to evaluate the expectation of Eq. (3.41) of any observables. Any new configuration \mathbf{U} should be generated by probability of Boltzmann factor

$$\rho(\mathbf{U}) \propto \exp\{-S_{SU(2)}^{\text{latt}}[\mathbf{U}]\}. \quad (3.9)$$

When we generate configuration according to probability Eq. (3.9), then a new configuration can be generated,

$$\{U_\mu^1(x)\} \rightarrow \{U_\mu^2(x)\} \rightarrow \{U_\mu^3(x)\} \rightarrow \dots \rightarrow \{U_\mu^N(x)\}. \quad (3.10)$$

This is called *Markov process* or *Markov chain*. The index N represents the time at which the configuration is generated. Under the ergodicity, it satisfy two conditions: 1) any configurations in ensemble should be produced from other configuration in ensemble within a finite Markov steps. 2) After performing a finite Markov steps, it cannot return to previous configuration. Finally the generated configuration can reach the thermalized state. Most of configurations will have the same particular

energy. That is, any new configurations generating from this state will satisfy the detail balance:

$$e^{-S(\mathbf{U})}P(\mathbf{U} \rightarrow \mathbf{U}') = e^{-S(\mathbf{U}')}P(\mathbf{U}' \rightarrow \mathbf{U}). \quad (3.11)$$

When each configuration is satisfied with Eq. (3.11), we assume that it reaches into the equilibrium state, or the thermalized state. Only few configurations have high or small energy. Then we can generate many configuration as we believe they satisfy the same condition(action). Any observable is measured from averaging of those configurations:

$$\langle \mathcal{O} \rangle \simeq \frac{1}{N_{\text{MC}}} \sum_{i=1}^{N_{\text{MC}}} \mathcal{O}(U_i), \quad (3.12)$$

where N_{MC} is the Monte Carlo steps of simulation.

3.2.1 Heatbath algorithm

This algorithm comes from the original work of the pioneer, Michael Creutz,(Creutz, 1980; Creutz et al., 1983) who first brought the Markov process into lattice gauge simulation, and that allows one measure any object of lattice gauge theory by Monte Carlo simulation. For our work, this algorithm is able to be used for only the group $SU(2)$ and cannot be readily developed into other Lie groups. The usual Monte Carlo sampling is to update the whole configuration with probability Eq. (3.9). But the heatbath algorithm choose to update only one or a few degrees of freedom and let the remaining ones are kept fixed. This also use the Boltzmann factor of $SU(2)$ Yang-Mills theory. Suppose we want to update the link variable $U_{\mu'}(x')$, the Boltzmann factor is factorized into two parts, one containing $U_{\mu'}(x')$ and no containing $U_{\mu'}(x')$:

$$\exp\{-S_{SU(2)}^{\text{latt}}[\mathbf{U}]\} = \exp\{-\bar{S}_{SU(2)}^{\text{latt}}[\mathbf{U}]\} \cdot \exp\{-S_{SU(2)}^{\text{latt}}[\mathbf{U}/U_{\mu'}(x')]\} \quad (3.13)$$

where

$$\begin{aligned} \exp\{-\bar{S}_{SU(2)}^{\text{latt}}[\mathbf{U}]\} &= \beta \sum_{\nu} \left(1 - \frac{1}{4} \text{Tr}[P_{\mu'\nu}(x') + P_{\mu'\nu}^{\dagger}(x')] \right) \\ &= \beta \sum_{\nu} \left(1 - \frac{1}{2} \text{Re Tr}[P_{\mu'\nu}(x')] \right) \end{aligned} \quad (3.14)$$

with $\mu \neq \nu$ and $\mu, \nu = 0, \pm 1, \pm 2, \pm 3$. The action $S_{SU(2)}^{\text{latt}}[\mathbf{U}/U_{\mu'}(x')]$ contains plaquette which does not include the link variable $U_{\mu'}(x')$. The acceptance probability of the new link variables depends on the six plaquettes contain the considered link. It requires to consider their contribution to the action. The headbath algorithm satisfies the detail balanced condition Eq. (3.11) and is reasonable to sampling update to $U_{\mu'}(x')$ by keeping $\mathbf{U}/U_{\mu'}(x')$ fixed.

We parameterize the $SU(2)$ -link variables as quaternion representation

$$U_{\mu}(x) = a_0(x)I + i\vec{a}(x) \cdot \vec{\sigma}, \quad (3.15)$$

where a_{μ} is a real four-vector of unit length $a_0^2 + \vec{a}^2 = 1$. The invariant group measure is Haar measure form:

$$dU = \frac{1}{2\pi^2} \delta(a^2 - 1) d^4a = \frac{1}{4\pi^2} \sqrt{(1 - a_0^2)} da_0 d\Omega \quad (3.16)$$

where the vector \vec{a} was described in spherical coordinates (r, θ, ϕ) and variable r is to be integrated and $d\Omega$ represents the solid angle of \vec{a} . Let $\Omega_{\mu'}(x')$ be a link variable, its contribution of $\Omega_{\mu'}(x')$ to the action can be expressed as

$$\begin{aligned} S[\Omega_{\mu'}(x')] &= -\frac{1}{2} \text{tr} \left[\Omega_{\mu'}(x') \sum_{\nu} V(\nu, x', \mu') \right] \\ &\text{with } \nu \in \{\pm 0, \pm 1, \pm 2, \pm 3\} \text{ and } \nu \neq \pm \mu'. \end{aligned} \quad (3.17)$$

We can imagine as shown in Fig. 3.4.

Then, it requires the the part

$$S[\Omega] = -\frac{1}{2} \text{tr}[\Omega \cdot V(x)] + \text{terms indep. of } \Omega(x). \quad (3.18)$$

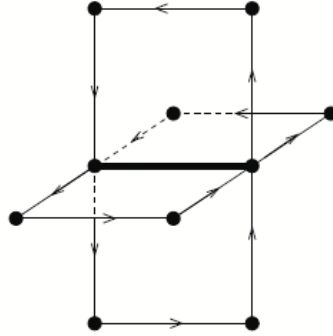


Figure 3.4 For each link $U_\mu(x)$, there are other nearest-neighbour link variables which have contribution to sampling.

Here $V(x)$ is a sum of all the $SU(2)$ matrices to which $\Omega(x)$ couples and therefore proportional to a $SU(2)$ matrix. Specific examples for this setting are Lorentz and Coulomb gauge fixing via simulated annealing or Wilson’s formulation of $SU(2)$ lattice Yang-Mills theory. In the latter case, the dynamical variables are the links $\Omega(x) \equiv U_\mu(x)$ and the action is (for $G = SU(N)$)

$$S_{\text{YM}}[U] = \sum_x \left[1 - \frac{1}{N} \text{Re tr } U_p(x) \right]. \quad (3.19)$$

Here, the plaquette variables are the products of links (holonomy) along an elementary lattice square,

$$U_P(x) \equiv U_{\mu\nu}(x) \equiv U_\nu^\dagger(x) \cdot U_\mu^\dagger(x + \hat{\nu}) \cdot U_\nu(x + \hat{\mu}) \cdot U_\mu(x). \quad (3.20)$$

Notice that $U_P(x)$ acting on a quark wave function $\psi(x)$ transports the quark along the contour in *clockwise* direction (the group multiplication $U_1 \cdot U_2$ means “apply U_1 after U_2 ”). This is consistent with the gauge transformation law for parallel transporters.

$$U_\mu(x) \rightarrow \Omega(x + \hat{\mu}) \cdot U_\mu(x) \cdot \Omega^\dagger(x) \quad (3.21)$$

which corresponds to the usual continuum relation for the gauge potential $U_\mu(x) =$

$$\exp(-aA_\mu(x)) = 1 - aA_\mu(x) + \mathcal{O}(a^2),$$

$$A_\mu(x) \rightarrow \Omega(x)A_\mu(x)\Omega^\dagger(x) + \Omega(x)\partial_\mu\Omega^\dagger(x) \equiv \Omega(x)(\partial_\mu + A_\mu(x))\Omega^\dagger(x) \quad (3.22)$$

$$\equiv \Omega(x)D_\mu\Omega^\dagger(x). \quad (3.23)$$

Each fixed link $U_\mu(x)$ in D space-time dimensions is attached to $2(D-1)$ plaquettes. Making use of $\text{Re tr}U^\dagger = \text{Re tr}U$, the relevant six terms of the Yang-Mills action can be simplified to

$$S[U_\mu(x)] = -\frac{1}{N}\text{Re tr} \sum_{\nu \neq \mu} U_\mu(x) \cdot \left[\underbrace{U_\nu^\dagger(x)U_\mu^\dagger(x + \hat{\nu})U_\nu(x + \hat{\mu})}_{\text{counter-clockwise}} \right. \\ \left. + \underbrace{U_\nu(x - \hat{\nu})U_\mu^\dagger(x - \hat{\nu})U_\nu^\dagger(x + \hat{\mu} - \hat{\nu})}_{\text{clockwise}} \right] + \dots \quad (3.24)$$

$$= -\frac{1}{N}\text{Re tr} \sum_{\nu \neq \mu} [U_\mu(x) \cdot V_{\mu\nu}(x)] + \text{terms indep. of } U_\mu(x) \quad (3.25)$$

The sum runs over the three directions different from the given μ and the term in brackets in the first line corresponds to the neighbour sum $V(x) \equiv V_{\mu\nu}(x)$ described above. Geometrically, $V_{\mu\nu}(x)$ can be interpreted as the sum over the six *staples* attached to the given link $U_\mu(x)$; the first term in brackets describes the *counter-clockwise* staples, the second term refers to the *clockwise* ones. In total, each given link $U_\mu(x)$ in $D = 4$ couples to six staples, i.e., 18 neighbouring links.

Returning to the general setting above, the heatbath algorithm for the $SU(2)$ valued quantum theory

$$Z = \int d\mu[\Omega] \exp\{-\beta S[\Omega]\} \\ = \int \prod_{y \neq x} d\mu[\Omega(y)] \int d\mu(\Omega(x)) \exp\{+\frac{\beta}{2}\text{tr}[\Omega(x) \cdot V(x)] + \dots\} \quad (3.26)$$

amounts to choosing *locally* a random $SU(2)$ matrix $\Omega(x) \equiv a_0 + ia_k\sigma_k$ distributed according to the density

$$P(\Omega) = d\mu(\Omega) \exp\{+\frac{\beta}{2}\text{tr}[\Omega(x) \cdot V(x)]\}, \quad (3.27)$$

where μ is the $SU(2)$ Haar measure. Since $V(x)$ is a sum of $SU(2)$ matrices, it is itself *proportional* to an $SU(2)$ matrix,

$$V = k \cdot \bar{V}, \quad k = \sqrt{\det V}, \quad \bar{V} \in SU(2). \quad (3.28)$$

Due to the invariance of the Haar measure,

$$P(\Omega) = d\mu(\Omega) \exp\left\{\frac{\beta}{2} k \operatorname{tr}[\Omega \cdot \bar{V}]\right\} = d\mu(\bar{\Omega}) \exp\left\{\frac{1}{2} k \beta \operatorname{tr} \bar{\Omega}\right\} \quad (3.29)$$

with $\bar{\Omega} \equiv \Omega \cdot \bar{V}$. Using the quaternion representation $\bar{\Omega} = b_0 + i b_k \sigma_k$ and the explicit form of the Haar measure

$$d\mu(\bar{\Omega}) = d^4(b_0, \mathbf{b}) \delta(b_0^2 + \mathbf{b}^2 - 1), \quad (3.30)$$

we can introduce spherical coordinates $\{|b|, \theta, \varphi\}$ for the 3-vector \mathbf{b} to find

$$P(\Omega) = db_0 d|\mathbf{b}| |\mathbf{b}|^2 \sin \theta \, d\theta \, d\varphi \delta(b_0^2 + \mathbf{b}^2 - 1) \cdot \exp\{\beta k b_0\}. \quad (3.31)$$

Eliminating $|\mathbf{b}|$ by means of the delta function, we have

$$P(\Omega) = db_0 \, d\theta \, d\varphi \, \sin \theta \cdot \frac{1}{2} \sqrt{1 - b_0^2} \cdot \exp\{\beta k b_0\}. \quad (3.32)$$

Next, we change variables from $b_0 \in [-1, 1]$ to $z \equiv \exp[\beta k (b_0 - 1)] \in [e^{-2\beta k}, 1]$ and introduce $t \equiv \cos \theta$. This yields

$$P(\Omega) \sim dz \, dt \, d\varphi \sqrt{1 - b_0^2(z)}, \quad \varphi \in [0, 2\pi], \quad t \in [-1, 1], \quad z \in [e^{-2\beta k}, 1].$$

The square root factor indicates that a given random $z \in [e^{-2\beta k}, 1]$ should only be accepted with probability $\sqrt{1 - b_0^2(z)}$, where

$$b_0(z) = 1 + (\beta k)^{-1} \log z \quad (3.33)$$

This can be accomplished by choosing repeatedly a random $z \in [e^{-2\beta k}, 1]$, then drawing a random $r \in [0, 1]$ uniformly and accepting the chosen z only if $r < \sqrt{1 - b_0^2(z)}$.

From the random number (z, t, φ) generated in this way, the coordinates (b, \mathbf{b}) of the $SU(2)$ matrix $\Omega = b_0 + ib_k \sigma_k$ can be reconstructed by

$$b_0 = 1 + (\beta k)^{-1} \log z \quad (3.34)$$

$$b_1 = \rho \sqrt{1 - t^2} \cos \varphi, \quad \rho \equiv |\mathbf{b}| = \sqrt{1 - b_0^2} \quad (3.35)$$

$$b_2 = \rho \sqrt{1 - t^2} \sin \varphi \quad (3.36)$$

$$b_3 = \rho t. \quad (3.37)$$

Finally, the initial matrix $\Omega = \Omega(x)$ is found by rotating back, $\Omega = \bar{\Omega}(b_0, \mathbf{b}) \cdot \bar{V}^\dagger$. For the explicit pseudocode of program, any interested reader can read more at Appendix B.

3.3 Observable as averaging from partition function

The Wilson action of $SU(N)$ Yang-Mills theory is given (Wilson, 1974) by

$$S_W[\beta, U] = \beta \sum_{P_{\mu\nu}} \left(1 - \frac{1}{N} \text{Re tr}[U_{P_{\mu\nu}}] \right), \quad \text{where } \beta = \frac{2N}{g_0^2} a^{D-4} \quad (3.38)$$

where g_0 is the bare coupling. This S_W is a gauge invariance of system. By using Eq. (3.7) and representation in Eq. (3.5) of $U_{P_{\mu\nu}}$, we obtain, for $SU(2)$,

$$S_W[\beta, U] = \frac{4a^{D-4}}{g_0^2} \sum_{P_{\mu\nu}} (1 - \cos \theta_{P_{\mu\nu}}) \approx \sum_x \sum_{\mu\nu} \sum_a \frac{a^D}{4g_0^2} F_{\mu\nu}^a F_a^{\mu\nu} \simeq \int d^D x \frac{1}{4g_0^2} F_{\mu\nu}^a F_a^{\mu\nu}. \quad (3.39)$$

This means, the Wilson action will be equivalent to the Yang-Mills action in the limit $a \rightarrow 0$.

In lattice gauge theory, we define the *partition function* by

$$Z(\beta) = \int DU e^{-S_W[\beta, U]}, \quad (3.40)$$

where S_W is the action in Euclidean space-time. The problem of Yang-Mills theory can be mapped into the problem of statistical mechanics by letting variables as

the link ensemble $\{U_\mu(x)\}$. The measure DU is operated on Haar measure and it satisfied the gauge invariance: $DU^g = DU$.

An Observable we want to find can be measured by averaging over all field configurations

$$\langle \mathcal{O} \rangle(\beta) = \frac{1}{Z(\beta)} \int DU \mathcal{O}[U] e^{-S_w[\beta, U]}. \quad (3.41)$$

3.4 Coulomb gauge fixing

Gauge fixing is choosing the gauge. Having gauge fixing in Yang-Mills theory is analogy with choosing a constraint into mechanical problem (Christ and Lee, 1980). Even we have freedom to choose any gauge, but in this research we choose Coulomb gauge $\nabla \cdot A = 0$, because from Gribov's quark confinement scenario (Gribov, 1978), which study with Coulomb gauge allowing us to extract potential between quarks within nucleon (combining by gluon exchanges).

The evaluation of Eq. (3.41) need to integrate over all continuous configuration which must include the redundant configurations of the gauge field, i.e. according Faddeev-Popov procedure and the effect of Gribov copies. We can eliminate some of redundant by implementing the gauge fixing, in our case, we must implement the Coulomb gauge fixing condition $\hat{\nabla} \cdot \hat{A} = 0^*$ into the lattice, which is expressed into numerical lattice condition as for all site \mathbf{x} in lattice,

$$\sum_i (\hat{A}_i(\mathbf{x}) - \hat{A}_i(\mathbf{x} - \hat{\mu})) = 0. \quad (3.42)$$

To try to reach this condition, we must minimize the following functional

$$F^t[g] = \sum_{\mathbf{x}} \sum_{i=1}^3 \frac{1}{2} \text{Re tr}[1 - U_i^g(\mathbf{x}, t)] \quad (3.43)$$

at fixed t -time slice, where U^g is gauge transformation by $SU(2)$ group attributing into lattice by

$$U_\mu^g(x) = g(x + \hat{\mu}) U_\mu(x) g^\dagger(x). \quad (3.44)$$

*We use the lattice notation which appear in Appendix E

The proof of this statement comes from the considering of derivative of the functional Eq. (3.43) with respect to subgroup

$$g(x) = e^{i\tau\omega(\mathbf{x})}, \quad (3.45)$$

where τ is a real parameter and $\omega(\mathbf{x})$ is an element of the Lie algebra. In terms of the τ parameter, if we found the configuration U_{\min} which lead the functional having minimum value

$$\left. \frac{d}{d\tau} F_{U_{\min}}^t \right|_{\tau=0} [\omega, \tau] = 0. \quad (3.46)$$

From Appendix E.6, we differentiate this functional and obtain

$$\frac{d}{d\tau} F^t[\omega, \tau] = \langle \omega, \hat{\nabla}^{(-)} \cdot \hat{\mathbf{A}} \rangle. \quad (3.47)$$

This condition yields the transversality of the lattice potential at the configuration g_{\min} . Therefore, we meet the conclusion at the implementing of Coulomb gauge into lattice is equivalent to minimize the gauge functional Eq. (3.43).

3.4.1 Iterated overrelaxation

The relaxation method consists of updating the lattice configuration. At each site \mathbf{x} , we could find the gauge transformation $g(x)$ which attributes into lattice by finding the best choice $g(x)$ from[†]

$$g(\mathbf{x}, t) = \frac{V^\dagger(x, t)}{\sqrt{\det V(x, t)}}, \quad (3.48)$$

where

$$V(x, t) = \sum_{k=1}^3 \left\{ U_k^\dagger(x, t) + U_k(x - \hat{k}, t) \right\}. \quad (3.49)$$

The $g(x)$ is computed from Eq. (3.48) and attributed into lattice until the gauge functional Eq. (3.43) relaxes to minimum. The number of steps of relaxation is not

[†]The proof appear in Appendix F.2

fixed, but the stopping of this procedure is done by means of a satisfied condition.

We always check the following quantity

$$\theta = \sum_{k=1}^3 [U_k^g(x + \hat{k}) - U_k^g(x)], \quad (3.50)$$

which gives rise to

$$\theta \simeq \int d^d x \text{Tr}[(\partial_i A_i)^2] \quad (3.51)$$

in the continuum limit. The value of θ decreased during the gauge-fixing process and should be zero when a minimum of the Functional in Eq. (3.43) has been reached.

In practise, the process should be stopped if θ drops below a certain small number ϵ which being fixed in advance. This is about the problem of critical slowing down, the minimum is accelerated by modifying the matrices

$$g_\alpha(x) \rightarrow [g(\mathbf{x}, t)]^\alpha, \quad (3.52)$$

where α is chosen in range $(1, 2)$. In our work, we use $\alpha = 1.75$, and set up the $\theta < 10^{-13}$ for accepting lattice Coulomb gauge condition. This can be implemented into lattice by the technique appeared in Appendix F.2.1.

3.5 Gribov's copy effect on Coulomb gauge

There are many configurations $U_\mu(x)$ satisfied Coulomb gauge condition, therefore whatever by numerical or theoretical point of view, it is very possible to have many configurations $U_\mu(x)$ satisfied $\vec{\nabla} \cdot \vec{A} = 0$ condition (or $\hat{\nabla} \cdot \hat{A} = 0$), we call this *Gribov gauge copies*, according to famous Gribov's paper (Gribov, 1978). In his original work, Gribov predicted the behaviour of some measurable quantity, the gluon propagator and ghost form factor, and lead us finally to static potential between quarks. This scenario is responsible for the quark confinement.

3.5.1 Finding best gauge copy

The influence of Gribov copies can be studied by taking various initial random gauge copies of the gauge field configuration before subjecting them to the standard overrelaxation (SOR) algorithm. Any $g(x) \in SU(2)$ can be randomly set and the transformation $U_\mu^g(x) = g(x + \hat{\mu})U_\mu(x)g^\dagger(x)$ is transformed randomly.

Then any observable quantities—the gauge-variant observables, such as gluon propagator, ghost form factor (ghost propagator), and Coulomb potential, can be computed from many gauge copy which being chosen from the lowest value of local minima F_{\min} [or the *best copy* (bc)] found for the gauge functional Eq. (3.43). We can hope to have found a copy belonging to the so-called *fundamental modular region* (Zwanziger, 1994) or at least not so far from it. In order to find the best copy for each thermalized gauge field configuration, we need to compare F_{\min} values for a large among of gauge copies, even it consumes a very long time of running of program. A reasonable question is if the use of only one gauge copy [the *first copy* (fc)] provides us with the same values, within error bars, of the propagator as the use of the best copy would. This consideration brings us to compare the propagator calculated on best copy (G^{bc}) with that on the first copies (G^{fc}).

We can enhance the effect of Gribov copies by finding the best gauge copy among the worst copies, i.e., by choosing the smaller F_{\min} values for being the better gauge copy, and, then, becomes finally the best gauge copy. This can be done from the repeated use of a given minimization method. The procedure have appeared in many research groups which working on Landau gauge (Bogolubsky et al., 2006; Bakeev et al., 2004) and Coulomb gauge (Voigt et al., 2008).

3.5.2 Flip Trick

Most of gauge transformation is implemented into lattice by periodic boundary condition. Nevertheless, we can enlarge the class of possible gauge transforma-

tion by also taking the *nonperiodic* gauge transformation. This will allow us to further minimize the gauge functional and to see the Gribov copies effect for gluon propagator or ghost form factor.

The observation of nonperiodic $SU(2)$ gauge field comes from the gauge transformation $U_\mu^g(x) = g(x + \hat{\mu})U_\mu(x)g^\dagger(x)$ is not necessarily periodic but differ by a group center element at the boundary:

$$g(x + L\hat{\nu}) = z_\nu g(x), \quad z_\nu = \pm 1 \in \mathbb{Z}(2) \quad (3.53)$$

where $\mathbb{Z}(2)$ is set of integers modulo 2. The algorithm we implemented into lattice is presented in Appendix F.2.2.

3.6 Renormalization

In Yang-Mills theories in 4-dimensions, there is the principle of renormalization, in brief, the coupling constant β acquires to depends on the large β value (ultraviolet regime). it allows us to include all any simulated data of lower β (infrared regime) combining them into one set of *renormalized* data by finding some constant to multiply each measurable observable, that is

$$O_{\text{REN}}(p) = \text{CONST} \cdot O_{\text{SIM}}(p). \quad (3.54)$$

With this procedure, the larger lattice and lower β can extract information at lower energy sector QCD. The renormalized data should be continuous from lower to high energy (momentum). The high energy QCD (ultraviolet regime) have been studied theoretically by Gross, Wilczek, and Politzer (David Politzer, 1973; Gross, 1973) and experiment of deep inelastic scattering.

3.7 Observables

For our framework of $SU(2)$ lattice gauge simulation in Coulomb gauge, there are three objects which are measured by considering Zwanziger confinement's

scenario (Zwanziger, 1994). They are gluon propagator, ghost form factor and Coulomb potential.

3.7.1 Gluon propagator

The gluon propagator we have measured in our project is defined along the same equal-time slice. That is

$$D_{ij}^{ab}(\mathbf{x} - \mathbf{y}) = \langle A_i^a(t_0, \mathbf{x}) A_j^b(t_0, \mathbf{y}) \rangle, \quad (3.55)$$

where t_0 is the fixed time. For the lattice calculation in Coulomb gauge, we define Fourier transformed connection which are a function of the lattice Matsubara momenta

$$\tilde{A}_i^k(\hat{p}_0, \hat{\mathbf{p}}) \equiv \sum_{\hat{x}} e^{-i\hat{p}\hat{x}} \cdot 2a_i^k(\hat{x}_0, \hat{\mathbf{x}}). \quad (3.56)$$

The (dimensionless) lattice propagator is then defined as

$$\hat{D}(\hat{p}_0, \hat{\mathbf{p}}) = \frac{1}{\hat{V}_3} \sum_{i=1}^3 \sum_{k=1}^3 \tilde{A}_i^k(-\hat{p}_0, -\hat{\mathbf{p}}) \tilde{A}_i^k(\hat{p}_0, \hat{\mathbf{p}}) = \frac{1}{\hat{V}_3} \sum_{i=1}^3 \sum_{k=1}^3 \left| \tilde{A}_i^k(\hat{p}_0, \hat{\mathbf{p}}) \right|. \quad (3.57)$$

3.7.2 Ghost form factor

It begins from defining the ghost propagator as the expectation value of the inverse Faddeev-Popov operator $M = -\nabla \cdot D$, where D is the gauge covariant derivative. On lattice, it is computed from

$$D^{0ab}(\mathbf{x} - \mathbf{y}) = \langle M^{-1}[A]_{(\mathbf{x}, \mathbf{y})}^{ab} \rangle. \quad (3.58)$$

Then we can transform it into momentum space to be D^{0ab} . We are interested to know its behavior of dimensionless quantity, the so-called *ghost form factor*, $D(p)$

$$D(p) = \frac{D^{0ab}}{|p^2|}. \quad (3.59)$$

3.7.3 Coulomb form factor

In the framework of lattice gauge simulation in Coulomb gauge (Cucchieri and Zwanziger, 2001a; Cucchieri and Zwanziger, 2001b; Langfeld and Moyaert, 2004), we can simulate the (Coulomb) potential between quark and anti-quark by

$$V_{\text{Coul}}(x-y) \propto -g_0^2 \langle [M^{-1}[A](-\Delta)M^{-1}[A]] \rangle \quad (3.60)$$

at fixed time-slice t_0 , in momentum space, the Coulomb potential are computed from

$$\hat{V}_{\text{Coul}}(p) = -\frac{1}{4N_d} g_0^2 \sum_{a=1}^3 \sum_{\bar{x}, \bar{y}} \langle [M^{-1}[A](-\Delta)M^{-1}[A]] \rangle e^{-i\frac{2\pi}{N_d} \cdot (x-y)} \quad (3.61)$$

This potential was proved that it is the upper bound value of the true potential (Zwanziger, 2003). This is why we are interested to simulate it. However, its computing is very slow by using conjugate-gradient method. We must use the preconditioning technique to speed up the conjugate-gradient process (Sternbeck et al., 2005).

3.8 Set up at finite temperature

After we can simulate observable quantities, gluon propagator and ghost form factor, and Coulomb potential at zero temperature. It is interesting to explore those observables at finite temperature. Fortunately, it is not difficult to perform the lattice simulation at finite temperature, but before running the program, we need to be ensured the results at zero temperature. Finite temperature performance starts from considering of the partition function in field theory,

$$Z = \int d^4x \langle x | e^{-\beta \hat{H}} | x \rangle, \quad (3.62)$$

where $d^4x = dx_0 d^3x$. The x_0 is time dimension. In lattice framework, it is time slice lattice x_0 , then Eq. (3.62) becomes

$$\int dx_0 \approx N_0 a = \frac{1}{k_B T}, \quad (3.63)$$

where a is lattice space relating with coupling constant β . For convenient, we can set k_B Boltzmann's constant equal to 1, and we obtain the temperature of lattice simulation

$$T = \frac{1}{N_0 a(\beta)}. \quad (3.64)$$

By tuning up the time-slice N_0 lattice size or coupling constant β , we can study any observable quantities at finite temperature. We are interested to know at temperature $T < T_c$, $T = T_c$ and $T > T_c$ where T_c is critical temperature between lower temperature of confinement phase and higher temperature of de-confinement phase.

CHAPTER IV

LATTICE RESULTS

This chapter is devoted to report the result of simulation of Yang-Mill theory in Coulomb gauge at zero and finite temperature by the procedure we have described in the previous chapter. We choose to study $SU(2)$ gluon propagator, ghost form factor at zero temperature and finite temperature. For the Coulomb form factor, the result is not consistent with other group research. This inspires us to further study in the future.

4.1 Gibov gauge copies effect

Before simulating the gluon propagator of all range of energy, we check the Gibov effect to the gluon propagator at low energy as show in Fig. 4.1. We also found the similar suppression of ghost form factor by Gribov gauge copies influence as in Fig. 4.2.

4.2 Gluon propagator

4.2.1 Result: at zero temperature

In case of dimensions=2+1

In our simulations in $D = 2 + 1$, we consider the 2-momenta aligned along in the first time slice:

$$\mathbf{p} = (0, p). \tag{4.1}$$

The results for gluon propagator are shown in Fig. 4.3 and were obtained by measuring from the best gauge copies by averaging from 100 configurations for the lattice

Gluon propagator in Coulomb gauge at lowest momentum

USE FLIP TRICK, lattice 24^4 , $\beta=2.2$, #samples=100, autocor=5, violation $<10^{-13}$

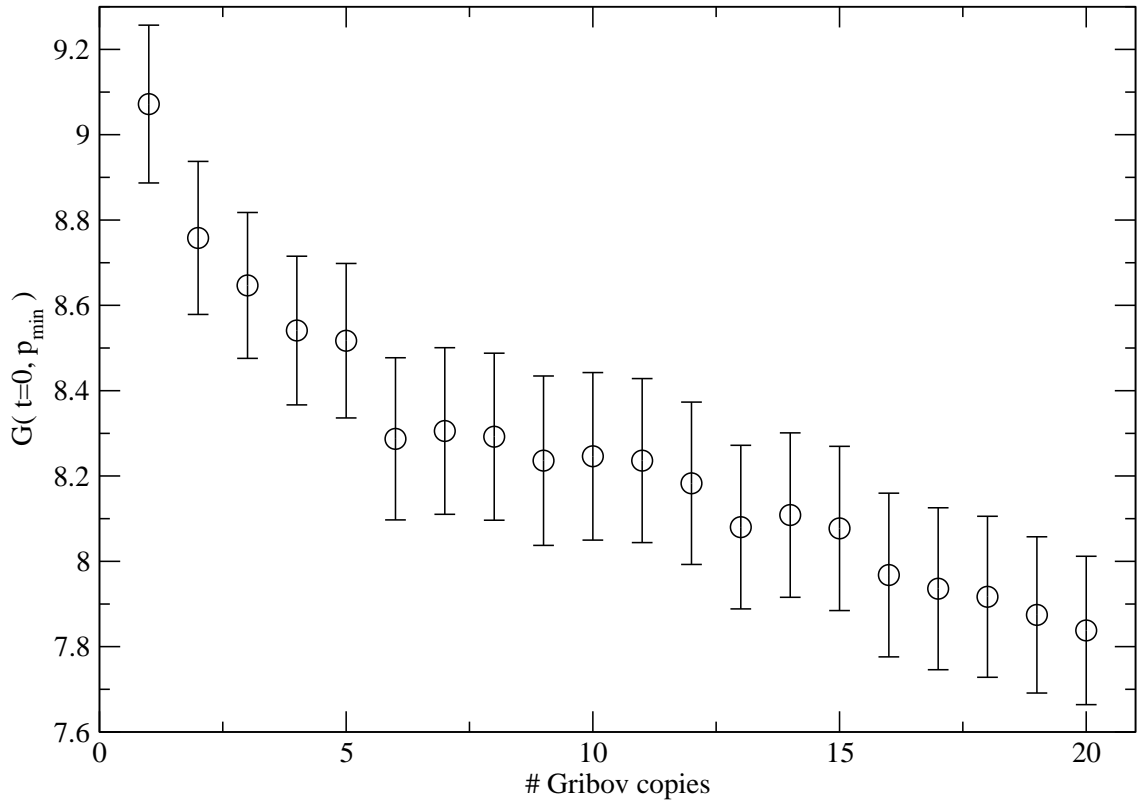


Figure 4.1 Gribov copies influence to gluon propagator at minimum momentum, p_{\min} , for lattice 24^4 at $\beta = 2.2$.

volume 68^3 and 48^3 . It shows clearly the suppression of gluon propagator at low momentum.

In case of Dimensions=3+1

The results for gluon propagator are shown in Fig. 4.4 and were obtained by measuring from the best gauge copies of 30 gauge copies by generating from 100 configurations for the lattice volume 36^4 . It shows clearly the suppression of gluon propagator at low momentum. It also shows that at IR region, the improved gauge fixing suppresses on propagator. At the UV region, it may be implied according the power law fitting $D(p) \sim p^{-\beta}$ in which $\beta = 1.57(8)$, but $1/(p \ln p)$ can be also possible.

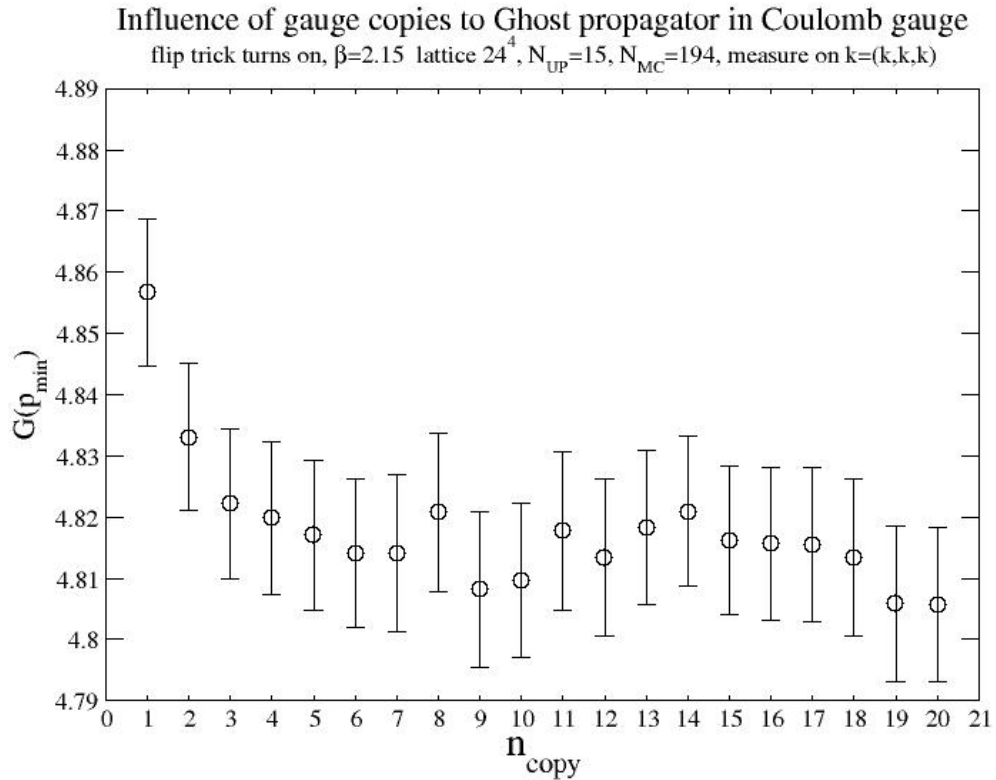


Figure 4.2 The suppression of Ghost propagator at lowest momentum.

For the result at zero temperature, we found that the gluon propagators approach zero at low energy. The Gibov copies effect influence the suppression of the gluon propagator at low energy.

4.2.2 Result: at finite temperature

The gluon propagator at finite temperature is shown in Fig. 4.5. We can fit them together by requiring that they should the same UV asymptotic freedom, then we plot the normalized gluon propagator in Fig. 4.6.

Any divergence of the ghost form factor at low temperature implies the existence of color charges, and the confinement of quark-antiquark is satisfied.

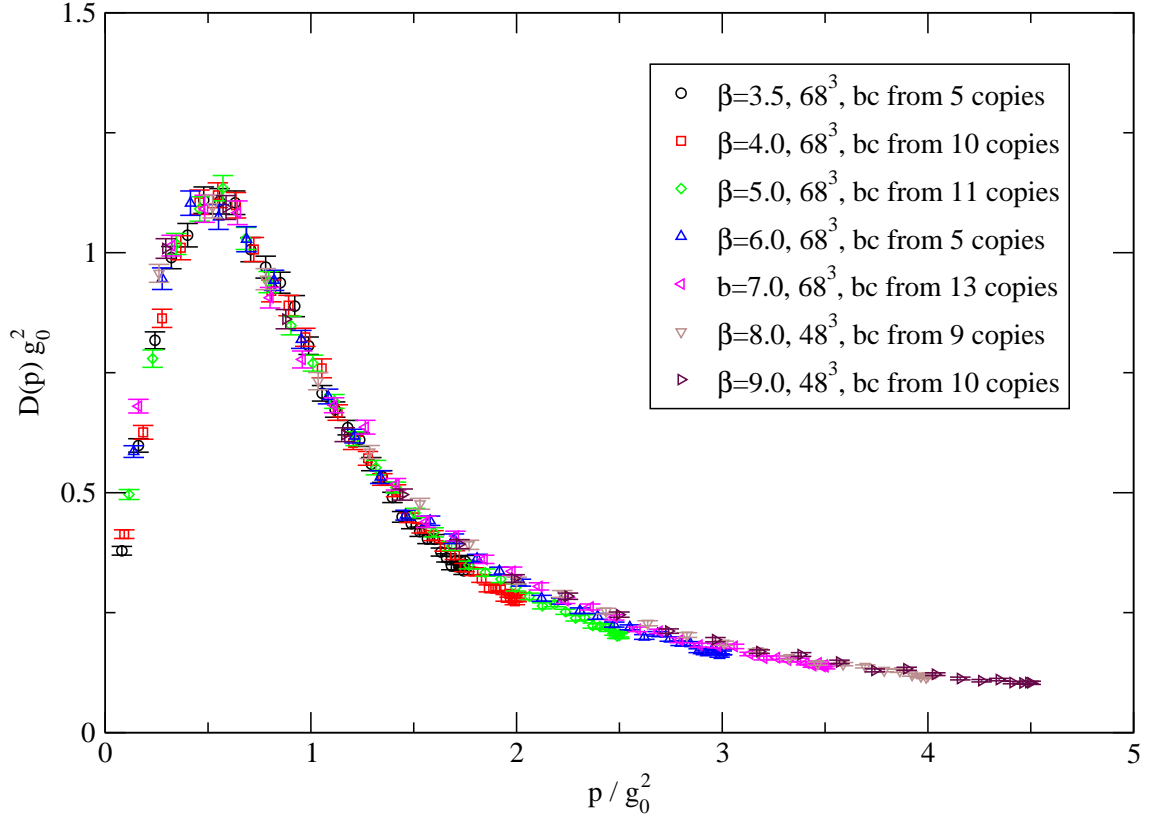


Figure 4.3 Gluon propagator in 2+1 dimensions at zero temperature

4.3 Ghost form factor

4.3.1 Result: curve fitting at IR and UV region

The ghost form factor data have been renormalized and been made the curve fitting of ghost form factor at zero temperature. It is shown in Fig. 4.7. The procedure we used to compute parameter at IR and UV region comes from (Langfeld and Moyaert, 2004). The rare data of simulations were fitted by choosing a cutoff from observing that, $d(p = 2.0 \text{ GeV}) = 0.49026$ and let it be the renormalisation condition. At high momentum regime, we have made a logarithmic ansatz supplemented with an anomalous dimension γ_0

$$d(\mathbf{p}) = \frac{a_{\mu\nu}}{\ln(|\mathbf{p}|/\Lambda_{\text{QCD}})^{\gamma_0}}, \quad p \gg \Lambda_{\text{QCD}}, \quad (4.2)$$

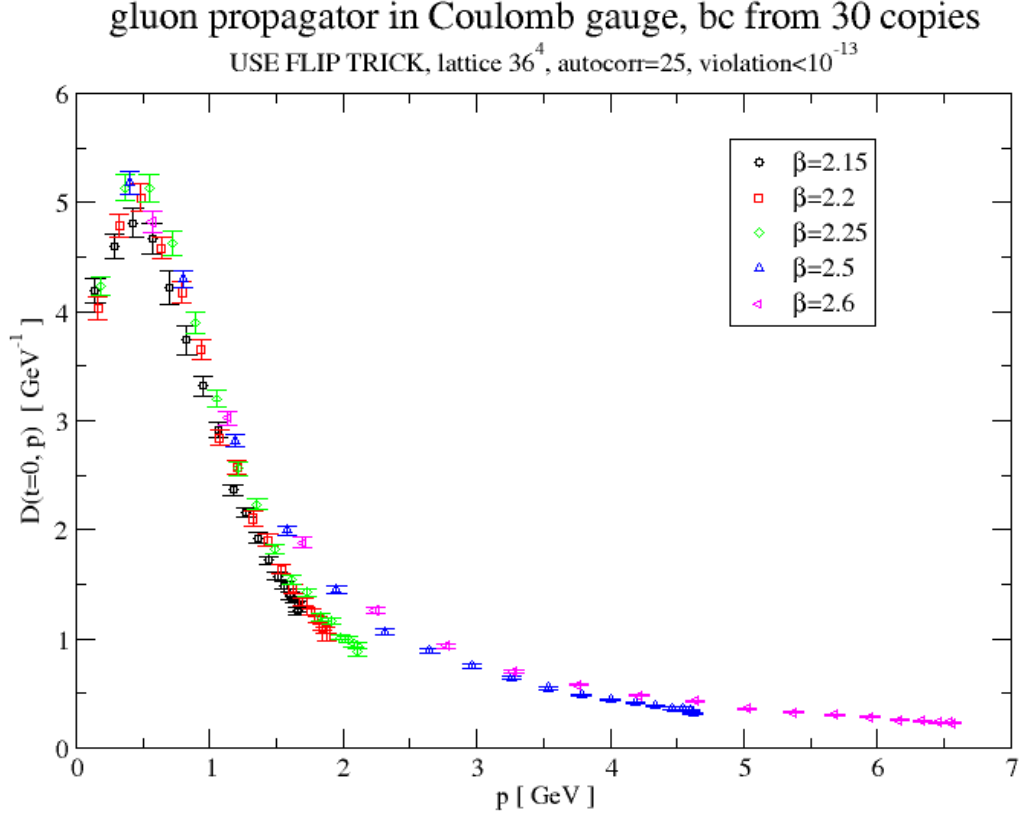


Figure 4.4 Gluon propagator in 3+1 dimensions at zero temperature.

where Λ_{QCD} is the renormalization group invariant scale parameter. After making curve fitting, we extract these parameters

$$a_{\mu\nu} = 0.443, \quad \gamma_{g_0} = 0.205. \quad (4.3)$$

After knowing these parameters, and the renormalisation condition, we can compute Λ_{QCD}

$$\Lambda_{\text{QCD}} = 1.08584 \text{ GeV}. \quad (4.4)$$

For the IR analysis, we adopt a scaling law:

$$d(\mathbf{p}) = \frac{a_{ir}}{(|\mathbf{p}^2|/\Lambda_{\text{QCD}}^2)^\kappa}, \quad p \ll \Lambda_{\text{QCD}}. \quad (4.5)$$

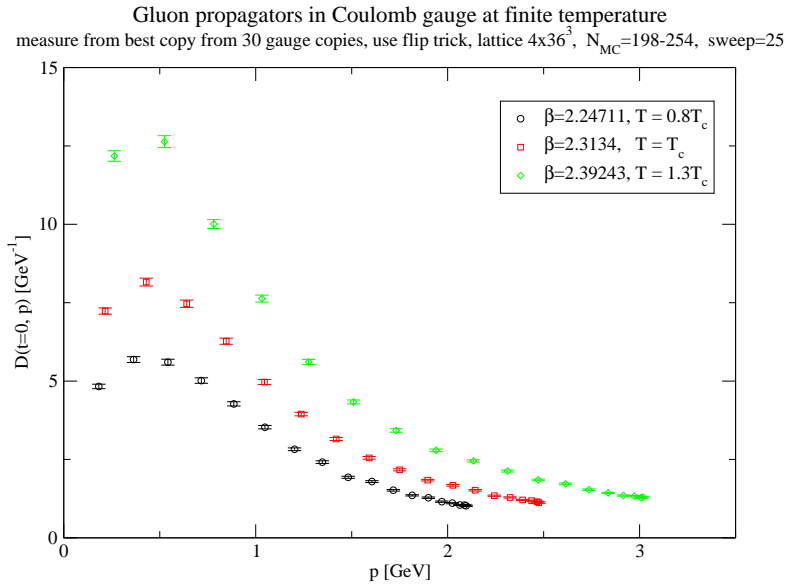


Figure 4.5 The gluon propagator at finite temperature.

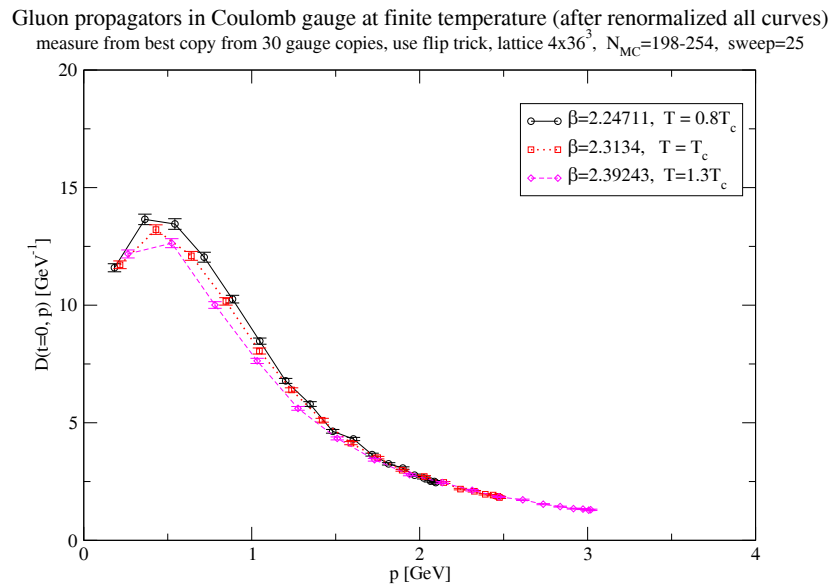


Figure 4.6 The gluon propagator at finite temperature after renormalizing data at high energy.

After having made the curve fitting, we found that

$$a_{ir} = 0.552, \quad \kappa_{g_0} = 0.130. \quad (4.6)$$

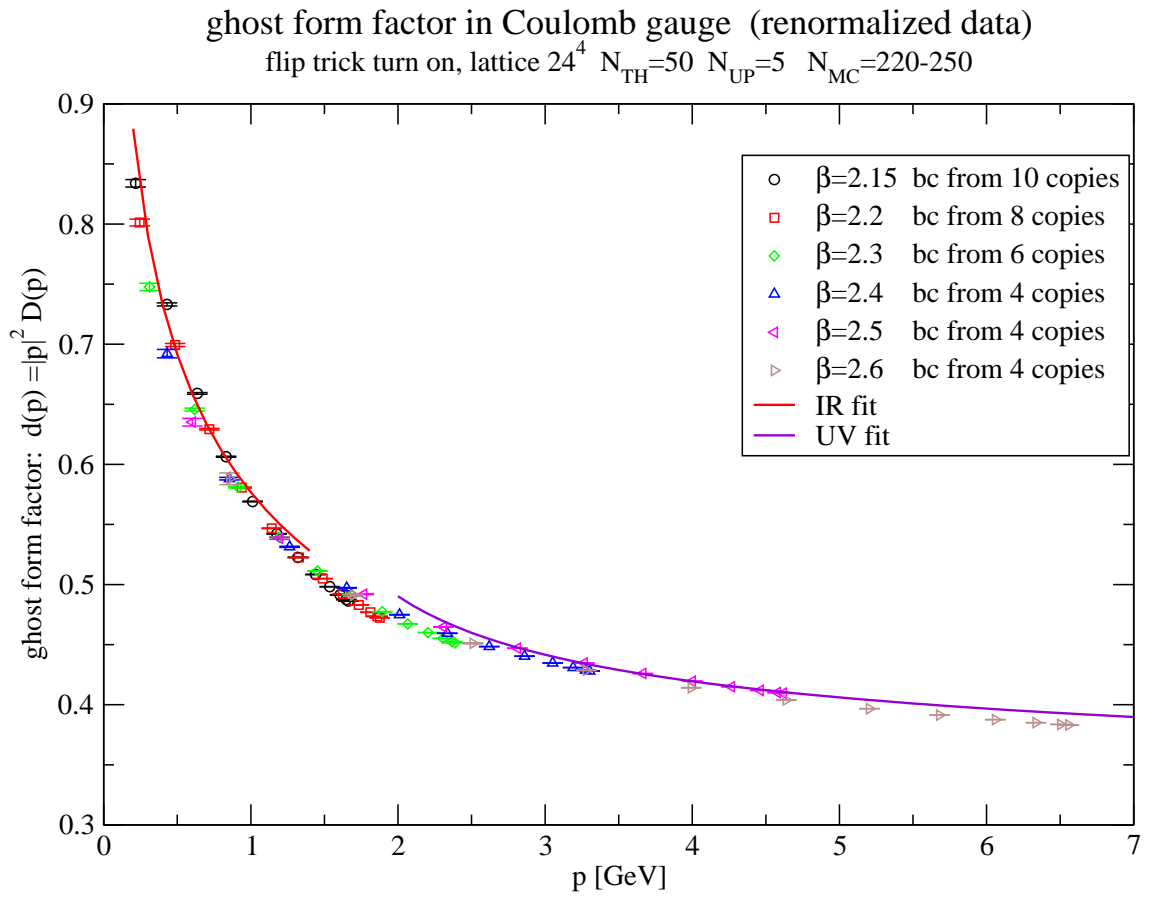


Figure 4.7 Ghost form factor at zero temperature, measured from best gauge copy of lattice 24^4 .

Combining with the previous data of the curve fitting, we summarize the value of parameter of UV region as shown in Table 4.1:

and at IR regime in Table 4.2:

Table 4.1 Parameters from curve fitting of the ghost form factor for UV region at zero temperature.

Temperature	$T = 0$	$T = 0.8T_c, T_c, 1.3T_c$
	$(\Lambda_{\text{QCD}} = 1.08584 \text{ GeV})$	$(\Lambda_{\text{QCD}} = 0.9935 \text{ GeV})$
$a_{\mu\nu}$	0.443	0.405
γ_0	0.205	0.196

Table 4.2 Parameters from curve fitting of the ghost form factor for IR region at zero temperature.

Temperature	$T = 0$	$T = 0.8T_c$	$T = T_c$	$T = 1.3T_c$
		$(\beta = 2.24711)$	$(\beta = 2.3134)$	$(\beta = 2.39243)$
a_{ir}	0.552	0.5659	0.5450	0.5307
κ	0.130	0.0926	0.0962	0.0997

4.3.2 Result: curve fitting for all range

We also have made the curve fitting of ghost form factor by using this Ansatz formula

$$\frac{A}{\left(|\log \frac{|p|}{\Lambda}|^{\frac{\gamma_0}{\alpha}} + \left(\frac{|p|^2}{\Lambda^2}\right)^{\frac{\kappa}{\alpha}}\right)^\alpha}$$

where Λ , A , γ_0 , α and κ are parameters which we want to extract from curve fitting. The plot of curve fitting is shown in Fig. 4.8. In the case of ghost form factor at $T = 0$, by using the curve fitting, we can extract these parameters as summarized in Table 4.3.

Table 4.3 Parameters from curve fitting of the ghost form factor for all range at zero temperature.

A	Λ	γ_0	α	κ
0.9756	0.0995	0.6562	0.0115	0.1085

In case of finite temperature, we have made the curve fitting as shown in Fig.

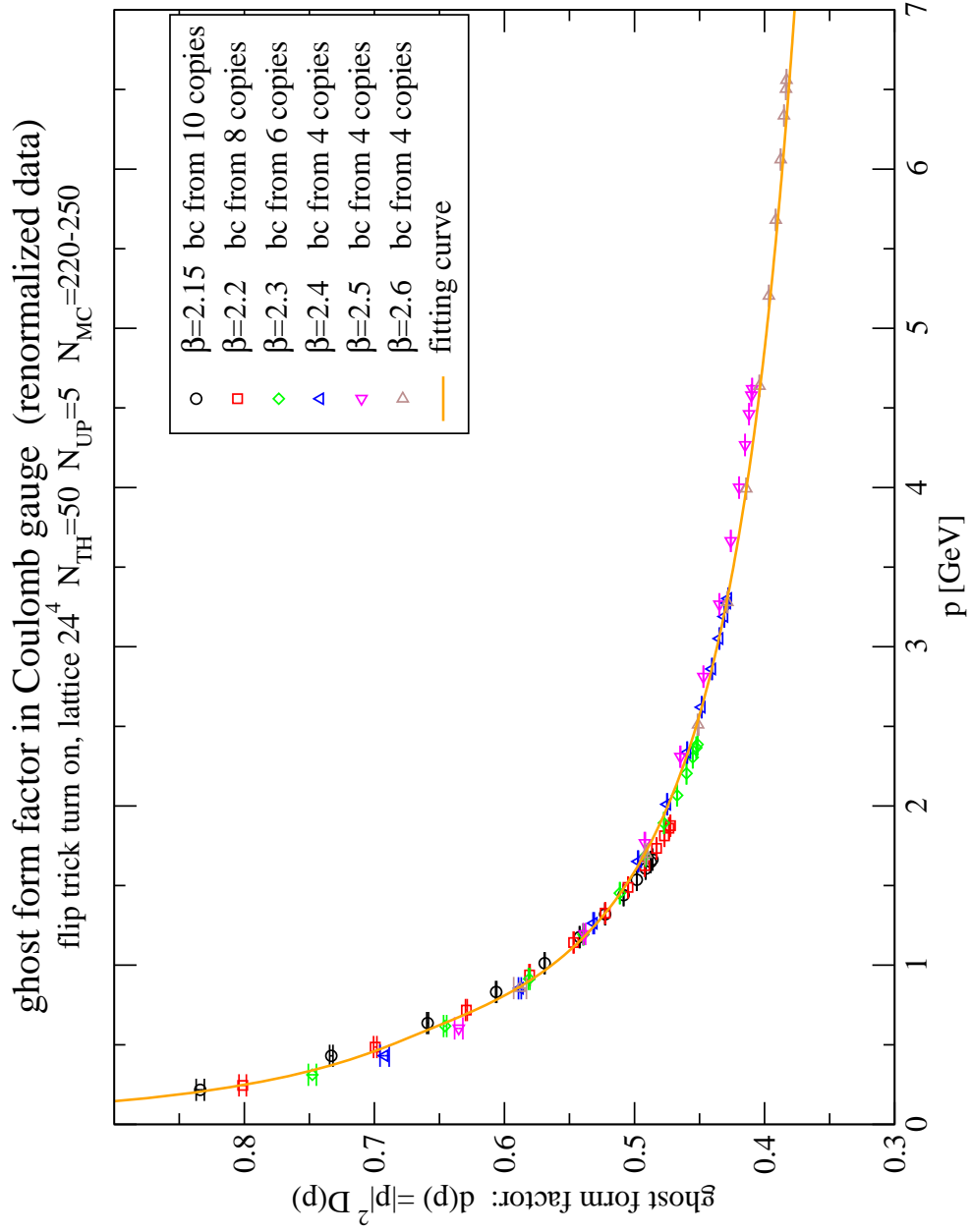


Figure 4.8 Ghost form factor at zero temperature, measured from best gauge copy of lattice 24^4

4.9. and obtain parameters as shown in the Table 4.4.

Table 4.4 Parameters from curve fitting of ghost form factor for all range at finite temperature.

	A	Λ	γ_0	α	κ
$T = 0.8T_c$	0.800508	0.148362	0.627315	0.0513664	0.0846121
$T = T_c$	0.814486	0.125575	0.619598	0.01991	0.0968555
$T = 1.3T_c$	0.709427	0.222751	0.564559	0.116498	0.0847839

4.4 Coulomb potential

The results of Coulomb potential are the measurement of three different quantities, which are $p^V(p)$, $p^4V(p)/8\pi\sigma$ and the Coulomb form factor. The latter quantity is the ratio of $p^2V(p)$ and the ghost form factor. All three objects are dimensionless which features confinement scenario in Coulomb gauge. Our result of $p^2V(p)$ as show in Fig. 4.10.

The $p^2V(p)$ result we obtain is similar to (Langfeld and Moyaert, 2004; Voigt et al., 2008), but the result of measuring $p^4V_{\text{Coul}}(p)$ is different from them. The $p^4V_{\text{Coul}}(p)$ of our simulation is shown in Fig. 4.11 which implies the vanishing of potential at low energy, while the reasonable result should be the finite potential at low energy as other research group, (see Fig. 4.12).

Then our work of measuring Coulomb potential is not agree with other. This is still the unfinished problem of our project. Even the results of Coulomb potential between other research groups (Langfeld and Moyaert, 2004; Voigt et al., 2008) are different in detail. Therefore, we cannot work future about the Coulomb potential at finite temperature.

We hope we can find the ultimate simulated results in the future.

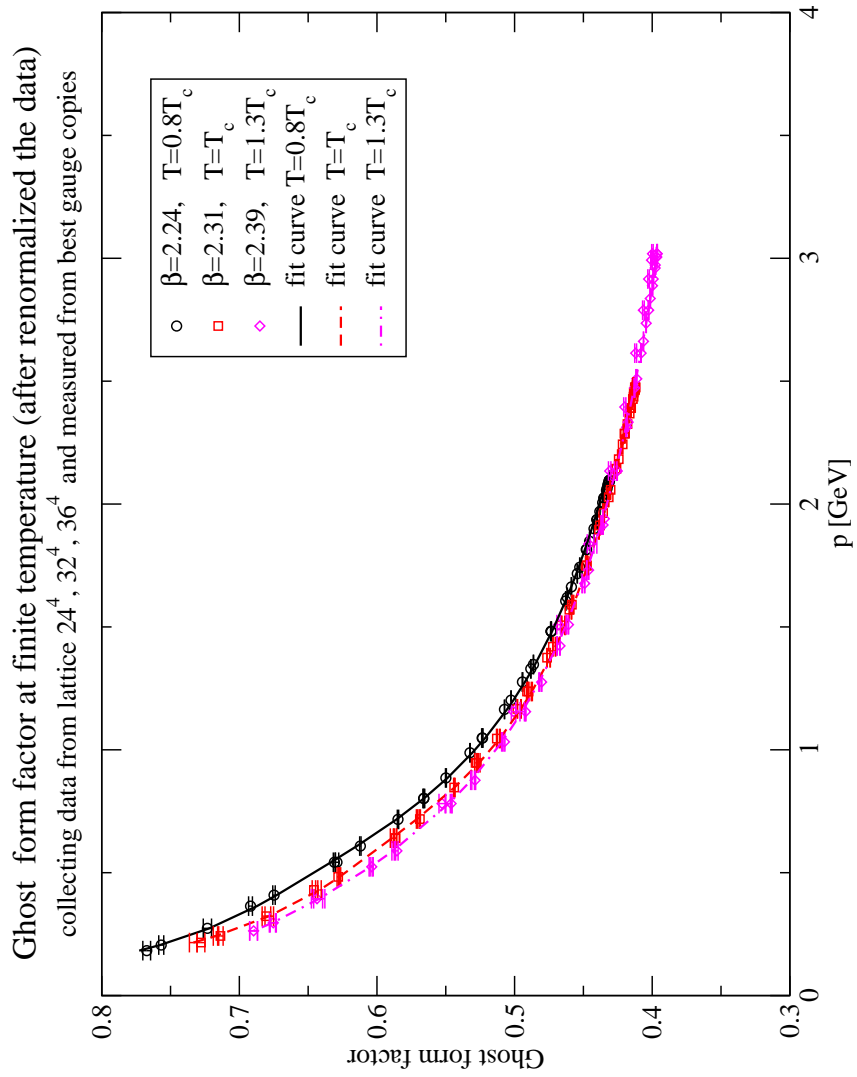


Figure 4.9 Ghost form factor at finite temperature, measured from the best gauge copy lattice 24^4 , 32^4 , 36^4 .

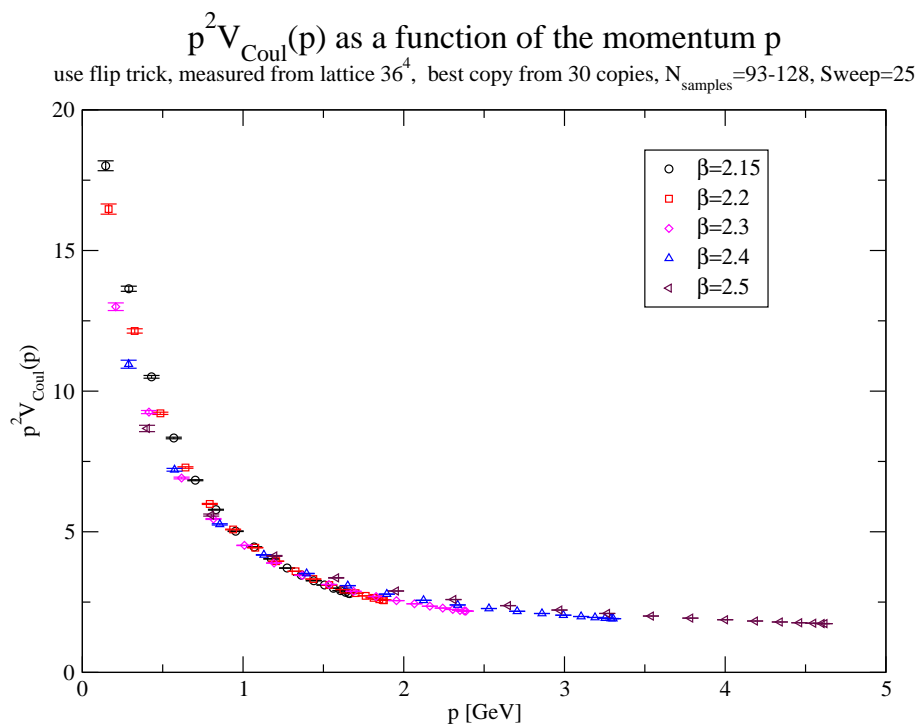


Figure 4.10 The dimensionless $p^2 V(p)$ measured from lattice 36^4 .

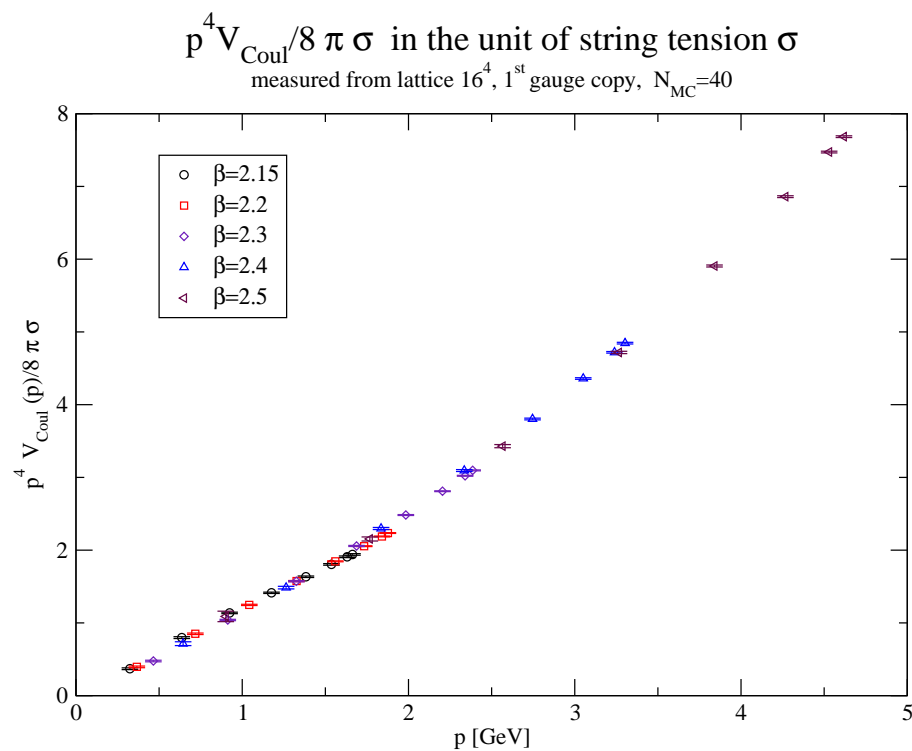


Figure 4.11 $p^4 V_{\text{Coul}}(p)$ in unit of the string tension σ , the result of our project, lattice 16^4 .

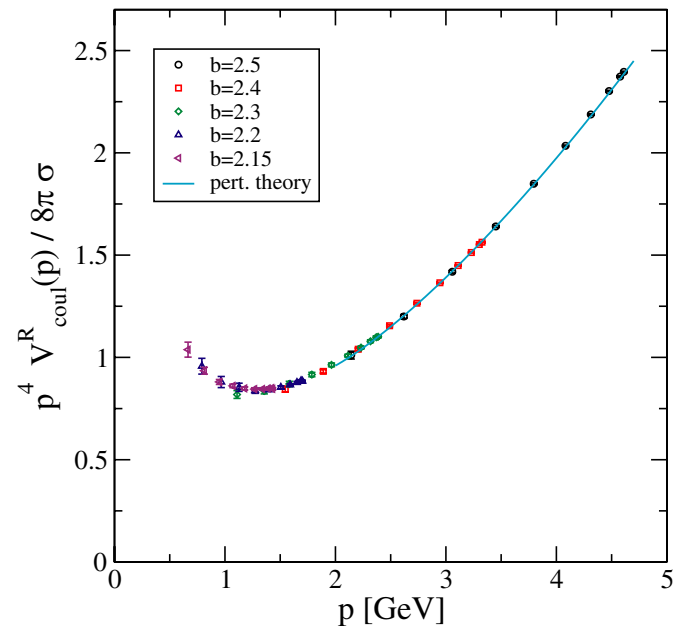


Figure 4.12 $p^4 V_{\text{Coul}}(p)$ in unit of the string tension σ , extracted from (Langfeld and Moyaert, 2004).

CHAPTER V

SUMMARY

We have studied the gluon propagators, ghost form factor and Coulomb potential of the pure $SU(2)$ Yang-Mills theory in Coulomb gauge by lattice simulation at zero and finite temperature. All objects we have measured were extracted at equal time slice. We review the Quantization of Yang-Mills theory and then describe the lattice method we used in our work. Especially, in our work, we implemented the gauge fixing by choosing the best gauge copies for avoid the problem of Gribov copies, and the improved gauge fixed by considering the anti-periodic lattice allowing us to have many choice for making the gauge orbit. This helps us to bring our configuration be near Coulomb gauge condition as it can.

We simulated the gluon propagator in $D = 2 + 1$ at zero temperature which is consistent with (Langfeld and Moyaert, 2004), but in $D = 3 + 1$, our result is different. However our results are consistent with the analytic results (Schleifenbaum et al., 2006; Feuchter and Reinhardt, 2004) which show the suppression of gluon propagator at low momentum. For the finite temperature, we simulated the gluon propagator at temperature $0.8T_c$, T_c and $1.3T_c$, this information will be guide theorists to consider in the future. For the ghost form factors, we simulated at $D = 3 + 1$ at zero temperature. The result agree with the other research group. And at finite temperature, again, we also have the results of ghost form factor at temperature $0.8T_c$, T_c and $1.3T_c$ and having made the fitting curve by the Ansatz formula

$$\frac{A}{(|\log \frac{|p|}{\Lambda}|^{\frac{\gamma_0}{\alpha}} + (\frac{|p|^2}{\Lambda^2})^{\frac{\kappa}{\alpha}})^{\alpha}},$$

and extracted all parameters α , κ and γ_0 . We hope this parameters can be infor-

mation theorist in the future.

Unfortunately, even we can simulate the Coulomb potential, but we have got the peculiar result at zero temperature, that is the glowing down of $p^4V(p)/\sigma$ at low momentum, as other group expect it should be constant at low momentum. With this unacceptable results, we cannot further simulated at finite temperature. In the future, we hope to find the correct result of Coulomb potential at zero temperature by finding some mistake in our code program and then move to investigate at finite temperature. Even in the other research group, they also have different result of Coulomb potential at zero temperature (Voigt et al., 2008; Langfeld and Moyaert, 2004). In future, it is rather possible to see that there may be the using of Coulomb potential as another new order parameter of confinement (Zwanziger, 2004).

REFERENCES

REFERENCES

- Alkofer, R. and Smekal, L. (2001). The infrared behaviour of QCD green's functions. **Phys. Rept.** 353: 281–465.
- Bakeev, A., Ilgenfritz, E.-M., Müller-Preussker, M., and Mitrijushkin, V. (2004). On practical problems to compute the ghost propagator in $SU(2)$ lattice gauge theory. **Phys. Rev. D** 69: 074507.
- Bogolubsky, I., Burgio, G., Müller-Preussker, and Mitrijushkin, V. (2006). Landau gauge ghost and gluon propagators in $SU(2)$ lattice gauge theory: Gribov ambiguity reexamined. **Phys. Rev. D** 74: 034503.
- Christ, N. H. and Lee, T. (1980). Operator ordering and Feynman rules in gauge theories. **Phys. Rev. D** 22: 939.
- Creutz, G. (1983). *Quarks, gluons and lattice*. Cambridge University Press, 1st edition.
- Creutz, M. (1980). Monte carlo study of quantized $SU(2)$ gauge theory. **Phys. Rev. D** 21: 2308–2315.
- Creutz, M., Jacobs, L., and Rebbi, C. (1983). Monte carlo computaions in lattice gauge theories. **Phys. Rept.** 95: 201.
- Cucchieri, A. and Mendes, T. (2007). Just how different are the $SU(2)$ and $SU(3)$ Landau-gauge propagators in the infrared regime? **Phys. Rev. D** 76: 114507.
- Cucchieri, A. and Zwanziger, D. (2001a). Numerical study of the gluon propagator

- and confinement scenario in the minimal Coulomb gauge. **Phys. Rev. D** 65: 014001.
- Cucchieri, A. and Zwanziger, D. (2001b). Renormalization-group calculation of the color-Coulomb potential. **Phys. Rev. D** 65: 014002.
- David Politzer, H. (1973). Reliable perturbative results for strong Interactions. **Phys. Rev. Lett.** 30: 1343.
- Di Giacomo, A. (1988). Monopole condensation and colour confinement. **Prog. Theor. Phys. Suppl.** 131: 161–188.
- Di Giacomo, A., Lucini, B., M. L., and Paffuti, G. (2000a). Colour confinement and dual superconductivity of the vacuum -I. **Phys. Rev. D** 61: 034503.
- Di Giacomo, A., Lucini, B., M. L., and Paffuti, G. (2000b). Colour confinement and dual superconductivity of the vacuum -II. **Phys. Rev. D** 61: 034504.
- Feuchter, C. and Reinhardt, H. (2004). Variational solution of the Yang-Mills Schrödinger equation in Coulomb gauge. **Phys. Rev. D** 70: 105021.
- Greensite, J. (2003). The Confinement problem in lattice gauge theory. **Prog. in Part. and Nucl. Phys.** 51: 1–83.
- Gribov, V. (1978). Quantization of non-abelian gauge theories. **Nucl. Phys. B** 139: 1.
- Gross, J. D., W. F. (1973). Asymptotically free gauge theories I. **Phys. Rev. Lett.** 30: 1346.
- Langfeld, K. and Moyaert, L. (2004). Propagators in Coulomb gauge from $SU(2)$ lattice gauge theory. **Phys. Rev. D** 70: 074504.
- Montvay, I. and Münster, G. (1994). *Quantum Field on a Lattice*. Cambridge University Press, 1st edition.

- Quandt, M., Burgio, G., Chimchinda, S., and Reinhardt, H. (2007). Coulomb gauge Green functions and Gribov copies in $SU(2)$ lattice gauge theory. **arXiv:0710.0549v1[hep-lat]**.
- Rothe, H. J. (2005). *LATTICE GAUGE THEORIES: An Introduction*. World Scientific Lecture Notes in Physics, 3rd edition.
- Schleifenbaum, W., Leder, M., and Reinhardt, H. (2006). Infrared analysis of propagators and vertices of Yang-Mills theory in Landau and Coulomb gauge. **Phys. Rev. D** 73: 125019.
- Shewchuk, J. (1994). *An Introduction to the Conjugate Gradient Method Without the Agonizing Pain*. <http://www.cs.cmu.edu/quake-papers/painless-conjugate-gradient.pdf>.
- Sternbeck, A., Ilgenfritz, E.-M., and Müller-Preussker, M. (2005). Towards the infrared limit in $SU(3)$ Landau gauge lattice gluodynamics. **Phys. Rev. D** 72: 014507.
- 't Hooft, G. (1981). Topology of the gauge condition and new confinement phases in non-abelian gauge theories. **Nucl. Phys. B** 190: 455.
- Voigt, A., Ilgenfritz, E.-M., Müller-Preussker, and Sternbeck, A. (2008). Effective Coulomb potential in $SU(3)$ lattice gauge theory. **Phys. Rev. D** 78: 014501.
- Wilson, K. (1974). Confinement of quarks. **Phys. Rev. D** 10(1): 2445.
- Yang, C. and Mills, R. (1954). Conservation of isotopic spin and isotopic gauge invariance. **Phys. Rev.** 96(1): 191–195.
- Zwanziger, D. (1994). Fundamental modular region, Boltzmann factor and area law in lattice theory. **Nucl. Phys. B** 412: 657–730.

Zwanziger, D. (1998). Renormalization in the Coulomb gauge and the order parameter for confinement in QCD. **Nucl. Phys. B** 518: 237.

Zwanziger, D. (2003). No confinement without Coulomb confinement. **Phys. Rev. Lett.** 90: 102001.

Zwanziger, D. (2004). Analytic calculation of color-Coulomb potential. **Phys. Rev. D** 70: 657–730.

APPENDICES

APPENDIX A

LIST OF NOTATION

Table of notation

\mathcal{L}	Lagrangian function in the fundamental representation of $SU(3)$ group
$\psi(x)$	quark field at space-time point x
$G_\mu^a(x)$	gluon field in the adjoint representation at space-time point x
$U_\mu(x)$	unitary transformation at space-time point x in direction μ
T^α	a generator of $SU(3)$
g	bare coupling constant
D_μ	covariant derivative
$\theta^\alpha(x)$	generic element of the Lie algebra at space-time point x
H	Hamiltonian function
V	Potential
τ	imaginary time
S	action
Z	partition function
β	$4/g^2$ for $SU(2)$ group
Ω	lattice gauge transformation
t^a	hermitian generator
$F_{\mu\nu}$	field strength tensor
A	gauge field potential
Π	canonical conjugated momentum

 Table of notation (Continued)

J	external source
H_{\perp}	Coulomb gauge Hamiltonian
V_{Coul}	Coulomb potential
ρ	color charge density
M	Faddeev-Popov operator
σ	string tension
Ω	Gribov region
$G(t, \vec{p})$	ghost form factor at time t and momentum \vec{p}
$D(t, \vec{p})$	gluon propagator at time t and momentum \vec{p}
$P_{\mu\nu}$	plaquette
a	lattice spacing
L	lattice size
$\mathbb{Z}(2)$	set of integers modulo 2
N_0	lattice size in time direction
T_c	critical temperature
Λ_{QCD}	renormalization group invariant scale parameter

APPENDIX B

GLOSSARY

asymptotic freedom The interactions between quarks are weaker as the distance between them are smaller (at high energy interaction), and tends to zero as the distance between them tends to zero. Conversely, the attractive interaction between quarks are stronger as the distance between them are greater.

Coulomb gauge The gauge condition, or constraint $\nabla \cdot \mathbf{A} = 0$.

Coulomb potential The static potential that is measured from the static quark-antiquark pair by considering in Coulomb gauge. It has gauge invariant property and is the upper bound of the real (Wilson) static potential.

gauge fixing The produce of choosing or fixing the specific gauge into the gauge field which corresponds to put the constraint into the gauge field. The gauge fixing can eliminate the redundant degree of freedom in field variable.

gauge theory The quantum field theories which explain the fundamental interaction by involving a symmetry group of the fields and potentials(the gauge group). The interaction in this theory is explained by the exchange of particles, such as gluons, photon, and W and Z bosons.

ghost form factor One object in quantum field theory, especially in gauge field theory, which can be is measured for each gauge fixing (non-gauge invariant observable). In Coulomb gauge, it is the inverse of Faddeev-Popov operator which is related to the color charge density and is expected to be diverse at low energy QCD.

gluon propagator One object in quantum field theory, especially in gauge field theory, which can be measured for each gauge fixing (non-gauge invariant observable). It measures the correlation function of gluon field and is expected to show the violation of reflection positivity.

fundamental modular region The region of gauge field configurations which is satisfied Coulomb gauge, $\nabla \cdot \mathbf{A} = 0$, and having minimum value of the functional $F[g] = \int dx \text{tr}[A(x) \cdot A^g(x)]$ where $g(x) = \exp(ig_0 \omega^a T^a)$.

Gribov copies The many gauge field potential configurations $A_\mu(x)$ which are satisfied Coulomb or Landau gauge fixing condition.

Landau gauge The gauge condition, or constraint $\partial_\mu A^\mu = 0$.

lattice gauge theory The formulation of gauge theories in which space and time are taken to be lattice, not continuous. At the end of calculations in this theory, it must take the continuum limit.

Markov process A random process in which the rate of change a time-dependent quantity $\partial \mathcal{O} / \partial t$ depends on the present state $\mathcal{O}(t)$, where t is the time, but not on its previous history. That is, its random evolution is memoryless.

Monte Carlo method A type of computation that involves random sampling for the mathematical simulation of physical systems. It can be applied to problems that can be formulated in terms of probability and are carried out by computers.

overrelaxation The method that changes the link variables $U_\mu(x)$ as much as possible in order to relax the system into the gauge fixing condition as quick as it can. During this process, the average plaquette $\langle P_{\mu\nu} \rangle$ value must be constant.

plaquette The product of $SU(2)$ or $SU(3)$ along closed path in each pair μ, ν directions in space-time.

quantum chromodynamics (QCD) The non-Abelian gauge field theory that describes the strong interaction in terms of quarks and antiquarks and the exchange of massless gluon between them. It is similar to quantum electrodynamics with having color charges being analogous to electric charge and the gluon being the analogue of the photon.

quantum field theory A quantum theory combines with special relativity applied to systems that have an infinite number of degrees of freedom. Any particles in this theory are represented by fields that have quantized normal modes of oscillation.

quark confinement The hypothesis that free quarks can never be seen in isolation. It is a consequence of quantum chromodynamics.

Yang-Mills theory A gauge theory based on non-Abelian $SU(N)$ group and is used for an explanation of strong interactions.

APPENDIX C

LIE GROUP BACKGROUND

C.1 $SU(N)$ algebra

Any group element $g \in SU(N)$ defined by

$$g(\omega) = e^{i\omega^a T^a}, \quad (\text{C.1})$$

where T^a form the $N^2 - 1$ hermitian generators basis of Lie algebra and hermitian $\omega^\dagger = \omega$. The generators satisfy the commutation relations

$$[T^a, T^b] = i f^{abc} T^c \quad (\text{C.2})$$

where the numbers f^{abc} are the antisymmetric structure constants of group. They satisfy the Jacobi identity

$$f^{ade} f^{bcd} + f^{bde} f^{cad} + f^{cde} f^{abd} = 0. \quad (\text{C.3})$$

The matrices t^a of the fundamental representation obey the following orthogonality relation:

$$\text{tr}[t^a, t^b] = \frac{1}{2} \delta^{ab}. \quad (\text{C.4})$$

In gauge group $SU(2)$, we use the fundamental representation with the generators

$$t^a = \frac{\tau^a}{2}$$

where each τ^a is the spin Pauli matrix as

$$\tau^1 = \begin{pmatrix} 0 & 1 \\ 1 & 0 \end{pmatrix}, \quad \tau^2 = \begin{pmatrix} 0 & -i \\ i & 0 \end{pmatrix}, \quad \tau^3 = \begin{pmatrix} 1 & 0 \\ 0 & -1 \end{pmatrix}.$$

In this case, the structure constant is

$$f^{abc} = \epsilon^{abc}.$$

C.2 Lagrangian

The Lagrangian of the classical $SU(2)$ Yang-Mills theory is

$$\mathcal{L} = -\frac{1}{4}F_{\mu\nu}^a F_a^{\mu\nu}.$$

When the field is coupling to matter field, we take into account the term $g_0 A_\mu J^\mu$.

That is

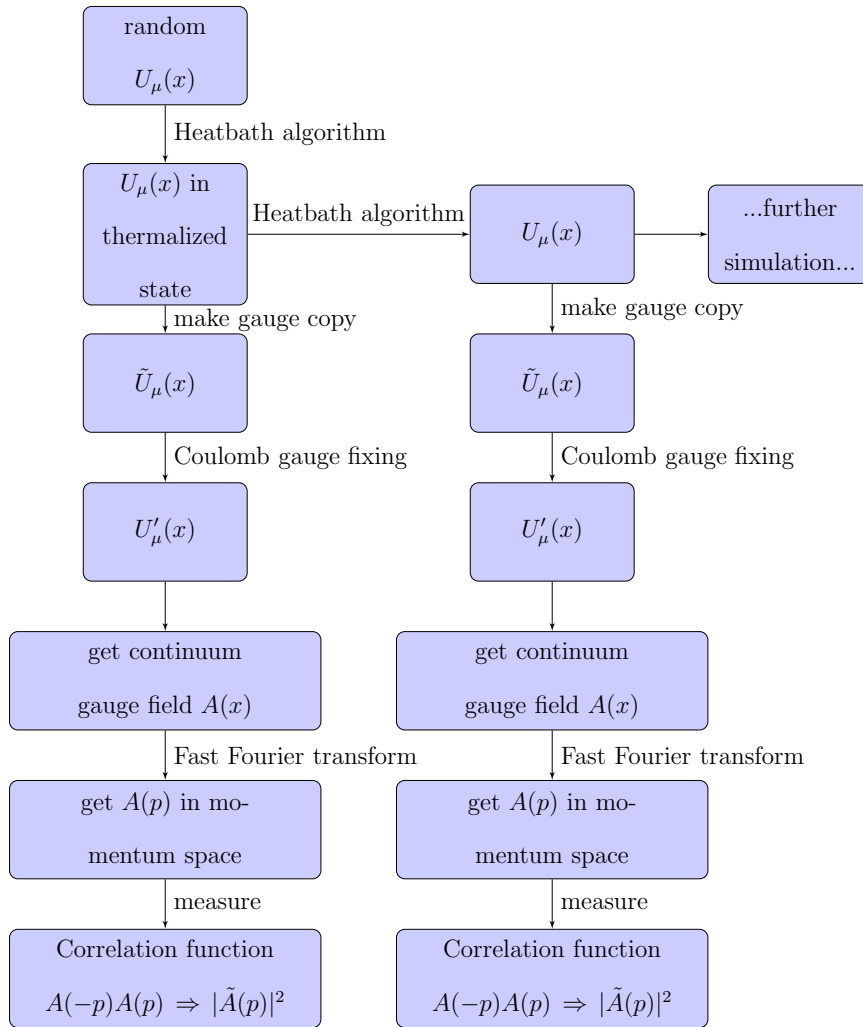
$$\mathcal{L} = -\frac{1}{4}F_{\mu\nu}^a F_a^{\mu\nu} + g_0 A_\mu J^\mu,$$

where g_0 is the coupling constant.

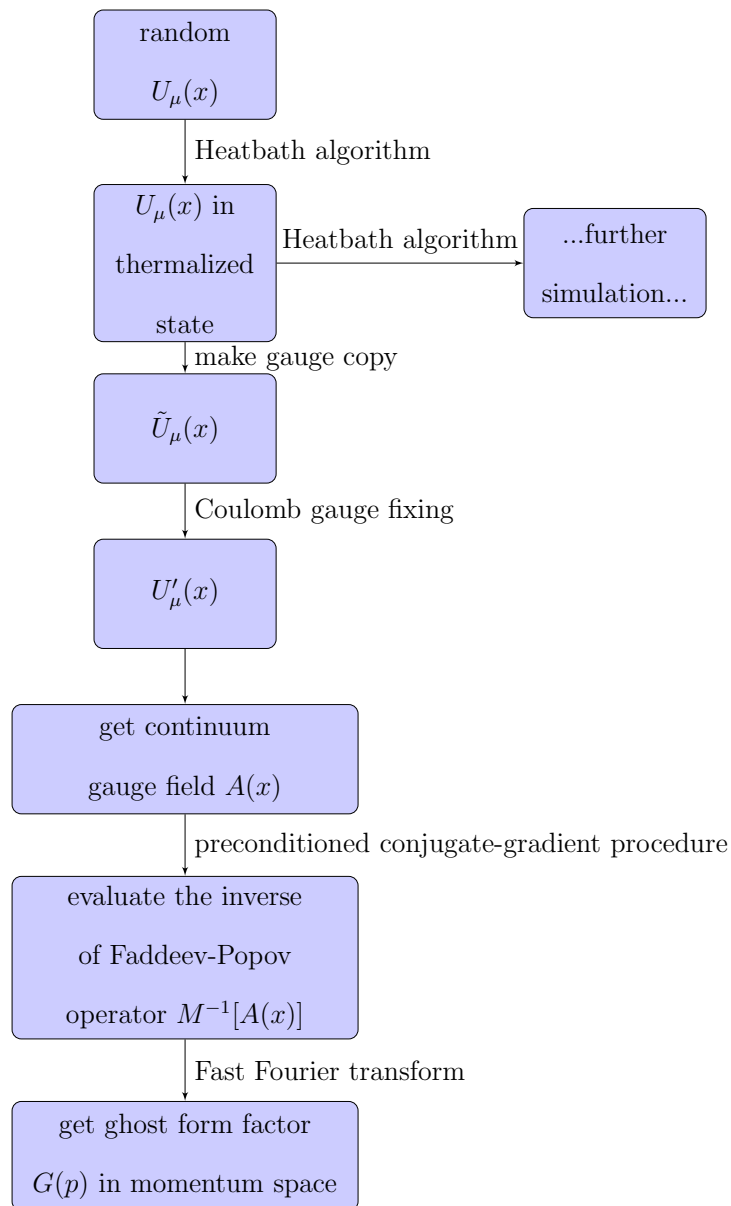
APPENDIX D

FLOWCHART OF PROGRAM

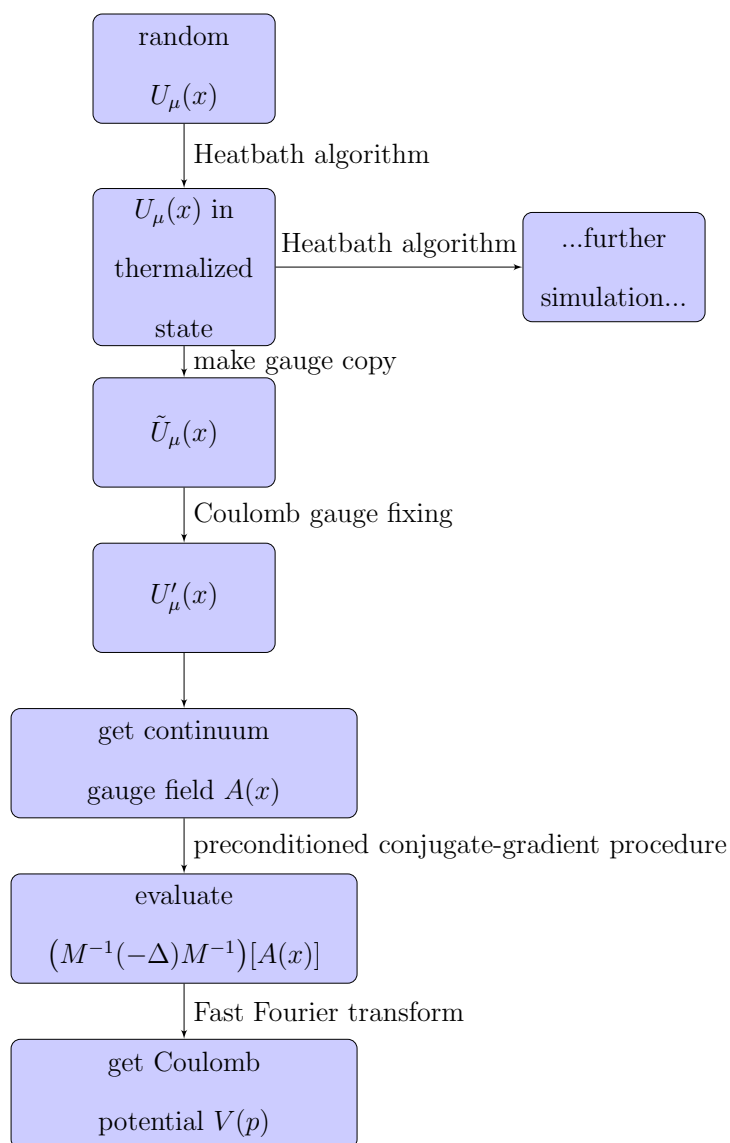
D.1 For gluon propagator measurement



D.2 For ghost form factor measurement



D.3 For Coulomb potential measurement



APPENDIX E

LATTICE CONVENTIONS

E.1 convention and notation

We use natural units $c = \hbar = 1$ and the metric $g_{\mu\nu} = \text{diag}(+, -, -, -)$ in Minkowsky space. Let D as the space-time dimension of spatial hyper-space by d , that is, $D = d + 1$. The Greek symbols: $\mu, \nu, \rho \in [0, 1, \dots, 3]$ are denoted for space-time indices, while Latin symbols: $i, j, k \in [1, \dots, 3]$ are denoted for spatial indices. The lattice is hypercubic, periodic, with edge of in integer length L , then the volume of lattice is $V = L^D$. The link variable $U_\mu(x) \in SU(N)$ associated to the link at space-time x in μ -direction from site x to site $x + \hat{\mu}$, where $\hat{\mu}$ is a unit vector in the positive μ -direction, with periodic boundary condition $U_\mu(x) = U_\mu(x + L\hat{\mu})$.

E.2 Covariant derivative - Gauge potential

The *gauge transformation* of a field $\phi(x)$ defined by

$$\phi(x) \rightarrow g(x)\phi(x) \quad \text{which} \quad g(x) = e^{ig_0\omega^a(x)T^a} \quad (\text{E.1})$$

where g_0 is the bare coupling constant and the number of generators is equal to the dimension of the field belongs. The covariant derivative operator is defined as

$$D_\mu = \partial_\mu - ig_0 A_\mu \quad (\text{E.2})$$

where the gauge potential A_μ is expanded by generator T^a as

$$A_\mu = A_\mu^a T^a. \quad (\text{E.3})$$

In gauge field theory, potential A_μ transforms according to

$$A_\mu = g A_\mu g^{-1} - \frac{i}{g_0} (\partial_\mu) g^{-1} \quad (\text{E.4})$$

for satisfying the being of covariant derivative $D_\mu \rightarrow gD_\mu$. By replacing Eq. (E.1) into Eq. (E.4) and we keep only the first order of α , we obtain

$$A_\mu \rightarrow A_\mu^\alpha + \partial_\mu \alpha^a + g_0 f^{abc} A_\mu^b \alpha^c \quad (\text{E.5})$$

To derive the covariant derivative, we can parametrize a subgroup of gauge group G as one-parameter:

$$g(\tau, x) = \exp(ig_0\tau\omega(x)), \quad (\text{E.6})$$

where ω is an element of the Lie group associated with G and τ is a real parameter.

Replacing Eq. (E.6) into the potential transformation Eq. (E.4), we obtain

$$A_\mu^g(x, \tau) = e^{ig_0\tau\omega(x)} A_\mu(x) e^{-ig_0\tau\omega(x)} + \tau \partial_\mu \omega(x).$$

When we differentiate it with respect to τ and taking the value at $\tau = 0$, we obtain

$$\left[\frac{d}{d\tau} A_\mu^g(x, \tau) \right]_{\tau=0} = \partial_\mu \omega(x) - g_0 [A_\mu, \omega(x)].$$

This formula is the covariant derivative applied to $\omega(x)$.

E.3 Lattice notation

Lattice of space-time and momentum space. The space-time is discretized as the lattice of D -dimensional lattice with lattice spacing a . Any lattice expression can be written as $N_0 \times N_1 \times N_2 \times N_3$. A lattice site is labeled by (x_0, x_1, x_2, x_3) or (n_0a, n_1a, n_2a, n_3a) or (n_0, n_1, n_2, n_3) by which the first number is the time-slice and the latter three numbers are spatial slice. For any function $\hat{f}(x)$ * we define associated with lattice must be satisfied with periodic boundary condition

$$\hat{f}(x + aN_\mu \hat{\mu}) = \hat{f}(x), \quad \mu \in [0, \dots, 3].$$

* \hat{f} or \bar{f} means f -value on lattice, f means f -value on continuum space-time.

The consequence of periodicity, we can transform any function $f(x)$ into a $f(p)$ momentum space by the Fourier transform:

$$\hat{f}(p) = \sum_{n_x=0}^{N-1} \hat{f}(n_x) e^{i\frac{2\pi}{N} n_x n_p}. \quad (\text{E.7})$$

And its inverse of Eq. (E.7) is

$$\hat{f}(x) = N \sum_{n_p=0}^{N-1} \hat{f}(n_p) e^{-i\frac{2\pi}{N} n_x n_p}. \quad (\text{E.8})$$

In practice, any observable G is defined on many variables \bar{x}_μ . We can use notion of Eq. (E.7) and Eq. (E.8) for defining G in momentum space,

$$G(\bar{p}_\mu) = \sum_{\bar{x}_\mu} e^{-i\frac{2\pi}{N} \bar{p}\bar{x}} G(\bar{x}_\mu), \quad (\text{E.9})$$

and

$$G(\bar{x}_\mu) = N \sum_{\bar{p}_\mu} e^{i\frac{2\pi}{N} \bar{p}\bar{x}} G(\bar{p}_\mu), \quad (\text{E.10})$$

Differential operators. We can define

$$\begin{aligned} \hat{\nabla} f(x)_\mu^{(-)} &= f(x) - f(x - \hat{\mu}), \\ \hat{\nabla} f(x)_\mu^{(+)} &= f(x + \hat{\mu}) - f(x). \end{aligned}$$

For the second derivative, we define

$$\hat{\nabla}^2 f(x) = f(x + \hat{\mu}) - 2f(x) - f(x - \hat{\mu}).$$

We can also define Laplacian operator $\hat{\nabla}_\mu^2$ on lattice by

$$\begin{aligned} \hat{\nabla}_\mu^2 G(\bar{x}_\mu) &= \hat{\nabla}^2 \left(N \sum_{\bar{p}_\mu} e^{i\frac{2\pi}{N} \bar{p}\bar{x}} G(\bar{p}_\mu) \right) \\ &= \left(i \frac{2\pi \bar{p}}{N} \right)^2 \left(N \sum_{\bar{p}_\mu} e^{i\frac{2\pi}{N} \bar{p}\bar{x}} G(\bar{p}_\mu) \right) \\ \hat{\nabla}_\mu^2 G(\bar{x}_\mu) &= \left(i \frac{2\pi \bar{p}}{N} \right)^2 G(\bar{x}_\mu) \end{aligned} \quad (\text{E.11})$$

From Eq. (E.11), we can define lattice momentum as

$$\hat{p}_\mu = 2 \sin \left(\frac{\pi}{N} \bar{p} \right).$$

where \bar{p} is Matsubara frequency defined on lattice.

E.4 Lattice gauge potential

For each link variable $U_\mu(x)$ which is the transport along the segment connecting the two adjacent lattice points, it gives the gauge potential from

$$U_\mu(x) = \exp(i\hat{A}_\mu(x)).$$

In order to extract the gauge potential \hat{A} , we consider that

$$U_\mu(x) - U_\mu^\dagger(x) = 2i\hat{A}_\mu(x) + \mathcal{O}(a^2).$$

For $SU(2)$ group, we represent

$$U_\mu(x) = a_\mu^0(x) + i\mathbf{a}_\mu \cdot \boldsymbol{\sigma}.$$

Then we can get \hat{A} by

$$\begin{aligned} \hat{A}_\mu^a &= 2\text{Im tr}[t^a U_\mu(x)] \\ &= 2a_\mu^a(x). \end{aligned}$$

E.5 Lattice gauge-covariant derivative

We can compute the derivative with respect to gauge group $g(x) = e^{i\tau\omega(\mathbf{x})}$, where τ is the parameter. The gauge transformation on lattice can have many conventions, however, in our work, we use the convention

$$U_\mu(\tau, x) = g(\tau, x + \hat{\mu})U_\mu(x)g^\dagger(\tau, x). \quad (\text{E.12})$$

And for the helpful calculating, we can let $g(\tau, x)$ is one-parameter subgroup defined in the other way by

$$g(\tau, x) = \exp(\tau\omega(x)), \quad \omega^\dagger(x) = -\omega(x) \quad (\text{E.13})$$

where τ is real parameter, $\omega(x)$ is a generic element of the local Lie algebra, $\omega(x) = t^a\omega^a(x)$, and t^a form the anti-hermitian basis of the Lie algebra, that is, $(t^a)^\dagger = -t^a$.

From definition of gauge potential $A_\mu^a(x)$ (Zwanziger, 1994)

$$A_\mu^a(x)t^a = \frac{1}{2}(U_\mu(x) - U_\mu^\dagger(x)) \quad (\text{E.14})$$

therefore,

$$A_\mu^a(x) = -2 \operatorname{Re} \operatorname{tr} [t^a U_\mu(x)]. \quad (\text{E.15})$$

Then we can calculate the lattice gauge-covariant derivative by

$$[D_\mu(U)\omega]^a(x) = \frac{d}{d\tau} A_\mu^a(\tau, x). \quad (\text{E.16})$$

E.6 Lattice gauge fixing

The differentiation of the gauge functional $F_U^t[g]$ in Sec. 3.4 with respect to the parameter τ of subgroup $g(x) = \exp(i\tau\omega)$ lead to the Coulomb gauge condition, $\hat{\nabla} \cdot \hat{A} = 0$. We start from the gauge transformation,

$$U_i^\tau(x) = g(x + \hat{\mu})U_i(x)g^\dagger(x).$$

We differentiate with respect to τ , and obtain

$$\frac{d}{d\tau} U_i^\tau(x) = i\omega(x + \hat{\mu})U_i^\tau(x) - iU_i^\tau(x)\omega(x)U_i^\tau(x).$$

Therefore, the derivative of F_U^t is

$$\begin{aligned} \frac{d}{d\tau} F_U^t[\omega, \tau] &= - \sum_{t,i,x} \operatorname{Re} \operatorname{Tr} [i\omega(x + \hat{\mu})U_i^\tau(x) - iU_i^\tau(x)\omega(x)] \\ &= - \sum_{t,i,x} \operatorname{Re} \operatorname{Tr} [i\omega(x)U_i^\tau(x - \hat{\mu}) - iU_i^\tau(x)\omega(x)] \\ &= - \sum_{t,i,x} \operatorname{Re} \operatorname{Tr} [i\omega(x)[U_i^\tau(x - \hat{\mu}) - iU_i^\tau(x)]] \end{aligned}$$

The term $U_i(x - \hat{\mu}) - U_i^\tau(x)$ is $\hat{A}_i^\tau(x - \hat{\mu}) - \hat{A}_i^\tau(x)$, therefore if we can find $U^{g_{\min}}$ which can make

$$\frac{d}{d\tau} F_{U^{g_{\min}}}^t[\omega, \tau] = 0.$$

We conclude that the condition $\hat{A}_i^\tau(x - \hat{\mu}) - \hat{A}_i^\tau(x) = 0$ is satisfied, and the Coulomb gauge condition, $\hat{\nabla} \cdot \hat{A} = 0$, is reached.

E.7 Gluon propagator

Gluon propagator is an observable from lattice simulation. It describes correlation function in momentum space from lattice gauge field. The computers do it by using (discrete) Fast Fourier transform,

$$A_\mu^a(x) \rightarrow \tilde{A}_\mu^a(p)$$

by

$$\tilde{A}_\mu^a(p) \sim \sum_{x_1=0}^{N_1-1} \sum_{x_2=0}^{N_2-1} \sum_{x_3=0}^{N_3-1} e^{-t\frac{2\pi}{N_1}x_1} e^{-t\frac{2\pi}{N_2}x_2} e^{-t\frac{2\pi}{N_3}x_3} A_\mu^a(x) \quad (\text{E.17})$$

and getting the gluon propagator of the lattice momentum from the definition of correlation function, that is, $\langle \tilde{A}_\mu^a(p) \tilde{A}_\nu^b(p') \rangle$ and we can take advantage that let $p' = p$ then our computation is

$$\begin{aligned} \langle \tilde{A}_\mu^a(p) \tilde{A}_\nu^b(p') \rangle &= \langle \tilde{A}_\mu^a(p) \tilde{A}_\nu^b(-p) \rangle \\ &= \langle |\tilde{A}_\mu^a(p)|^2 \rangle \end{aligned}$$

Therefore, gluon propagator is a function of Matsubara frequency l , from the formula,

$$G(l) = \left\langle \sum_{a=1}^3 \sum_{\mu=0}^4 \frac{1}{3} (|\tilde{A}_\mu^a(l, 0, 0)|^2 + |\tilde{A}_\mu^a(0, l, 0)|^2 + |\tilde{A}_\mu^a(0, 0, l)|^2) \right\rangle \quad (\text{E.18})$$

where for each integer $l_i \in [-\frac{N}{2}, \frac{N}{2}]$ corresponds for each $p_i = \frac{2\pi l}{N_i}$ (Matsubara frequency).

E.8 Faddeev-Popov operator

The lattice Faddeev-Popov operator $M = -\nabla \cdot D$ is defined on lattice by

$$(M[U]\omega)^a(x) = -\hat{\nabla}_\mu^{(-)} \cdot (\hat{D}[U]\omega)^a(x).$$

By using the convention, $U_\mu(\tau, x) = g(\tau, x + \hat{\mu})U_\mu(x)g^\dagger(\tau, x)$, we prove the lattice Faddeev-Popov formular by starting from proving the lattice gauge-covariant

derivative,

$$\begin{aligned}
A_\mu^a(\tau, x) &= -2 \operatorname{Re} \operatorname{tr} \{ t^a U'_\mu(\tau, x) \} \\
&= -2 \operatorname{Re} \operatorname{tr} \left\{ t^a \frac{d}{d\tau} [g(x + \hat{\mu}) U_\mu(x) g^\dagger(x)] \right\} \\
&= -2 \operatorname{Re} \operatorname{tr} \left\{ t^a \frac{d}{d\tau} [\exp(\tau\omega(x + \hat{\mu})) U_\mu(x) \exp(-\tau\omega(x))] \right\} \\
&= -2 \operatorname{Re} \operatorname{tr} \{ t^a [\omega(x + \hat{\mu}) U_\mu(\tau, x) - U_\mu(\tau, x) \omega(x)] \} \\
&= -2 \operatorname{Re} \operatorname{tr} \{ t^a \omega(x + \hat{\mu}) U_\mu(\tau, x) - t^a U_\mu(\tau, x) \omega(x) \} \\
&= -2 \operatorname{Re} \operatorname{tr} \{ t^a \omega(x + \hat{\mu}) U_\mu(\tau, x) - \omega(x) t^a U_\mu(\tau, x) \}. \tag{E.19}
\end{aligned}$$

Consider the term

$$\begin{aligned}
&-2 \operatorname{Re} \operatorname{tr} \{ t^a \omega(x + \hat{\mu}) U_\mu(\tau, x) - \omega(x) t^a U_\mu(\tau, x) \} \\
&= -\operatorname{tr} \{ t^a \omega(x + \hat{\mu}) U(\tau, x) - \omega(x) t^a U(\tau, x) \\
&\quad + (t^a \omega(x + \hat{\mu}) U(\tau, x))^\dagger - (\omega(x) t^a U(\tau, x))^\dagger \} \\
&= -\operatorname{tr} \{ t^a \omega(x + \hat{\mu}) U(\tau, x) - \omega(x) t^a U(\tau, x) \\
&\quad + U^\dagger(\tau, x) (t^a \omega(x + \hat{\mu}))^\dagger - U^\dagger(\tau, x) (\omega(x) t^a)^\dagger \} \\
&= -\operatorname{tr} \{ t^a \omega(x + \hat{\mu}) U(\tau, x) - \omega(x) t^a U(\tau, x) \\
&\quad + \omega(x + \hat{\mu}) t^a U^\dagger(\tau, x) - t^a \omega(x) U^\dagger(\tau, x) \}. \\
&= -\operatorname{tr} \{ (\star\star) \},
\end{aligned}$$

where

$$(\star\star) \equiv t^a \omega(x + \hat{\mu}) U(\tau, x) - \omega(x) t^a U(\tau, x) + \omega(x + \hat{\mu}) t^a U^\dagger(\tau, x) - t^a \omega(x) U^\dagger(\tau, x).$$

Therefore,

$$\begin{aligned}
&-2 \operatorname{Re} \operatorname{tr} \{ t^a \omega(x + \hat{\mu}) U_\mu(\tau, x) - \omega(x) t^a U_\mu(\tau, x) \} \\
&= -\operatorname{tr} \{ t^a \omega(x + \hat{\mu}) U(\tau, x) + \omega(x + \hat{\mu}) t^a U(\tau, x) - \omega(x + \hat{\mu}) t^a U(\tau, x) \\
&\quad - \omega(x) t^a U(\tau, x) - t^a \omega(x) U(\tau, x) + t^a \omega(x) U(\tau, x) \\
&\quad + \omega(x + \hat{\mu}) t^a U^\dagger(\tau, x) + t^a \omega(x + \hat{\mu}) U^\dagger(\tau, x) - t^a \omega(x + \hat{\mu}) U^\dagger(\tau, x) \\
&\quad - t^a \omega(x) U^\dagger(\tau, x) - \omega(x) t^a U^\dagger(\tau, x) + \omega(x) t^a U^\dagger(\tau, x) \}
\end{aligned}$$

$$\begin{aligned}
&= -\text{tr}\{ \{\omega(x + \hat{\mu}), t^a\}U(\tau, x) - \omega(x + \hat{\mu})t^aU(\tau, x) \\
&\quad - \{\omega(x), t^a\}U(\tau, x) + t^a\omega(x)U(\tau, x) \\
&\quad + \{\omega(x + \hat{\mu}), t^a\}U^\dagger(\tau, x) - t^a\omega(x + \hat{\mu})U^\dagger(\tau, x) \\
&\quad - \{\omega(x), t^a\}U^\dagger(\tau, x) + \omega(x)t^aU^\dagger(\tau, x) \} \\
&= -\text{tr}\{ \{\omega(x + \hat{\mu}) - \omega(x), t^a\}U(\tau, x) + \{\omega(x + \hat{\mu}) - \omega(x), t^a\}U^\dagger(\tau, x) \\
&\quad - \omega(x + \hat{\mu})t^aU(\tau, x) + t^a\omega(x)U(\tau, x) \\
&\quad - t^a\omega(x + \hat{\mu})U^\dagger(\tau, x) + \omega(x)t^aU^\dagger(\tau, x) \} \\
&= -\text{tr}\{ \{\omega(x + \hat{\mu}) - \omega(x), t^a\}(U(\tau, x) + U^\dagger(\tau, x)) \\
&\quad - \omega(x + \hat{\mu})t^aU(\tau, x) + t^a\omega(x)U(\tau, x) \\
&\quad - t^a\omega(x + \hat{\mu})U^\dagger(\tau, x) + \omega(x)t^aU^\dagger(\tau, x) \} \\
&= -\text{tr}\{ \{\omega(x + \hat{\mu}) - \omega(x), t^a\}(U(\tau, x) + U^\dagger(\tau, x)) \\
&\quad - \omega(x + \hat{\mu})t^aU(\tau, x) + t^a\omega(x + \hat{\mu})U(\tau, x) - t^a\omega(x + \hat{\mu})U(\tau, x) \\
&\quad + t^a\omega(x)U(\tau, x) - \omega(x)t^aU(\tau, x) + \omega(x)t^aU(\tau, x) \\
&\quad - t^a\omega(x + \hat{\mu})U^\dagger(\tau, x) + \omega(x + \hat{\mu})t^aU^\dagger(\tau, x) - \omega(x + \hat{\mu})t^aU^\dagger(\tau, x) \\
&\quad + \omega(x)t^aU^\dagger(\tau, x) - t^a\omega(x)U^\dagger(\tau, x) + t^a\omega(x)U^\dagger(\tau, x) \} \\
&= -\text{tr}\{ \{\omega(x + \hat{\mu}) - \omega(x), t^a\}(U(\tau, x) + U^\dagger(\tau, x)) \\
&\quad - [\omega(x + \hat{\mu}), t^a]U(\tau, x) - t^a\omega(x + \hat{\mu})U(\tau, x) \\
&\quad - [\omega(x), t^a]U(\tau, x) + \omega(x)t^aU(\tau, x) \\
&\quad + [\omega(x + \hat{\mu}), t^a]U^\dagger(\tau, x) - \omega(x + \hat{\mu})t^aU^\dagger(\tau, x) \\
&\quad + [\omega(x), t^a]U^\dagger(\tau, x) + t^a\omega(x)U^\dagger(\tau, x) \} \\
&-2 \text{Re tr} \{ t^a\omega(x + \hat{\mu})U_\mu(\tau, x) - \omega(x)t^aU_\mu(\tau, x) \}
\end{aligned}$$

$$\begin{aligned}
&= -\text{tr}\{ \{ \omega(x + \hat{\mu}) - \omega(x), t^a \} (U(\tau, x) + U^\dagger(\tau, x)) \\
&\quad - [\omega(x + \hat{\mu}) + \omega(x), t^a] U(\tau, x) \\
&\quad + [\omega(x + \hat{\mu}) + \omega(x), t^a] U^\dagger(\tau, x) \\
&\quad - t^a \omega(x + \hat{\mu}) U(\tau, x) + \omega(x) t^a U(\tau, x) \\
&\quad - \omega(x + \hat{\mu}) t^a U^\dagger(\tau, x) + t^a \omega(x) U^\dagger(\tau, x) \} \\
&= -\text{tr}\{ \{ \omega(x + \hat{\mu}) - \omega(x), t^a \} (U(\tau, x) + U^\dagger(\tau, x)) \\
&\quad - [[\omega(x + \hat{\mu}) + \omega(x)], t^a] (U(\tau, x) - U^\dagger(\tau, x)) \\
&\quad - t^a \omega(x + \hat{\mu}) U(\tau, x) + \omega(x) t^a U(\tau, x) \\
&\quad - \omega(x + \hat{\mu}) t^a U^\dagger(\tau, x) + t^a \omega(x) U^\dagger(\tau, x) \} \tag{E.20}
\end{aligned}$$

$$\begin{aligned}
&= -\text{tr}\{ \{ , \} (U + U^\dagger) - [,] (U - U^\dagger) \} \\
&\quad - \text{tr} \{ -t^a \omega(x + \hat{\mu}) U(\tau, x) + \omega(x) t^a U(\tau, x) \\
&\quad \quad - \omega(x + \hat{\mu}) t^a U^\dagger(\tau, x) + t^a \omega(x) U^\dagger(\tau, x) \} \\
&= -\text{tr}\{ \{ , \} (U + U^\dagger) - [,] (U - U^\dagger) \} \\
&\quad + \text{tr} \{ t^a \omega(x + \hat{\mu}) U(\tau, x) - \omega(x) t^a U(\tau, x) \\
&\quad \quad + \omega(x + \hat{\mu}) t^a U^\dagger(\tau, x) - t^a \omega(x) U^\dagger(\tau, x) \} \\
&= -\text{tr}\{ \{ , \} (U + U^\dagger) - [,] (U - U^\dagger) \} \\
&\quad + \text{tr} \{ (\star\star) \} \tag{E.21}
\end{aligned}$$

$$\begin{aligned}
-2\text{tr}[(\star\star)] &= -\text{tr}\{ \{ , \} (U + U^\dagger) - [,] (U - U^\dagger) \} \\
-\text{tr}[(\star\star)] &= -\frac{1}{2}\text{tr}\{ \{ , \} (U + U^\dagger) - [,] (U - U^\dagger) \} \tag{E.22}
\end{aligned}$$

$$\begin{aligned}
A_\mu^{ta}(\tau, x) &= -\text{tr}(\star\star) \\
&= -\frac{1}{2}\text{tr}(\{ [\omega(x + \hat{\mu}) - \omega(x)], t^a \} (U(\tau, x) + U^\dagger(\tau, x)) \\
&\quad - [[\omega(x + \hat{\mu}) + \omega(x)], t^a] (U(\tau, x) - U^\dagger(\tau, x))) \tag{E.23}
\end{aligned}$$

Consider each term,

$$\begin{aligned}
& \bullet - \frac{1}{2} \text{tr} (\{ [\omega(x + \hat{\mu}) - \omega(x)], t^a \} (U(\tau, x) + U^\dagger(\tau, x))) \\
& \bullet - \frac{1}{2} \text{tr} ([\omega^b(x + \hat{\mu}) - \omega^b(x)] \{ t^b, t^a \} (U(\tau, x) + U^\dagger(\tau, x))) \\
& \bullet - \frac{1}{2} \text{tr} (\{ t^a, t^b \} (U(\tau, x) + U^\dagger(\tau, x))) \underbrace{[\omega^b(x + \hat{\mu}) - \omega^b(x)]}_{G_\mu^{ab}(x)}. \tag{E.24}
\end{aligned}$$

and another term,

$$\begin{aligned}
& \bullet + \frac{1}{2} \text{tr} ([[\omega(x + \hat{\mu}) + \omega(x)], t^a] (U(\tau, x) - U^\dagger(\tau, x))) \\
& \bullet + \frac{1}{2} \text{tr} ((\omega^b(x + \hat{\mu}) + \omega^b(x)) [t^b, t^a] (U(\tau, x) - U^\dagger(\tau, x))) \\
& \bullet + \frac{1}{2} \text{tr} ((\omega^b(x + \hat{\mu}) + \omega^b(x)) f^{bac} t^c (U(\tau, x) - U^\dagger(\tau, x))) \\
& \bullet + \frac{1}{2} \text{tr} (f^{abc} (\omega^b(x + \hat{\mu}) + \omega^b(x)) (-t^c (U(\tau, x) - U^\dagger(\tau, x)))) \\
& \bullet + \frac{1}{2} f^{abc} (\omega^b(x + \hat{\mu}) + \omega^b(x)) \underbrace{-\text{tr} (t^c (U(\tau, x) - U^\dagger(\tau, x)))}_{A_\mu^c(x)} \\
& \bullet + \frac{1}{2} f^{abc} (\omega^b(x + \hat{\mu}) + \omega^b(x)) A_\mu^c(x) \\
& \bullet - \frac{1}{2} f^{abc} A_\mu^b(x) (\omega^c(x + \hat{\mu}) + \omega^c(x)). \tag{E.25}
\end{aligned}$$

Therefore, we have the explicit form of the gauge-covariant derivative,

$$\begin{aligned}
A_\mu^a(\tau, x) &= G_\mu^{ab} [\omega^b(x + \hat{\mu}) + \omega^b(x)] \\
&\quad - \frac{1}{2} f^{abc} A_\mu^b(x) [\omega^c(x + \hat{\mu}) + \omega^c(x)]. \tag{E.26}
\end{aligned}$$

Then we compute directly the lattice Faddeev-Popov operator,

$$\begin{aligned}
M &= -\nabla \cdot D(U) \\
&= -\nabla \cdot (G_\mu^{ab}[\omega(x + \hat{\mu}) + \omega(x)]^b - \frac{1}{2}f^{abc}A_\mu^b(x)[\omega(x + \hat{\mu}) + \omega(x)]^c) \\
&= -\{G_\mu^{ab}(x)(\omega^b(x + \hat{\mu}) - \omega^b(x)) - G_\mu^{ab}(x - \hat{\mu})\mu(\omega^b(x) - \omega^b(x + \hat{\mu})) \\
&\quad - \frac{1}{2}f^{abc}[A_\mu^b(x)[\omega(x + \hat{\mu}) + \omega(x)]^c - A_\mu^b(x - \hat{\mu})[\omega(x) + \omega(x - \hat{\mu})]^c]\} \\
&= G_\mu^{ab}(x)(\omega^b(x) - \omega^b(x + \hat{\mu})) - G_\mu^{ab}(x - \hat{\mu})(\omega^b(x - \hat{\mu}) - \omega^b(x)) \\
&\quad + \frac{1}{2}f^{abc}[A_\mu^b(x)\omega^c(x + \hat{\mu}) + \underbrace{A_\mu^b(x)\omega^c(x) - A_\mu^b(x - \hat{\mu})\omega^c(x) - A_\mu^b(x - \hat{\mu})\omega^c(x - \hat{\mu})}_{(A_\mu^b(x) - A_\mu^b(x - \hat{\mu}))\omega^c(x) \rightarrow \nabla \cdot A = 0}] \\
M &= G_\mu^{ab}(x)(\omega^b(x) - \omega^b(x + \hat{\mu})) - G_\mu^{ab}(x - \hat{\mu})(\omega^b(x - \hat{\mu}) - \omega^b(x)) \\
&\quad + \frac{1}{2}f^{abc}[A_\mu^b(x)\omega^c(x + \hat{\mu}) - A_\mu^b(x - \hat{\mu})\omega^c(x - \hat{\mu})]. \tag{E.27}
\end{aligned}$$

Finally, we obtain

$$\begin{aligned}
(M[U]\omega)^a(x) &= \sum_\mu \{G_\mu^{ab}(x)\hat{\nabla}_\mu^{(+)}\omega^b(x) - G_\mu^{ab}(x - a\hat{e}_\mu)\hat{\nabla}_\mu^{(+)}\omega^b(x - a\hat{e}_\mu) \\
&\quad - \frac{1}{2}f^{abc}[\hat{A}_\mu\omega^c(x + ae_\mu)]\}. \tag{E.28}
\end{aligned}$$

Then the practical formula we use in the program is

$$\begin{aligned}
[\hat{M}[U]\omega^a(x)] &= \sum_\mu \{ a_\mu^0(x)(\omega^a(x) - \omega^a(x + \hat{\mu})) \\
&\quad - a_\mu^0(x - \hat{\mu})(\omega^a(x - \hat{\mu}) - \omega^a(x)) \\
&\quad + \frac{1}{2}f^{abc}[2a_\mu^b(x)\omega^c(x + \hat{\mu}) - 2a_\mu^b(x - \hat{\mu})\omega^c(x - \hat{\mu})]\}.
\end{aligned}$$

E.9 Coulomb potential

In order to compute Coulomb potential in momentum space from Eq. (3.61).

We implement the program according to the following procedure.

1. We set the goal that we will compute $\langle M^{-1}[A](-\Delta)M^{-1}[A]e^{-i\vec{k}\cdot\vec{x}} \rangle$.

2. Then we will compute the inverse matrix by conjugate-gradient method

$$\left(M[A](-\Delta)^{-1}M[A]\right)\phi^a(x) = \{\delta^{ac}e^{-ikx}\} \quad (\text{E.29})$$

$$\phi^a(x) = \left(M^{-1}[A](-\Delta)M^{-1}[A]\right)\delta^{ac}e^{-i\vec{k}\cdot\vec{x}} \quad (\text{E.30})$$

where c is color index, in set $\{1, 2, 3\}$. Therefore, we must find the appropriate representation of inverse Laplacian, $(-\Delta)^{-1}$.

The representation of $(-\Delta)^{-1}$ is found from

- (a) starting from the assumption that any lattice function in space-time, $f(\hat{x})$, can be represented by Fourier series in momentum- k -space, (3-dimensions for Coulomb gauge)

$$f(\hat{x}) = \frac{1}{N_1N_2N_3} \sum_{\hat{k}=0}^{N-1} f(\hat{k})e^{-i\frac{2\pi}{N}\hat{x}\hat{k}}.$$

When we operate $(-\Delta)$ on $f(\hat{x})$, I obtain

$$-\Delta f(\hat{x}) = \frac{1}{N_1N_2N_3} \sum_{\hat{k}=0}^{N-1} (\hat{k}_1^2 + \hat{k}_2^2 + \hat{k}_3^2) f(\hat{k})e^{-i\frac{2\pi}{N}\hat{x}\hat{k}}. \quad (\text{E.31})$$

That means $(-\Delta)$ can be represented as \hat{k}^2 , therefore $(-\Delta)^{-1}$ should be represented as $\frac{1}{\hat{k}^2}$,

- (b) When applying $(-\Delta)^{-1}$ to the field $f(\hat{x})$, it should be represented by the formula,

$$(-\Delta)^{-1}f(\hat{x}) = \frac{1}{N_1N_2N_3} \sum_{\hat{k}=0}^{N-1} \frac{f(\hat{k})}{(\hat{k}_1^2 + \hat{k}_2^2 + \hat{k}_3^2) + \frac{1}{N^2}} e^{-i\frac{2\pi}{N}\hat{x}\hat{k}}. \quad (\text{E.32})$$

Eq. (E.32) is able to implemented by 3-dimensional-Fast-Fourier from *complex* to *real* numbers. In summary,

$$(-\Delta)^{-1} \rightarrow \mathcal{F}^{-1} \frac{1}{p^2} \mathcal{F}$$

where \mathcal{F} is Fourier Transform.

3. computing $(M(-\Delta)^{-1}M)\phi(x) = \{\delta^{ac}e^{-i2\pi\vec{k}\cdot\vec{x}}\}$ by

(a) let $M\phi(x) \Rightarrow M_{xy}\phi(y) = \varphi(x)$

(b) then $(-\Delta)^{-1}\varphi(x) \Rightarrow (-\Delta)^{-1}\varphi(x) \equiv \xi(x)$

(c) then we operate with Faddeev-Popov operator again,

$$\begin{aligned} M_{xy}\xi(y) &\equiv \eta(y) = \delta^{ac}e^{-i\vec{k}\cdot\vec{x}} \\ \phi^a(x) &= \eta^{-1}(y)\delta^{ac}e^{-i\vec{k}\cdot\vec{y}} \end{aligned} \quad (\text{E.33})$$

4. Made the Fourier transform of $\phi^a(x) = \langle M^{-1}[U](-\Delta)M^{-1}[U] \rangle$:

$$\begin{aligned} \hat{V}_{\text{Coul}}(\hat{k}) &= \frac{-1}{4N_d}g_0^{2d-4} \sum_{a=1}^3 \sum_{\hat{x},\hat{y}}^{N_d} \langle M^{-1}[U](-\Delta)M^{-1}[U] \rangle \exp(-i\frac{2\pi}{N_d}\vec{p}\cdot(\vec{x}-\vec{y})) \\ \hat{V}_{\text{Coul}}(\hat{k}) &= \frac{-1}{4N_1N_2N_3}g_0^{2d-4} \sum_{a=1}^3 \sum_{\hat{x}} \phi^a(x)e^{-i\hat{k}\cdot\hat{x}} \\ &= \frac{-1}{4N_1N_2N_3}\frac{4}{\beta} \sum_{a=1}^3 \sum_{\hat{x}} \phi^a(x)e^{-i\hat{k}\cdot\hat{x}} \\ \hat{V}_{\text{Coul}}(\hat{k}) &= \frac{-1}{N_1N_2N_3}\frac{1}{\beta} \sum_{a=1}^3 \sum_{\hat{x}} \phi^a(x)e^{-i\hat{k}\cdot\hat{x}} \end{aligned} \quad (\text{E.34})$$

Eq. (E.34) is used in case of $d = 3$ (spatial dimensions), and $\beta = \frac{4}{g_0^2}$ (bare coupling constant for $SU(2)$).

APPENDIX F

LATTICE ALGORITHM

F.1 Heatbath algorithm : pseudocode

```
//INPUT: - Sum of neighbouring matrices V for the local variable U
coupling constant beta

//OUTPUT: -A SU(2) matrix U distributed w.r.t. Gibb's measure

k = sqrt(det(V)); V1 = V / k;

k1 = k * beta;

for(;;)
{
z = ran(exp(-2*k1),1); // uniform distribution
b0 = 1 + log (z)/k1;
rho = sqrt{1 - b0 * b0 };
r = ran(0,1); // uniform distribution
if (r< rho) break;
}

phi = ran(0, 2*Pi); // uniform distribution
t = ran(-1, 1); // uniform distribution
u = rho * sqrt{ 1- t*t}
b1 = u * cos(phi);
b2 = u * sin(phi);
b3 = rho * t;
U1 = SU2(b0,b1,b2,b3);
U = U1 * inverse(V1);
```

F.2 Relaxation

From the gauge transformation $U_\mu^g(x) = g(x + \hat{\mu})U_\mu(x)g^\dagger(x)$, an element $g(x)$ of $SU(2)$ group can attribute in the gauge transformation at site x by

$$U_\mu^g(x, t) = U_\mu(x, t)g^\dagger(x)$$

$$U_\mu^g(x - \hat{k}, t) = g(x, t)U_k(x - \hat{k}, t).$$

We want to find $g(x)$ which can minimize the functional Eq. (3.43) at fixed t_0 time-slice. By considering the attributing of $g(x, t)$ into lattice, the best choice is computed from the following procedure:

$$F^t[g] = \sum_{\mathbf{x}} \sum_{i=1}^3 \frac{1}{2} \text{tr}[1 - U_i^g(\mathbf{x}, t)]$$

$$= \sum_{\mathbf{x}} \sum_{i=1}^3 \frac{1}{2} \text{tr}[1 - g(x + \hat{i})U_i(x, t)g^\dagger(x)],$$

$$F^t[g] = \text{const} - \frac{1}{2} \sum_x \text{tr} \left\{ \sum_{i=1}^3 g(x + \hat{i})U_i(x, t)g^\dagger(x) \right. \\ \left. + \sum_{i=1}^3 g(x)U_i(x - \hat{i}, t)g^\dagger(x - \hat{i}, t) \right\},$$

$$F^t[g] = \text{const} - \frac{1}{2} \sum_x \text{Re tr} \left\{ \sum_{i=1}^3 (g(x + \hat{i})U_i(x, t))^\dagger \right. \\ \left. + U_i(x - \hat{i}, t)g^\dagger(x - \hat{i}, t) \right\} g(x, t),$$

$$F^t[g] = \text{const} - \frac{1}{2} \sum_x \text{Re tr} \left\{ \left[\sum_{i=1}^3 (g(x + i, t)U_i(x, t))^\dagger \right. \right. \\ \left. \left. + (U_i(x - i, t)g^\dagger(x - i, t)) \right] \right\},$$

$$F^t[g] = \text{const} - \frac{1}{2} \sum_x \text{Re tr} \left\{ \underbrace{g(x, t)}_{\neq \mathbb{I}} \left[\sum_{i=1}^3 \underbrace{(g(x + i, t)U_i(x, t))^\dagger}_{=1} \right. \right. \\ \left. \left. + (U_i(x - i, t) \underbrace{g^\dagger(x - i, t)}_{=1}) \right] \right\},$$

$$\begin{aligned}
F^t[g] &= \text{const} - \frac{1}{2} \sum_x \text{Re tr} \left\{ g(x, t) \underbrace{\left[\sum_{i=1}^3 (U_i^\dagger(x, t) + U_i(x - i, t)) \right]}_{\text{Let it be } V(x, t)} \right\}, \\
&= \text{const} - \frac{1}{2} \sum_x \text{Re tr} g(x, t) V(x, t).
\end{aligned}$$

The solution comes from $g(x, t)V(x, t) \sim \mathbb{I}$, therefore,

$$g(\mathbf{x}, t) = \frac{V^\dagger(x, t)}{\sqrt{\det V(x, t)}},$$

where

$$V(x, t) = \sum_{k=1}^3 \left\{ U_k^\dagger(x, t) + U_k(x - k, t) \right\}.$$

F.2.1 Overrelaxation

In gauge transformation, $U_\mu^g(x) = g(x + \hat{\mu})U_\mu(x)g^\dagger(x)$, the $g(x) \in SU(2)$ can be approximated as

$$\begin{aligned}
g(x) &\approx \mathbb{I} \\
g(x) &= \exp \left\{ i\theta^a(x) \frac{\sigma^a}{2} \right\} \\
&= \cos\theta(x)\mathbb{I} + i\hat{\theta}_k(x)\sigma_k(x) \sin\theta.
\end{aligned}$$

The overrelaxation in Sec. 3.4.1 is implemented by set $\alpha = 1.75$. Therefore,

$$\begin{aligned}
g^\alpha(x) &= \exp \left\{ i\alpha\theta^a(x) \frac{\sigma^a}{2} \right\} \\
&= \cos\theta(x)\mathbb{I} + i\alpha\theta_k\sigma_k(x) \sin\theta(x)
\end{aligned}$$

To accelerate the relaxation process, we can modify $g(x)$ when $F_t^g(x) < 10^{-3}$

by starting the following procedure:

$$\begin{aligned}
 &\text{if } (a_0 < 0), \quad g(x) = -g(x), \\
 &\quad a_1 \leftarrow a_1 \cdot \alpha, \\
 &\quad a_2 \leftarrow a_2 \cdot \alpha, \\
 &\quad a_3 \leftarrow a_3 \cdot \alpha, \\
 &g(x) \leftarrow \frac{g(x)}{\sqrt{\det g(x)}}.
 \end{aligned}$$

These can accelerate the decreasing of $F_t^g[g(x)]$, and avoid the critical slowing down.

F.2.2 Flip trick

We use the flip trick by monitoring the gauge functional value from Eq. (3.43). Because we want to minimize, when $F_t^g[g(x)] > 0$, we implement the antiperiodic condition $g(x + L\hat{\nu}) = -g(x)$, by for all time slice t

$$\begin{aligned}
 &\text{if } \sum_x \text{Re tr} U_0(t, x) > 0, \\
 &\quad \text{then } U_0(t, x) = -U_0(t, x) \text{ for all } x,
 \end{aligned}$$

and at the fixed t time slice

$$\begin{aligned}
 &\text{if } \sum_{x_j, x_k \neq x_i} \text{Re tr} U_i(t, x_i, x_j, x_k) > 0, \\
 &\quad \text{then } U_i(t, x_i, x_j, x_k) = -U_i(t, x_i, x_j, x_k) \text{ for all } t = 0, \dots, N_0 - 1,
 \end{aligned}$$

F.3 Conjugate gradient method

The conjugate gradient method we use in this thesis is used for solving the inverse problem for ghost field $\vec{\phi}$ from

$$M\vec{\phi}(x) = \vec{\psi}(x) \tag{F.1}$$

where $\vec{\psi}(x)$ is a plane wave $\vec{\psi}_c(x) = \{\delta_{ac} \exp(2\pi i \hat{k} \cdot x)\}$. The algorithm we got from the good lecture script by J.R. Shewchuk (Shewchuk, 1994). The Eq. (F.1) can be deposited along color index as

$$M\vec{x} = \vec{b}$$

where \vec{b} is the know vector and M is the known (operator), which is positive-definite matrix. We give the algorithm without proof. The principle of this algorithm is to finding a vector \vec{x} that minimizes the function

$$f(\vec{x}) = \frac{1}{2} \vec{x}^T M \vec{x} - \vec{b}^T \vec{x} + c.$$

Then we construct $\vec{d}_{(i)}$ denoting the direction of decent and $\vec{r}_{(i)}$ is the residual $\vec{r}_{(i)} = \vec{b}_{(i)} - M\vec{x}_{(i)}$ at the i^{th} iteration.

We Start the computing $\vec{d}_{(0)}$ and $\vec{r}_{(0)}$ from

$$\vec{d}(0) = \vec{r}(0) = \vec{b} - M\vec{x}(0),$$

by choosing any initial guess $\vec{x}(0)$. The recursive procedure runs as follows:

1. compute

$$\alpha_{(i)} = \frac{\vec{r}_{(i)}^T \cdot \vec{r}_{(i)}}{\vec{d}_{(i)}^T M \vec{d}_{(i)}},$$

2. recompute the residual \vec{r} and the vector \vec{x}

$$\vec{r}_{(i+1)} = \vec{r}_{(i)} - \alpha_{(i)} M \vec{d}_{(i)},$$

$$\vec{x}_{(i+1)} = \vec{x}_{(i)} + \alpha_{(i)} \vec{d}_{(i)},$$

3. compute

$$\beta_{(i)} = \frac{\vec{r}_{(i+1)}^T \cdot \vec{r}_{(i+1)}}{\vec{r}_{(i)}^T \cdot \vec{r}_{(i)}},$$

4. recompute the direction of decent

$$\vec{d}_{(i+1)} = \vec{r}_{(i+1)} - \beta_{(i)} \vec{d}_{(i)}.$$

The iteration is stopped when the norm of the residual is below than a given small constant number ϵ :

$$\vec{r}_{(i)}^T \cdot \vec{r}_{(i)} < \epsilon.$$

The vector \vec{x} is solved by projecting matrix M back as the numerical estimate of $M^{-1}\vec{b}$.

F.4 Preconditioned conjugate gradient method

Even the conjugate gradient (CG) can be used to solve $M\vec{\phi}(x) = \vec{\psi}(x)$, but it takes the very long time to compute. The speed of convergence rate depends on the condition number which is the ratio of largest to lowest eigenvalue of operator M . There are many kind of precondition CG. The method we use in our work is developed by (Sternbeck et al., 2005) by instead of solving $M\vec{\phi}(x) = \vec{\psi}(x)$ we can solve another form of equation

$$[M\Delta^{-1}](\Delta\vec{\phi}) = \vec{\psi}.$$

Running the procedure in this way, the condition number is reduced.

This kind of preconditioned CG algorithm (PCG) has algorithm as follows:
initialize:

$$\begin{aligned}\vec{r}^{(0)} &= \vec{\phi}_{(i)} - M\vec{\phi}^{(0)}, & \vec{p}^{(0)} &= \Delta^{-1}\vec{r}^{(0)} \\ \gamma^{(0)} &= (\vec{p}^{(0)}, \vec{r}^{(0)}),\end{aligned}$$

implement the loop in problem: $k = 0, 1, \dots$

$$\begin{aligned}
\vec{z}^{(k)} &= M\vec{p}^{(k)} & \alpha^{(k)} &= \gamma^{(k)} / (\vec{z}^{(k)}, \vec{p}^{(k)}) \\
\vec{\phi}^{(k+1)} &= \vec{\phi}^{(k)} + \alpha^{(k)}\vec{p}^{(k)}, \\
\vec{r}^{(k+1)} &= \vec{r}^{(k)} - \alpha^{(k)}\vec{z}^{(k)}, \\
\vec{z}^{(k+1)} &= \Delta^{-1}\vec{r}^{(k+1)}, \\
\gamma^{(k+1)} &= (\vec{z}^{(k+1)}, \vec{r}^{(k+1)}) \\
&\text{if } (\gamma^{(k+1)} < \epsilon) \text{ exit the loop} \\
\text{update } \vec{p}^{(k+1)} &= \vec{z}^{(k+1)} + \frac{\gamma^{(k+1)}}{\gamma^{(k)}}\vec{p}^{(k)}
\end{aligned} \tag{F.2}$$

finish the loop.

Here (\cdot, \cdot) is the scalar product, and Δ^{-1} is performed by $\Delta^{-1} = \mathcal{F}^{-1}p^{-2}\mathcal{F}$ where \mathcal{F} is fast Fourier transformation.

APPENDIX G
PUBLICATION PAPER

Coulomb gauge ghost propagator and the Coulomb potential*

Markus Quandt[†]

University of Tübingen

E-mail: quandt@tphys.physik.uni-tuebingen.de

Giuseppe Burgio

University of Tübingen

E-mail: burgio@tphys.physik.uni-tuebingen.de

Songvudhi Chimchinda

University of Tübingen and Suranaree University of Technology

E-mail: chimchinda@tphys.physik.uni-tuebingen.de

Hugo Reinhardt

University of Tübingen

E-mail: hugo.reinhardt@uni-tuebingen.de

The ghost propagator and the Coulomb potential are evaluated in Coulomb gauge on the lattice, using an improved gauge fixing scheme which includes the residual symmetry. This setting has been shown to be essential in order to explain the scaling violations in the instantaneous gluon propagator. We find that both the ghost propagator and the Coulomb potential are insensitive to the Gribov problem or the details of the residual gauge fixing, even if the Coulomb potential is evaluated from the A_0 -propagator instead of the Coulomb kernel. In particular, no signs of scaling violations could be found in either quantity, at least to well below the numerical accuracy where these violations were visible for the gluon propagator. The Coulomb potential from the A_0 -propagator is shown to be in qualitative agreement with the (formally equivalent) expression evaluated from the Coulomb kernel.

8th Conference Quark Confinement and the Hadron Spectrum

September 1-6, 2008

Mainz, Germany

*Supported by DFG under contract Re-856/6-1,2

[†]Speaker.

1. Introduction

Yang–Mills theory in the Coulomb gauge has recently drawn a renewed attention, both in the continuum [1, 2, 3] and on the lattice [5, 4, 6, 7, 8]. This is mainly due to the fact that Gauß’ law can be resolved explicitly in this gauge, which allows for a neat Hamiltonian formulation with the transversal part of the remaining vector potential \mathbf{A}^\perp as the only physical degree of freedom. Much of the intuition and techniques from ordinary quantum mechanics can thus be carried over to the YM case. In particular, recent variational approaches in the Schrödinger picture, based on the notion of a weakly interacting constituent gluon and the Gribov–Zwanziger confinement scenario [12], proved to be very successful [3]; similar calculations are presently carried out in the renormalisation flow approach.

All these continuum formulations, in one way or the other, give rise to relations between low-order Green functions of the constituent gluon \mathbf{A} and the Faddeev–Popov ghosts. It is therefore important to obtain non-perturbative information on such correlators from the lattice. Careful studies of the equal-times gluon propagator, for instance, reveal strong scaling violations and a UV behaviour at odds with simple dimensional arguments [5, 7, 6]. These surprising results reflect the renormalisation problems for instantaneous correlators in the continuum. One possible explanation of the lattice findings [9] is based on the idea that the residual gauge freedom left over by the Coulomb condition must be fixed in such a way that it resembles the Hamiltonian formulation as closely as possible.¹ A careful study of the energy dependence of the gluon propagator then allows to manipulate the data such that perfect scaling is observed even on finite lattices.

For the confinement scenario layed out by Gribov and Zwanziger [12], the more important correlators are, of course, the ghost propagator and, in particular, the Coulomb potential. Furthermore, the ghost form factor has been shown to represent the inverse of the colour dielectric function of the Yang–Mills vacuum [13], and is therefore of direct physical relevance. Initial studies of the ghost and Coulomb propagator for the gauge group $G = SU(2)$ with simple Coulomb and no residual gauge fixing [5] found no scaling violations at low momenta, but had inconclusive results about the Coulomb string tension in the deep infrared. Moreover, these results were partially at odds with more careful $SU(3)$ studies using a residual gauge fixing different from ours [11], which featured a peculiar saddle-like behaviour in the Coulomb potential at low momenta. In the present talk, I will report about recent $SU(2)$ calculations of ghost form factors and the Coulomb potential, using exactly the same gauge fixing techniques which proved essential for the resolution of the scaling violations in the gluon propagator.

2. Gauge Fixing

Our gauge fixing procedure employs both simulated annealing and the microcanonical flip procedure layed out in [7] as a preconditioning with subsequent (over)relaxation to complete the gauge fixing within machine precision. To reduce the Gribov noise and bring the lattice configs closer to the fundamental modular region, we perform up to 40 restarts with random gauge transformations as starting points, and take the copy with the best minimum of the gauge fixing functional. While this procedure proved to be important for the correct extraction of the gluon propagator in

¹For the first-order formalism in the continuum, renormalisability has been proven algebraically [10].

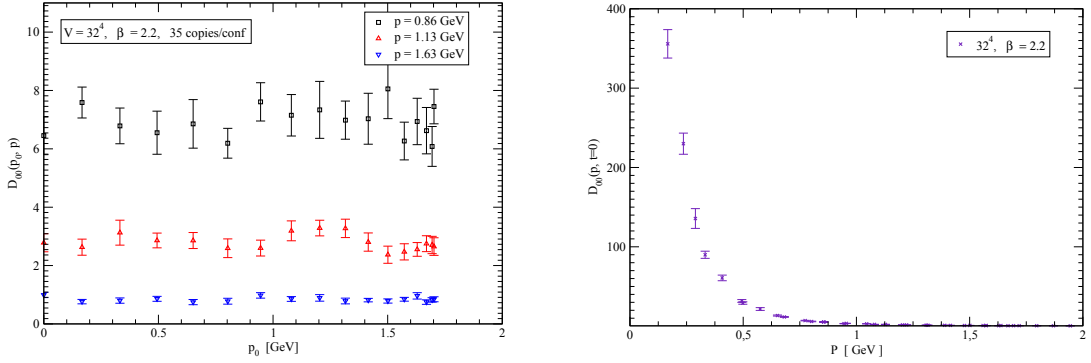


Figure 1: Left panel: Energy dependence of the A_0 -propagator $D_{00}(\mathbf{p}, p_0)$ after improved Coulomb and residual gauge fixing, for various spatial momenta $|\mathbf{p}|$. Right panel: The equal-times A_0 -propagator $D_{00}(\mathbf{p}, t = 0)$ as a function of the spatial momentum $|\mathbf{p}|$.

the deep infrared [7], the ghost correlators exhibit a much weaker dependence on the quality of gauge fixing. This can be clearly seen in the left panel of fig. 2: The value of the ghost propagator at the lowest diagonal momentum $\hat{\mathbf{p}} = (1, 1, 1)$ is only very slightly suppressed as the number n of Gribov restarts is increased, and the optimum is already reached for n as low as $n \approx 2..3$. All this is in contrast to the corresponding findings for the gluon propagator, where a 20% effect was seen that required up to $n = 40$ for saturation.

The second important ingredient is the residual gauge fixing. To make contact with the Hamiltonian approach in Weyl gauge, we would like to put the spatial average $u(t) = L^{-3} \sum_{\mathbf{x}} U_0(t, \mathbf{x})$ to unity. However, periodic boundary conditions only allow us to make $u(t)$ time-independent, $u(t) \equiv \overline{U}_0 = \text{const.}$ In the infinite volume limit (and in praxis also for $L \geq 32$), \overline{U}_0 approaches unity. Although this only enforces $\partial_0 U_0 = 0$ on the spatial average, the A_0 -propagator is, within statistical errors, independent of energy (see left panel of fig. 1). In the right panel of fig. 1, we thus plot only the instantaneous A_0 -propagator which is strongly enhanced in the infrared. This result will be related to the Coulomb potential below.

3. Results

The right panel of figure 2 shows our results for the ghost propagator and its form factor,

$$G(p) = \langle \bar{c}(-\mathbf{p}) c(\mathbf{p}) \rangle = L^{-3} \sum_{\mathbf{x}} e^{i\mathbf{p}\mathbf{x}} \langle \mathbf{M}(\mathbf{x}, \mathbf{0})^{-1} \rangle \equiv \frac{d(|\mathbf{p}|)}{\mathbf{p}^2} \quad (3.1)$$

where $\mathbf{M} \equiv (-\nabla \mathbf{D})$ is the Faddeev–Popov operator and the ghost form factor $d(p)$ measures the deviation from the perturbative result. The form factor is infrared enhanced, which agrees with the horizon condition $d^{-1}(0) = 0$ necessary in the Zwanziger confinement criterion [12]. Our infrared exponent $\kappa \approx 0.22$ for the divergence $d(p) \sim 1/(p^2)^\kappa$ is slightly smaller than the one obtained with naive gauge fixing [5], but agrees well with recent improved studies in $SU(3)$ [11].

Even more directly related to the confinement problem is the so-called Coulomb potential V_c , i.e. the response of the gluon vacuum to static colour charges. Since the constituent gluon \mathbf{A} and its wave functional are gauge-dependent, V_c is not directly the physical potential between static

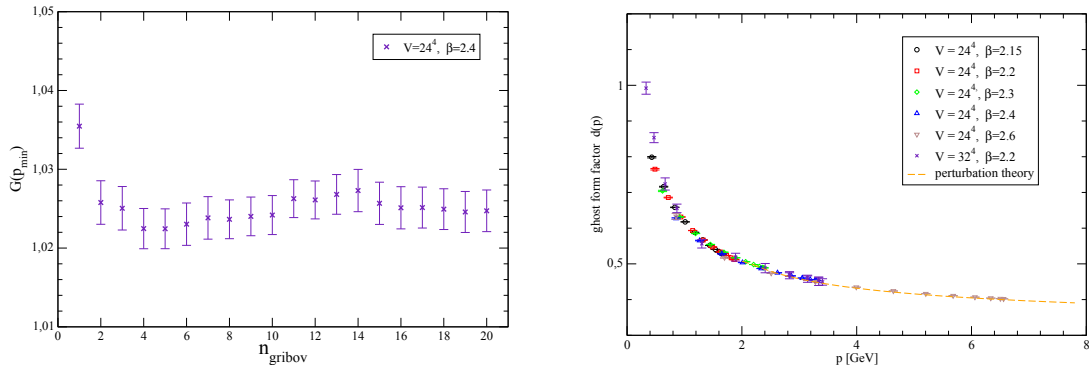


Figure 2: Left panel: The ghost propagator at the lowest diagonal momentum $\hat{\mathbf{p}} = (1, 1, 1)$ as a function of the number of Gribov copies considered in the Coulomb gauge fixing. (Note the scale on the y -axis.) Right panel: The ghost form factor $d(p)$ as a function of the spatial momentum $|\mathbf{p}|$.

quarks (as extracted from Wilson loops or Polyakov lines), but an upper bound, $V_c(r) \geq \frac{4}{3}V(r)$. This implies that there is no confinement without Coulomb confinement [12], but a linear Coulomb potential may persist even in the deconfined phase.

Formally, $V_c(r)$ can be computed in one of two equivalent ways,

$$V_c(|\mathbf{x} - \mathbf{y}|) = \langle A_0(t, \mathbf{x}) A_0(t, \mathbf{y}) \rangle = g^2 \langle (M^{-1} \cdot \Delta \cdot M^{-1})_{\mathbf{x}, \mathbf{y}} \rangle. \quad (3.2)$$

The formal equivalence of these two expressions can be shown in the first order formalism upon explicitly resolving Gauß' law [10, 14]. This leaves possible renormalisation issues aside and the lessons learned from the scaling violations in the gluon propagator indicate that some caution is required when connecting bare instantaneous correlators. Of course, the A_0 -propagator is numerically much simpler than the complicated Coulomb kernel involving two inversions of the FP operator.

The strong Ward identities in Coulomb gauge [10] imply that the special combination in momentum space

$$\mathbf{p}^2 V_c(\mathbf{p}) \sim g^2(p) \quad (3.3)$$

is a renormalisation group invariant which can be taken as a definition of the running coupling constant. Simulations with different β should thus fall on top of each other without further multiplicative renormalisation. We have tested this conjecture for numerous values of β on relatively small 16^4 lattices. (On 32^4 lattices, we have only been able to complete the analysis of the complicated Coulomb kernel for a single value of β). The β -invariance was much better for the A_0 -correlator, while V_c constructed from the Coulomb kernel still showed noticeable scaling violations. At present, it is not known whether these deviations are pure numerical or finite volume effects, or if they have any more significant meaning. (Similar observations were made in ref. [11]). Simulations with improved statistics on larger lattices have to be conducted to resolve this issue.

Finally, the most direct approach to the confinement issue is given by the expression

$$\mathbf{p}^4 V_c(\mathbf{p}). \quad (3.4)$$

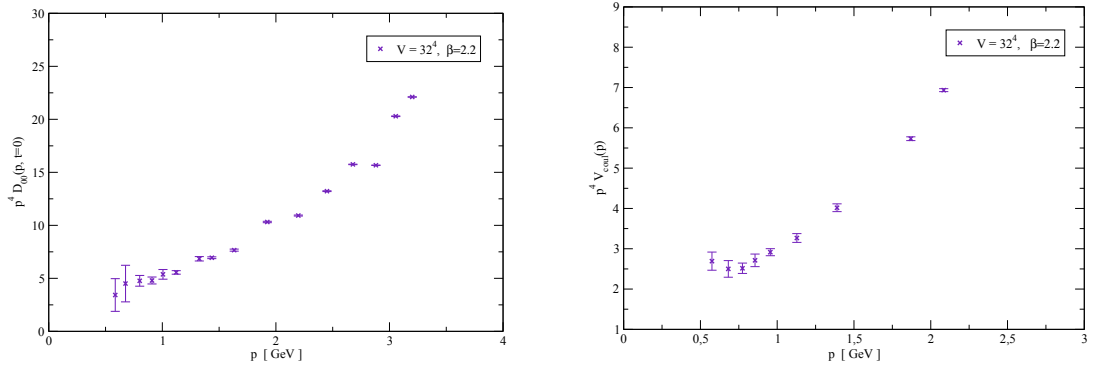


Figure 3: Left panel: The combination $\mathbf{p}^4 V_c(|\mathbf{p}|)$ with the Coulomb potential V_c extracted from the A_0 -propagator $D_{00}(\mathbf{p}, t=0)$. Right panel: The same quantity, with V_c extracted from the Coulomb kernel.

From the Fourier transformation of a linear potential, $V_c(r) = \sigma_c r$, it is readily seen that

$$\mathbf{p}^4 V_c(\mathbf{p}) \rightarrow 8\pi\sigma_c, \quad |\mathbf{p}| \rightarrow 0.$$

The *Coulomb string tension* σ_c is an upper bound for the real string tension σ extracted from Wilson loops. Previous and current lattice studies are inconclusive as to whether $\sigma_c = \sigma$, since the approach to $|\mathbf{p}| \rightarrow 0$ is not as uniform as expected: Early simulations without improved/residual gauge fixing saw a slight but noticeable rise in the quantity (3.4) below $|\mathbf{p}| \approx 1$ GeV, which seemed compatible with σ_c/σ anywhere in the range $1 \dots 3$. More recent computation for the gauge group $G = SU(3)$ prefer a value $\sigma_c/\sigma \approx 1.6$, but the extrapolation to zero momentum is again uncertain due to a peculiar "bump" in the quantity (3.4) at momenta between $0.1 \dots 1$ GeV.

Our result on a $V = 32^4$ lattice in figure 3 using all improved gauge fixing techniques give reliable results (for cylinder cut momenta) only down to $|\mathbf{p}| \simeq 0.5$ GeV. In this range, the results for (3.4) are compatible with V_c computed either from the A_0 -propagator or from the Coulomb kernel. The latter result show a more pronounced plateau at the smallest momenta, which is reminiscent of the slight rise observed in [5]. However, the numerical data can equally well be fitted with a constant. (V_c from the A_0 -propagator is compatible with the Coulomb kernel results within statistical errors). For both definitions of V_c , we do not see the "bump" reported for $SU(3)$ in ref. [11]. While the approach to a constant seems promising, better statistics and larger lattices are required for a reliable extrapolation of σ_c/σ .

4. Conclusion

The computation of ghost correlators and the Coulomb potential in $G = SU(2)$ show qualitative agreement with continuum calculations in the variational approach [2, 3]. The scaling violations observed previously for the equal-times gluon propagator $D(\mathbf{p})$ have no counter part in the ghost correlators studied here. In particular, the dependence on the Gribov noise and the details of the improved gauge fixing are negligible. Likewise, the residual gauge fixing, which is essential for the resolution of the scaling violations in $D(\mathbf{p})$, seems to have little or no influence on the ghost propagator or Coulomb potential, even when the latter is extracted from the the A_0 -propagator.

Our residual gauge fixing removes the energy dependence on A_0 not only in the spatial average, but effectively for arbitrary A_0 -correlators. There is thus no issue with renormalisation and the results for the instantaneous A_0 -correlators resemble the ones with unfixed residual symmetry. (Similar observations are made for the ghost propagator and the Coulomb potential as extracted from the Coulomb kernel.) It is therefore not surprising that our findings agree with other calculations, even if these fixed the Coulomb gauge naively, or left the residual symmetry unfixed.

The statistics in the deep infrared are not sufficient to make reliable quantitative extrapolations for the Coulomb string tension σ_c , or the Coulomb form factor $f(p)$ whose infrared behaviour is an important ingredient in the variational approaches [2, 3]. We intend to improve on this and accumulate data for 32^4 lattices with various β , and A_0 -correlators on even larger lattices. These results will be published in a forthcoming paper.

References

- [1] A.P. Szczepaniak and E.S. Swansen, Phys. Rev. **D65** (2002) 025015, [hep-ph/0107078].
- [2] C. Feuchter and H. Reinhardt, Phys. Rev. **D70** (2004) 105021, [hep-th/0408236];
H. Reinhardt and C. Feuchter, Phys. Rev. **D71** (2005) 105002.
- [3] D. Epple, H. Reinhardt and W. Schleifenbaum, Phys. Rev. **D75** (2007) 045011;
W. Schleifenbaum, M. Leder and H. Reinhardt, Phys. Rev. **D73**, (2006) 125019.
- [4] A. Cucchieri and D. Zwanziger, Phys. Rev. **D65** (2002) 014001, [hep-lat/0008026].
- [5] K. Landfeld and L. Moyaerts, Phys. Rev. **D70** (2004) 074507, [hep-lat/0406024].
- [6] A. Voigt et al. , *PoS LAT2007*, (2007) 338; [arXiv:0709.4585].
- [7] M. Quandt et al. , *PoS LAT2007* (2007) 325, [arXiv:0710.0549].
- [8] I. L. Bogolubsky et al. , Phys. Rev. **D74** (2006) 034503, [hep-lat/0511056] ;
I. L. Bogolubsky et al. , Phys. Rev. **D77** (2008) 014504, [arXiv:0707.3611].
- [9] G. Burgio, M. Quandt and H. Reinhardt, [arXiv:0807.3291] (2008).
- [10] D. Zwanziger, Nucl. Phys. **B518** (2002) 014001.
- [11] A. Voigt, M. Ilgenfritz, M. Müller-Preussker, Phys. Rev. **D78** (2008) 14501.
- [12] D. Zwanziger, Nucl. Phys. **B485** (1997) 185 ; [hep-th/9603203].
- [13] H. Reinhardt, Phys. Rev. Lett. **101** (2008) 061602, [arXiv:0803.0504].
- [14] P. Watson, H. Reinhardt, Phys. Rev. **D76** (2007) 125016, [arXiv:0709.0140].

Coulomb gauge Green functions and Gribov copies in $SU(2)$ lattice gauge theory*

Markus Quandt[†]

University of Tübingen

E-mail: quandt@tphys.physik.uni-tuebingen.de

Giuseppe Burgio

University of Tübingen

E-mail: burgio@tphys.physik.uni-tuebingen.de

Songvudhi Chimchinda

University of Tübingen

E-mail: chimchinda@tphys.physik.uni-tuebingen.de

Hugo Reinhardt

University of Tübingen

E-mail: hugo.reinhardt@uni-tuebingen.de

We reconsider the lattice measurement of Green functions in Coulomb gauge, both in $2+1$ and $3+1$ dimensions, using an improved gauge fixing scheme. The influence of Gribov copies is examined and we find clear indications that Green functions are more strongly affected than previously assumed, in particular for low momenta. Qualitatively, our improved lattice results in the infra-red compare more favourably with recent continuum calculations in the Hamiltonian approach.

*The XXV International Symposium on Lattice Field Theory
July 30 - August 4 2007
Regensburg, Germany*

*Supported by DFG under contract *DFG-Re856/6-1,2*.

[†]Speaker.

1. Introduction

Yang-Mills theory in the Coulomb gauge has recently drawn a renewed attention, both in the continuum [1, 2] and on the lattice [4, 5, 6]. In the continuum at least, this interest is mostly due to the remarkable fact that Gauß' law can be resolved explicitly in Coulomb gauge, which gives the remaining vector potential \mathbf{A} a very intuitive notion similar to electrodynamics [8]. Recent variational approaches in the Schrödinger picture even support the idea of a *constituent gluon* [1, 2], which is almost non-interacting in the infrared and thus completely determined by its dispersion relation $\omega(\mathbf{p})$, i.e. the (inverse) equal-time gluon propagator $D(\mathbf{p}) = \frac{1}{2}\omega(\mathbf{p})^{-1}$.

The obvious drawback of the Coulomb gauge is that *manifest* Lorentz invariance is lost at intermediate stages; it may only be recovered at the end of the calculation. Perturbatively, this problem is reflected in the (tree-level) propagators of some fundamental fields, which are instantaneous in time so that many loop integrands are independent of the temporal loop momentum component k_0 . Such integrals are notoriously difficult to regulate with conventional techniques, though they are believed to cancel in the full theory [8]. Still, the issue of renormalisation in Coulomb gauge remains cumbersome, even at the one-loop level [9].

Similar problems arise on the lattice as well. While initial studies of the gluon propagator in Coulomb gauge displayed almost perfect scaling [4, 5], recent studies using improved gf. techniques indicate that the quality of gauge fixing has a significant impact on Green functions; in particular, substantial scaling violations may result [6]. The same conclusion has been drawn earlier in Landau gauge, where careful gauge fixing may alter the infrared behaviour of the propagator quantitatively by as much as 20 % [7].

Even more severe discrepancies arise in the comparison of early lattice results with the variational approach mentioned above. While both methods show good agreement in $D = 2 + 1$, their results in $D = 3 + 1$ differ *qualitatively*, both in the infra-red and the ultra-violet:

	IR	UV
lattice [4, 5]	$D(\mathbf{p}) \rightarrow \text{const}$	$D(\mathbf{p}) \sim \mathbf{p} ^{-\frac{3}{2}}$
variation [1]	$D(\mathbf{p}) \rightarrow 0$	$D(\mathbf{p}) \sim \mathbf{p} ^{-1}$

All these findings emphasise the need for a thorough corroboration of lattice results in Coulomb gauge, in particular with regard to the quality of gauge fixing. In the present talk, I will present the first results in this program, viz. the equal time gluon propagator in $D = 2 + 1$ and $D = 3 + 1$. Further studies on the ghost propagator and the Coulomb form factor are currently underway and will be presented elsewhere.

The plan of this talk is as follows: In the next section, I will briefly discuss our gf. techniques and demonstrate that they are effective in reducing the Gribov problem which is at the heart of most gf. issues. Section three presents our findings for the gluon propagator. Some of this data is still preliminary, and so is the quantitative analysis, but our results so far imply both scaling violations in the UV and a significant suppression in the IR. The last point improves the qualitative agreement with variational studies, although the quantitative agreement is still unsatisfactory. In the last section, I will conclude with a brief summary and outlook.

2. Gauge fixing techniques

Coulomb gauge on the lattice can be defined as the maximisation of the functional¹

$$F_t[U] \equiv \frac{1}{3V_3} \text{tr} \sum_{\mathbf{x}} \sum_{i=1}^3 \frac{1}{2} \text{tr} U_i(\mathbf{x}, t) \stackrel{!}{=} \max, \quad V_3 \equiv \prod_{i=1}^3 N_i. \quad (2.1)$$

Here, $U_\mu(x)$ are the link variables, the sum over \mathbf{x} runs over all sites in a fixed *time-slice* $t = \text{const}$ and the maximisation is along the gauge orbit, i.e. with respect to all gauge rotations $\Omega(\mathbf{x}, t)$ of the link field $U_\mu(x)$. As indicated, the Coulomb condition $F_t \stackrel{!}{=} \max$ can be implemented at each time-slice t *independently*. This leaves a residual invariance of space-independent but time dependent gauge transformations $\Omega(t)$, i.e. a global gauge rotation in every time slice.

For the equal-time gluon propagator²

$$D(\mathbf{p}) \sim \int d^3 \mathbf{x} e^{i\mathbf{p} \cdot (\mathbf{x}-\mathbf{y})} \sum_{i=1}^3 \sum_{c=1}^3 \langle A_i^c(\mathbf{x}, t) A_i^c(\mathbf{y}, t) \rangle = |\mathbf{p}|^{-1} + \mathcal{O}(\hbar) \quad (2.2)$$

the residual gauge fixing is irrelevant and it is sufficient to fix only the time slice in which the measurement is taken. This is no longer true for other correlators such as the $A_0 - A_0$ propagator related to the static Coulomb potential. Moreover, recent perturbative studies [9] indicate that possible scaling violations in $D(\mathbf{p})$ may be attributed to the loss of covariance at equal times; it will then be necessary to consider the full gluon propagator at all (unequal) times, and Coulomb gauge fixing at all time slices must be augmented by a suitable choice for the residual symmetry.

The Gribov problem, which is at the heart of most g.f. issues, can be expressed as the fact that (2.1) has many *local* maxima which may, however, give inequivalent contributions to non-gauge invariant quantities such as the Green functions. Uniqueness can be enforced by searching for the *global* maximum of (2.1), an NP-hard problem. Our strategy to reduce the influence of Gribov copies is to prepend the standard (over)relaxation algorithm by an initial *preconditioning* step combined with multiple *Gribov repetitions* from random starts. This method is a less expensive substitute for full simulated annealing and works well for small to medium size volumina up to $V \approx 36^4$.

2.1 Preconditioning

The periodic boundary conditions on the lattice allow for a somewhat larger symmetry than just the periodic local gauge rotations. This is well-known from the $SU(2)$ lattice center symmetry: In this case, one multiplies all links $U_0(t, \mathbf{x})$ pointing out of a fixed time-slice³ $t = \text{const}$ by (-1) . This construction flips the sign of all Polyakov lines, but it leaves all plaquettes (and thus the action) invariant; it is therefore a genuine symmetry of the system. In Landau gauge, one can generalise this construction to all four directions, giving a total of 2^4 possible combinations of *flips* [7].

¹For simplicity, we work exclusively with the colour group $G = SU(2)$.

²Gauge potentials are extracted from the link variables in the usual fashion via an $\mathcal{O}(a^2)$ improvement of the basic formula $A_\mu = \frac{1}{2a} [U_\mu(x) - U_\mu^\dagger(x)]$.

³The actual location of the time slice t is irrelevant, since a center flip at a different time-slice t' can be decomposed into a flip at t followed by a strictly local, periodic gauge transformation.

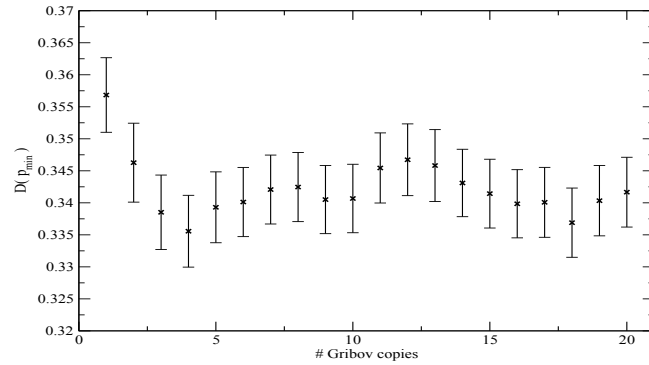


Figure 1: The equal-time gluon propagator at the smallest non-zero lattice momentum, measured as a function of the number N of Gribov repetitions. Data was collected on a 24^4 lattice with $\beta = 2.15$ (left) and $\beta = 2.20$ (right); a total of 200 thermalised configuration were analysed for each data point.

In the Coulomb case, the gauge fixing is carried out in a fixed $3D$ time-slice, i.e. the flips are only carried out in spatial directions, and only the $2D$ sub-planes perpendicular to a given direction (at fixed t) are flipped. The *preconditioning* consist of trying all 2^3 twists to maximise $F_t[U]$ prior to the actual relaxation step. This can be viewed as a non-local update representing a large symmetry transformation that no local relaxation algorithm is likely to find. Flips can also be interspersed at any time during relaxation, although they are most efficient early on, when the algorithm has not yet converged onto a target maximum.⁴

2.2 Multiple Gribov repetitions

The gf. sequence consisting of preconditioning, relaxation and overrelaxation can be repeated multiple times with random starting points. This inspects different regions of the search space and converges to distinct Gribov copies. What makes this repetition effective is that a relatively small number N of copies gives a large increase in the gf. functional, while subsequent repetitions beyond a certain *plateau* point do not give any substantial improvement within reasonable computation time.

This can be seen in figure 1, which plots the equal-time Gluon propagator $D(\mathbf{p})$ at the smallest non-zero lattice momentum, as a function of the number N of Gribov repetitions. The net effect of the improved gauge fixing is generally to suppress $D(\mathbf{p}_{\min})$. Even for N as small as $N = 2, \dots, 5$, the corrections are in the range of 10%. Further copies give smaller corrections; it is then a matter of experiment to find the optimal tradeoff between CPU time and gf. quality. The optimal N will depend quite sensitively on the lattice size and other simulation parameters. In fig. 1 one can see the plateau setting in rather quickly, while our largest lattices ($V = 36^4$) required up to $N = 30$ repetitions.

⁴The (over)relaxation algorithm is iterated until the local gf. violation, i.e. the (maximal norm at all sites \mathbf{x} of the) local gradient of (2.1) is smaller than 10^{-13} .

3. Results

3.1 $D = 2 + 1$

In this case, our findings in fig. 2 are in fair agreement to previous lattice calculations [4, 5]. Our improved gauge fixing scheme has again the tendency to suppress the gluon propagator in the infra-red, but since $D(|\mathbf{p}|) \rightarrow 0$ at small $|\mathbf{p}|$ even without gf. improvement, the *qualitative* behaviour of the gluon propagator is unchanged.

In the UV, we observe scaling in the sense that the various propagator curves for different values of the coupling β can be multiplied by a momentum-independent factor $Z(\beta)$ such that all curves coalesce to a single line. There is a tendency for the scaling to be less perfect than without the gf. improvement, but this is well below the error bars of our numerical simulation.

Quantitatively, the suppression of the gluon propagator in the infra-red is as large as 10% – 15%. To fit the curve in the deep IR and UV region, we have placed two cuts on the data. In the IR, a power ansatz yields

$$D(|\mathbf{p}|) = |\mathbf{p}|^\alpha \cdot (c_1 + c_2|\mathbf{p}|^2 + \dots), \quad \alpha \approx 0.85(10). \quad (3.1)$$

Since the curve flattens towards the maximum, the exponent α is somewhat depending on the exact location of the IR cut. At $\Lambda = 0.5 \text{ GeV}$, we have $\alpha = 0.81$, while it increases to the above value $\alpha = 0.85$ for $\Lambda = 0.4 \text{ GeV}$. With our present lattice sizes, we cannot go much lower with the IR cut, but the present trend does certainly not rule out the value $\alpha = 1$ preferred by Hamiltonian approaches [1].

In the ultra-violet, a power-law decay

$$D(|\mathbf{p}|) \sim |\mathbf{p}|^{-\gamma}, \quad \gamma \approx 1.5(1) \quad (3.2)$$

is possible, but the exact value of the exponent γ depends quite sensitively on the location of the UV cut. A double-logarithmic plot in the deep UV is *not* a straight line at large momenta, which points to sizeable logarithmic corrections. In fact, an ad-hoc ansatz

$$D(p) \sim \frac{1}{|\mathbf{p}| \cdot \ln|\mathbf{p}|^\delta}$$

with $\delta \approx 0.51$ can fit the data equally well. The conclusion is that our present data does not contain large enough momenta to distinguish between a logarithmic or a power-like behaviour in the UV.

3.2 $D = 3 + 1$

The left panel of fig. 3 shows the results for the largest lattice that we considered. The improved gf. scheme is now seen to make a *qualitative* difference, both in the IR and the UV.

At low momenta, the propagator is clearly *suppressed* as compared to less intricate gf. procedures. The power-law fit explained in the last subsection reveals a IR exponent of

$$\alpha \approx 0.24(12),$$

again with significant variations as the IR cut on the data is changed. However, a value $\alpha = 0$, i.e. a gluon propagator going to a constant as $\mathbf{p} \rightarrow 0$ [4, 5] seems much more unlikely than the vanishing

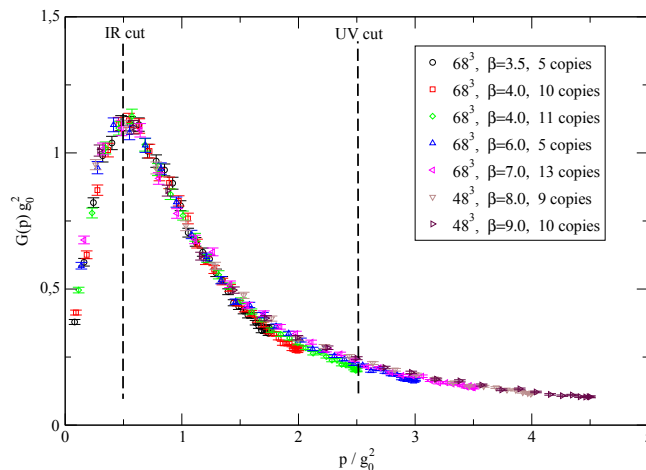


Figure 2: The renormalised equal-time gluon propagator for various couplings and lattice sizes. For the significance of the two data cuts, see the main text.

$D(0) = 0$ predicted by variational calculations [1]. On the other hand, the comparison with the $D = 2 + 1$ case indicates that much smaller momenta must be sampled to rule out one or the other option.

In the UV, the most striking difference to previous lattice results is the absence of perfect scaling, i.e. the gluon propagator does not seem to be multiplicatively renormalisable. This can be clearly seen in the logarithmic plot in the right panel of fig. 3. In a multiplicatively renormalisable situation, we would expect the curves for all couplings β to have the same *slope* at large momenta – which is clearly not the case.

One can now proceed and renormalise anyway such that a common curve can be observed in one p -region or the other (the right panel of fig. 3 has been renormalised to fit well in the IR). In particular, one could try to fit the deep UV region, at the expense of sacrificing a common curve in the IR. From such a fit, it is even possible to extract a power-like behaviour

$$D(\mathbf{p}) \sim |\mathbf{p}|^{-\alpha}, \quad \alpha = 1.57.$$

which is in fair agreement with ref. [4]. Our present data, however, does not warrant such a procedure. In particular, an ad-hoc logarithmic ansatz as in the last subsection would work equally well. To summarize, the scaling violations displayed by our improved gf. scheme are so severe that any attempt to extract a consistent UV behaviour from a multiplicative renormalisation seems ill-advised.

Comparable problems with renormalisation were also found in other studies employing improved gf. schemes. Continuum perturbation theory [9] attributes the scaling violations to the instantaneous nature of the propagator considered here.

4. Summary and conclusions

In this talk, I have presented first results for the equal-time gluon propagator measured in an

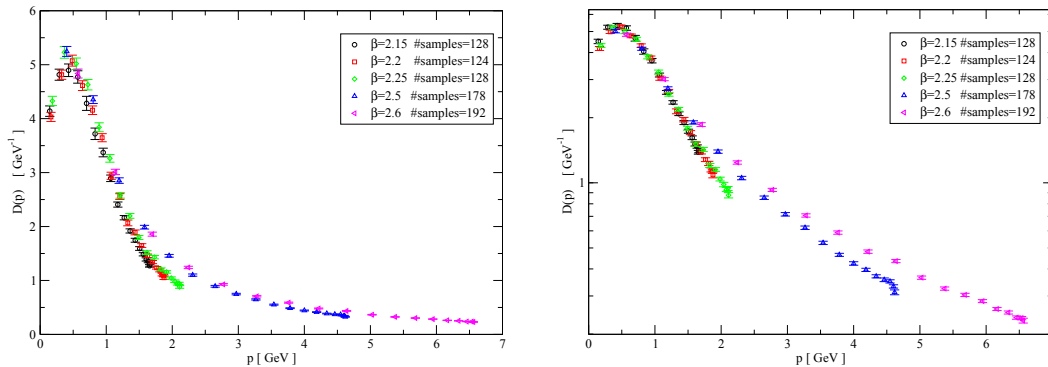


Figure 3: Left panel: The equal-time gluon propagator for various values of the coupling constant. The gauge fixing includes preconditioning and a minimum of 30 Gribov repetitions for each measurement; multiplicative renormalisation focused on the IR data. Right panel: The same data in a logarithmic plot.

improved Coulomb gauge fixing scheme. The general observation is a significant *suppression* of the propagator in the infrared, and a *loss of scaling* at very large momenta. Although the numerics is not fully compelling, the IR data points to $D(0) = 0$ as a likely scenario even for $D = 3 + 1$. The failure of multiplicative renormalisation in the UV has also been observed in other studies treating Coulomb gauge with improved gf. techniques; in perturbation theory, this failure can presumably be attributed to a loss of covariance for the equal-time propagator.

To make the present numbers more convincing, we have to go to smaller momenta, which may involve a simulated annealing step in the gf. pipeline. To get a handle on the scaling issue, it would also be interesting to study the gluon propagator at non-equal times, using a complete gauge fixing that also destroys the residual symmetry in Coulomb gauge. Further investigations involve the ghost propagator and the Coulomb form factor, which are of immediate relevance for the physics of the gauge system. These studies are currently underway and will be presented elsewhere.

References

- [1] C. Feuchter and H. Reinhardt, Phys. Rev. **D70** (2004) 105021;
H. Reinhardt and C. Feuchter, Phys. Rev. **D71** (2005) 105002.
- [2] A.P. Szczepaniak and E.S. Swansen, Phys. Rev. **D65** (2002) 025015.
- [3] D. Epple, H. Reinhardt and W. Schleifenbaum, Phys. Rev. **D75** (2007) 045011;
H. Reinhardt, W. Schleifenbaum, D. Epple, C. Feuchter, arXiv:0710.0316 [hep-th]
- [4] K. Landfeld and L. Moyaerts, Phys. Rev. **D70** (2004) 074507.
- [5] A. Cucchieri and D. Zwanziger, Phys. Rev. **D65** (2002) 014001.
- [6] A. Voigt et. al. , arXiv:0709.4585 [hep-lat]
- [7] I.L. Bogolubsky et. al. , Phys. Rev. **D74** (2006) 034503.
- [8] D. Zwanziger, Nucl. Phys. **B518** (1998) 237.
- [9] P. Watson and H. Reinhardt, arXiv:0709.0140 [hep-th].

CURRICULUM VITAE

NAME Mr. Songvudhi Chimchinda
DATE OF BIRTH November 11, 1974
PLACE OF BIRTH Bangkok, Thailand
PERSONAL ADDRESS 47, lane Romkraw 21/8, Romkraw Road ,
Khlongsampravej Ladkrabang, Bangkok, 10520
Thailand
Tel. 66-2-3609181, Mobile. 66-87-5054803
E-MAIL songvudhi@buu.ac.th, songvudhi@gmail.com

EDUCATIONS

Degree of Doctor of Philosophy (2002 - present)

School of Physics, Suranaree University of Technology, Nakhon Ratchasima,
Thailand

Supervisors: Prof. Dr. Yupeng Yan and Asst. Prof. Dr. Chinorat Kobdaj

Master of Science (1996 - 2000)

Department of Physics, Faculty of Science, Chulalongkorn University,
Bangkok, Thailand

Supervisor: Dr. Pornthep Nisamaneepong

Bachelor of Science (1991 - 1995)

Department of Physics, Faculty of Science, Mahidol University, Bangkok,
Thailand